T. & A. M. Report No. 394

# THE INFLUENCE OF SPECIMEN DIMENSIONS ON A $J_M$ FRACTURE TOUGHNESS TEST

by

Frank Zaverl, Jr.

This research was performed in the Department of Theoretical and Applied Mechanics at the University of Illinois at Urbana-Champaign, Illinois 61801 with support of the Advanced Research Projects Agency of the Department of Defense under Grant Nos. DAHC 15-72-G-10 and DAHC 15-73-G-7; ARPA Order No. 2169 w/Amend. 1, Req. No. 1001/191; Methods and Applications of Fracture Control. The period of the Grants is from June 15, 1972 through June 14, 1974 and the amount is $100,000/year. Professor H. T. Corten 217/333-3175 is Principal Investigator and Professors G. M. Sinclair 217/333-3173, JoDean Morrow 217/333-4167 and H. R. Jhansale 217/333-1835 have participated as Project Scientists.

Department of Theoretical and Applied Mechanics
University of Illinois
Urbana, Illinois
September, 1974

# FOREWORD

Recent requirements for increased strength and service life of machines and structures have been met by the use of higher strength materials and new fabrication and joining methods. Simultaneously, failures due to fracture have increased relative to those resulting from excessive deformation. Frequently service conditions are such that low temperature brittle fracture, fatigue fracture, and high temperature creep rupture must be considered in a single system. National concern with increased safety, reliability, and cost has focused attention upon these problems.

Methods are now available to predict both fatigue crack initiation life and crack propagation life. Paradoxically the materials properties required for long fatigue crack initiation life are incompatible with the requirements of high fracture toughness. Thus, the conflicting design approaches and requirements placed on the material are confusing and often impossible to satisfy.

Numerous publications dealing with a variety of fracture problems have led to many new and useful developments. However, the synthesis of the concepts into methods for design, testing and inspection has lagged.

This program of study is intended to contribute to the integration, correlation, and organization of mechanics and materials concepts and research information into a form that will permit enlightened decisions to be made regarding fracture control. Reports are in preparation in three categories:

1. Research reports designed to explore, study and integrate isolated and/or conflicting concepts and methods dealing with life prediction,

2. Reports to introduce and summarize the state-of-the-art concepts and methods in particular areas, and

3. Example problems and solutions intended to illustrate the use of these concepts in decision making.

H. T. Corten
Principal Investigator

## ACKNOWLEDGMENT

Support was provided for this research by the Advanced Research Projects Agency of the Department of Defense under U. S. Department of the Army No. DAHC-15-72-G-10, ARPA Order No. 2169.

The author wished to thank his advisor, Professor H. T. Corten, for his guidance and patience throughout the course of this investigation. A debt of gratitude is also expressed to R. H. Sailors for his helpful discussions and experimental assistance, and M. R. Mitchell, whose aid was deeply appreciated.

Thanks are also due to Mrs. R. A. Mathine and Karen Hageman, who typed the manuscript, and to H. T. James, who prepared the figures for this report.

# INTRODUCTION

For cracked bodies exhibiting a limited amount of plasticity, linear-elastic fracture mechanics adequately describes the singular stress field existing near the crack tip. The fracture toughness parameter, $K_{Ic}$, characterizing this singularities magnitude for crack extension, has had sufficient investigation to provide an extremely useful tool for judging a material's susceptibility towards onset of crack extension from flaws. Unfortunately, not all engineering structures can be analyzed with this linear elastic approach due to the high toughness of the material being used or the large crack tip plastic zone relative to the dimensional characteristics of the structure at fracture. In such situations, an analysis must be made describing the singularity within the plastic zone at the crack tip.

The J-integral, a path independent line integral, has been shown useful in describing this singularity [1]. Rice has defined the J-integral for linear elastic and non-linear elastic materials as [2]:

$$J = \int_{\Gamma} W\,dy - \overline{T} \cdot \left( \frac{d\overline{u}}{dx} \right) ds \qquad (1)$$

where $\Gamma$ = path of integration taken counterclockwise around the crack tip

$W$ = strain energy density

$\overline{T}$ = traction vector defined by the outward normal vector along the path $\Gamma$

$\overline{u}$ = displacement vector

$s$ = arc length along the path $\Gamma$

Its importance lies in its path independence, leading to the ability to evaluate near crack tip characteristics in a region far removed from the crack tip. Deformation-type elastic-plastic materials can now be analyzed by approximating them as non-linear elastic materials, but such an analysis is theoretically limited by allowing no unloading.

For a cracked body exhibiting linear elastic behavior, the J-integral is found to be equivalent to the strain energy release rate, G [3]. Thus if near crack tip conditions control the onset of crack extension, the value of J should be identical for a body exhibiting limited crack tip plasticity, where G can be determined, to that of a body made of the same material exhibiting fully plastic behavior.

The J-integral may also be interpreted as the difference in potential energy between two identically loaded bodies having neighboring crack lengths [4]. This can be expressed as:

$$J = -\frac{\Delta U}{\Delta d} \tag{2}$$

where $U$ = potential energy per unit thickness

$d$ = crack length

Using this expression, Begley and Landes experimentally evaluated the J-integral at maximum load for specimens exhibiting fully plastic behavior, and found general agreement with the value of $G_{Ic}$ [5].

The general size requirements placed on specimens used in evaluating the fracture toughness using linear elastic fracture mechanics [6], arise from two conditions which must exist during the evaluation. The first condition being that the plastic zone at the crack tip, where linear-elasticity is no longer applicable, must be small relative to the specimen thickness and crack length. Secondly, the fracture toughness is defined for the plane strain situation, therefore, in-plane deformation must occur in the region of the crack tip. The criterion used to insure this places a lower bound on the specimen thickness as compared to the plastic zone size.

If the value of the J-integral near the onset of crack extension is to be used as an accurate material parameter, two similar conditions must also be met during its evaluation. As with a linear-elastic fracture toughness test, a plane strain condition must

prevail. But since the J-integral can be used within the plastic zone, a fully plastic situation may now be present. With the J-integral, concern centers on a region of intense strain ahead of the crack caused by blunting. This zone, on the order of $J_{critical}$ divided by the yield stress, has been suggested by Paris, [7], as the size parameter to be used in the criteria specifying the size limitation on the J-integral. Expressed as:

$$B \geq \alpha \frac{J_{critical}}{S_y} \tag{3}$$

The data presented by Begley and Landes using maximum load as measurement point indicated the constant $\alpha$, to be on the order of 25 to 50 [5, 8]. They also expressed concern with the size of the uncracked ligament and its effect on $J_{critical}$.

The effect of strain state on $J_c$ has been investigated by Sailors [9] for compact tension specimens. Using maximum load as measurement point, his results indicate that the plastic plane strain behavior occurs as long as the thickness to remaining ligament ratio exceeds two. Any ratio less than two has the effect of increasing the value of $J_{critical}$.

The major purpose of this investigation was to determine the effect of dimensional variables on the value of J determined at the maximum load. In addition, an attempt was made to measure the point of the onset of crack extension for fully plastic behavior. Because it is found that the measurement point and specimen dimensions interact to influence the value of J, in this paper the critical value of J determined using the maximum load as a measurement point will be designated $J_{Mb}$. The subscript "Mb" indicates J at "maximum load" for a specimen with remaining ligament of size b.

## EXPERIMENTAL PROCEDURE

All tests were conducted using a quenched and tempered 4340 steel with composition given in Table 1. Two strength levels were achieved by tempering at different temperatures and the mechanical properties for each heat treatment are given in Table 2.

Bend specimens, shown in Fig. 1, with variations in crack length and thickness were used to investigate the size effects on $J_{Mb}$ and the amount of crack advancement involved. Specimens were machined from a three-inch thick plate with the longitudinal axis along the rolling direction of the plate (L-T); the specific orientations are shown in Fig. 2. Specimens were taken from random locations in the plate to insure any trend in the data would not reflect location in the plate.

The value of $J_{Mb}$ was evaluated using the single specimen formula [10] and by the compliance method [5]. The actual evaluation of $J_{Mb}$ from one specimen, as described in Appendix A, involved two separate tests on one specimen. The first test was conducted to obtain load-deflection curves for the uncracked specimen; and the second, to obtain similar curves for the cracked specimen. The compliance method of obtaining $J_{Mb}$ outlined in Appendix B, was used on a series of similar thickness specimens to enable a comparison of the two evaluation techniques.

The bend specimens with thicknesses ranging from $\frac{1}{4}$" to 2" are illustrated in Fig. 1 (a). For thin bars with deep cracks, slight modifications in specimen design were necessary to eliminate difficulties of specimen alignment and buckling. Thus, for specimens with a thickness of $\frac{1}{4}$" or less, the specimen configuration shown in Fig. 1 (b) was used.

Four point loading was employed on the bend bars using a span length of 2" (see Appendix A). The loading apparatus is shown in Fig. 3. Relative vertical displacements of the bars connecting the contact rollers were measured on both sides of the specimen.

These bars were fastened loose enough to allow roller movement in the longitudinal direction without excessive wobbling of the bars. Vertical displacements were monitored by clip gages mounted on the bars. Both gages were calibrated to produce identical displacement-voltage output. During a test the output of both gages were then added together and the resulting output corresponded to twice the average displacement. This procedure compensated for any longitudinal rotation of the specimen due to small misalignments and irregularities of the fatigue crack front. Load-deflection records were obtained during tests conducted on an Instron test machine using a crosshead speed of 0.02 inches per minute.

Unnotched bend specimens were first heat treated to the desired strength level and then individual load-displacement diagrams were produced. These specimens were initially loaded to produce indentations from the contact rollers, then reloaded to produce the actual load-deflection records. Thin specimens were not subjected to this first loading procedure for it was felt the deflection corresponding to the unnotched specimen was insignificant relative to the deflection of the cracked specimen.

The bend specimens were then notched and fatigue cracked on an MTS closed-loop, servo controlled hydraulic test system using the apparatus previously described. Fatigue cracks were allowed to progress 1/16" or more from the notch tip using a $\Delta K$ between 30 and 35 ksi$\sqrt{\text{in}}$ calculated using the expression:

$$K_I = 4 \frac{M}{b^{3/2} B} \tag{4}$$

for deep cracked bars [11]. It should be noted that for the thin specimens, the fatigue crack was allowed to progress a distance of approximately 1/16", then specimens were remachined to produce the desired remaining ligament length.

With the cracked specimen, the final load-deflection curves were produced. A microphone attached near the crack was used to monitor the audible acoustic emission

from the specimen. This was attempted with both materials but only the higher strength steel produced a well defined initial emission which could be attributed to crack advancement.

For the lower strength steel, a series of bend specimens with different crack lengths were used to investigate the amount of crack growth during loading. Heat tinting was used to identify crack fronts at different portions of the load-displacement diagram. The crack specimen was loaded to a certain displacement, then a wedge was inserted in the notch to hold it open. After unloading, the specimen was placed in a furnace for tinting. The procedure was repeated several times on the same specimen. The times and temperatures for each subsequent tinting were:

1. 20 minutes at $620^{o}$ F.
2. 25 minutes at $540^{o}$ F.
3. 35 minutes at $460^{o}$ F.
4. 45 minutes at $400^{o}$ F.

## RESULTS AND DISCUSSION

The experimental results for the bend specimens are presented in Tables 3 through 6. Specimens numbered A1 through A104 are the lower strength steel specimens with a lower yield point of 113 ksi and specimens number BO through B55 are the higher strength steel with a yield stress of 174 ksi. Unless otherwise specified, the value of $J_{Mb}$ was calculated at maximum load. The values of $J_{Mb}$ obtained from the compliance method for the B specimens and the single specimen formula show general agreement.

In Figs. 4 through 7, the J-integral data for both series of tests are compared to the dimensional variables under consideration. The dependence of $J_{Mb}$ on the remaining ligament and the thickness to remaining ligament ratio, B/b, must be individually considered and interactions between the two variables must be separated in order to identify the dependence on each variable. From these figures, three dominant points are noted:

1. For specimens with remaining ligaments greater than a defined value, $J_{Mb}$ increases if the B/b ratio is less than 1.8. For ratios greater than 1.8, the value of $J_{Mb}$ remains essentially constant.
2. For specimens with B/b ratios greater than 1.8, the value of $J_{Mb}$ decreases with remaining ligament if the remaining ligament is below a certain value. If the remaining ligament is larger than this value, $J_{Mb}$ is unaffected by remaining ligament.
3. The combination of small remaining ligament and small B/b ratio causes a large amount of scatter in the value of $J_{Mb}$ with no apparent trend with remaining ligament or B/b ratio. Small values of remaining ligament tend to decrease the value of $J_{Mb}$ while the small B/b ratio increases the expected value.

The values of $J_{Mb}$ which show no dependence on remaining ligament size and B/b ratio provide the desired consistency and are proposed as a potentially suitable measure of fracture toughness comparable to $K_{Ic}$. These values of $J_{Mb}$ are hereafter referred to as consistent values of $J_{Mb}$.

The following expression was used to evaluate $J_{Mb}$ from a single specimen (see Appendix A):

$$J = \frac{2}{bB} \int_0^{\delta_c} P \, d\delta_c \tag{5}$$

In the following discussion, each variable contributing to the above integral (i.e. P, $\delta_c$ and b) is used to interpret the variations of $J_{Mb}$ with the specimen dimensional variables. The B/b ratio is employed as a measure of constraint and used to interpret the effect of strain state on the value of $J_{Mb}$.

The effect of the B/b ratio is readily seen for the higher strength steel as shown in Fig. 5, with $J_{Mb}$ for specimens having a B/b ratio less than 1.8 increasing above the consistent values. For the lower strength steel (Fig. 4), the effect of this ratio is present but not as apparent. The interaction between insufficient remaining ligament and B/b ratio now produce considerable scatter around the region of B/b equal to 1.8.

The increase of $J_{Mb}$ for B/b ratios less than 1.8 can be attributed to the loss of constraint such that through the thickness deformation is occurring, no longer producing a plane strain situation. A general check on the constraint was made by plotting maximum load versus remaining ligament and comparing this to the limit solution from Green and Hundy [12]:

$$M_1 = \frac{1}{2} P_1 L = 1.261 (2\tau_o) \frac{Bb^2}{4} \tag{6}$$

The value of the flow stress, $\tau_o$, was taken as the ultimate stress divided by $\sqrt{3}$, to take into account strain hardening and the von Mises yield criteria. From Figs. 8 and 9, it is seen that the limit load is approached as the remaining ligament is reduced but no apparent deviations from the general trend occur in these specimens with B/b ratios less than 1.8. One can therefore conclude that as the remaining ligament becomes large, the digression of this data from the limit solution is primarily due to the fact that the limit load could not be achieved due to crack advancement occurring at lower loads.

The effect of constraint at the crack tip can be made more visible by employing the dimensionless parameters $M/Bb^2$ and $\theta_c$ (for one material). Since a constant span length of two inches was used for all specimens, a $P/Bb^2$ versus $\delta_c$ diagram will allow all bend specimens of a given material to be represented on one load-displacement diagram, independent of thickness and remaining ligament. A model of such a diagram is shown in Fig. 10, with the limit solution of $P/Bb^2$ designated as maximum load. By plotting $P_{max}/Bb^2$ versus $\delta_c$ at $P_{max}$, as shown in Figs. 11 and 12, the general shape of the $P/Bb^2$ versus $\delta_c$ can be determined. From these figures, it is apparent that crack initiation, thus maximum load, frequently occurred before the limit load occurred. They also show why the lower strength material appears to approach the limit solution (Fig. 8) while the higher strength material shows a much larger deviation (Fig. 9). The shape of the load-deflection curve is strongly reflected in the comparison between the maximum load and the limit load due to crack initiation prior to limit load. Thus materials exhibiting relatively flat-topped load deflection responses will show the maximum load approaching the limit solution more readily because the difference between the two is undetectable.

In the above discussion, by representing all specimens on a single dimensionless load-displacement diagram, the assumption that all specimens exhibited a plane strain

behavior was used. Should the strain state differ, a family of load-deflection curves would result, each representing a different state of strain. By looking at the dimensionless load at a fixed value of $\delta_c$ prior to $P_{max}$, the effect of constraint may be examined without the influence of crack extension. This procedure was used for the lower strength steel by comparing $P/b^2B$, at $\delta_c = 0.025"$, to the B/b ratio. As seen in Fig. 13, the data is somewhat scattered but there does appear to be a trend for the load to be somewhat lowered for small values of B/b: for large values of B/b plane strain is approached. As a basis for an arbitrary limit on B/b, the apparent knee in this curve corresponds approximately with the value of B/b = 1.8 noted previously in Figs. 4 and 5.

Considering the shapes of the load-displacement diagrams, a variable move sensitive to constraint should be that of displacement rather than load. As seen from Fig. 10, if the limit moment is achieved at maximum load, the displacement due to the crack should be a constant at maximum load. From Figs. 14 and 15, where displacement due to the crack at maximum load is compared to the remaining ligament, it is apparent this is not the case. Instead, the data shows that displacement increases as the remaining ligament is reduced. In general, the effect of a small B/b ratio is to increase the expected displacement, with a slight decrease in load (as seen in Fig. 13). For specimens with B/b ratios near 1.8 the two effects seem to cancel each other out and produce a $J_{Mb}$ nearly equal to the consistent values of $J_{Mb}$. Only when the loss of constraint is large ($B/b < 1.8$) will $\delta_c$ sufficiently increase to produce a $J_{Mb}$ which is considerably larger than the consistent values of $J_{Mb}$.

The point of onset of crack extension was found for the higher strength material using the audible acoustic emission of the specimen. The values of $J_A$ determined by audible acoustic emission are tabulated in Table 5 and shown as a function of B/b in

Fig. 16. As expected, the $J_A$ values determined from audible emission fall below those taken at maximum load. Scatter in $J_A$ exceeds that observed with consistent values of $J_{Mb}$ and no dependence on B/b ratio was found. Thus defining a procedure for measuring $J_{Mb}$, the criteria used to define the measurement point, also influences the size requirements.

Through the use of subsequent heat tintings during loading, a qualitative measure of crack advancement was made for several specimens on the lower strength material. The tinting procedure produced a strain aging effect causing an abnormal increase in subsequent load-deflection diagrams when compared to similar specimens, as seen in Appendix C. Though this effect rendered the load-displacement data inaccurate for calculating the J-integral, the assumption that displacement was unaffected, or little affected, as far as crack advancement was concerned, allowed a comparison to previous data. Table 7 presents the data obtained from a series of 1" thick specimens which were heat tinted. A diagram of the percentage of crack advance versus displacement due to the crack is shown in Fig. 17. Using Fig. 14 to determine the displacement at maximum load is in the neighborhood of 2% for all crack lengths. This is approximately the same amount of crack advancement specified for a $K_{Ic}$ test evaluated using the ASTM E-399 Test Method.

Referring back to Figs. 10, 11 and 12, it was previously mentioned that maximum load was generally governed by crack advancement before the limit load (corresponding to the initial crack length) was achieved. As the remaining ligament, b, was decreased, the onset of crack extension occurred at larger values of $\delta_c$, and the limit load (corresponding to the initial crack length) was approached. If the maximum load were governed by reaching limit load (in the absence of crack extension), then dimensional similitude would apply and the deflection (angle of bend) at this point would be constant. On a diagram of $P/Bb^2$ ($M/Bb^2$) versus $\delta_c(\theta)$, for specimens with full constraint

$(B/b \geq 1.8)$, the area, A, under the curve would be constant (see Appendix A). Using the single specimen formula for deep cracked bend bars for these conditions, the J-integral can be evaluated at maximum load (limit load) as:

$$J = \frac{2}{Bb} \int_0^{\delta_c \text{ at } P_{max}} P d\delta_c = 2b \int_0^{\delta_c \text{ at } P_{max}} \left(\frac{P}{Bb^2}\right) d\delta_c \qquad (7)$$

Since the area A to $P_{max}$ is represented by the integral in Eq. 6,

$$J = 2bA \qquad (8)$$

Thus when the maximum load is used as the measurement point, but is not governed by crack advancement, J is not $J_{critical}$ a constant, but a linear function of the remaining ligament b. This linear relationship can be seen for the higher strength material for remaining ligaments less than 0.13 inch (Fig. 7). Whether J is actually linear above 300 in-lb/in$^2$, a small amount of crack advancement may be taking place as indicated by the acoustic emission data.

For the lower strength steel, $J_{Mb}$ begins to deviate from the consistent values of $J_{Mb}$ when the remaining ligament becomes smaller than about 0.26", as seen in Fig. 6. Now the linear relationship between $J_{Mb}$ and b is not as apparent. A small amount of crack extension may have taken place at maximum load but as the remaining ligament was reduced, this amount of extension approached zero. This was indicated by the heat tinting data. Although not conclusive, it does suggest a trend toward zero crack growth as the remaining ligament becomes smaller.

Consider different areas under the load-deflection curve, shown in Fig. 11, as representing different amounts of crack extension between zero and 2%, with zero percent occurring for the specimens exhibiting the largest deflection at maximum load. Now as the remaining ligament is reduced below 0.26" the amount of crack extension

at maximum load is reduced. As indicated in Fig. 6, this causes the apparent curvature in the $J_{Mb}$ versus b trend. If this same procedure was used to evaluate the higher strength material, the insignificant differences between the areas representing different amounts of crack extension would show very little deviation of the $J_{Mb}$ versus b data from linearity. Thus the $J_{Mb}$ data for the higher strength material appears to be linear with remaining ligament.

The restrictions on the remaining ligament and the B/b ratio imposed for consistent values of $J_{Mb}$, automatically places a lower limit on the allowable size of the thickness, given a specific remaining ligament. A diagram of the thicknesses and ligament sizes used for the specimens are shown in Figs. 18 and 19. Should the limit on thickness be somewhat larger than imposed by the limits on b and B/b, the only additional area which would be restrictive for a consistent value of $J_{Mb}$ would be the small triangle indicated in these diagrams. This added area would be so small that it is almost undetectable and generally could be ignored. Thus, with the restriction on b and B/b ratio, it is felt the automatic restriction on thickness is sufficient.

The fracture surfaces for all specimens are shown at the end of Appendix C.

## CONCLUSION

The results of the $J_{Mb}$ measurements, taking maximum load as the measurement point, can be summarized for bend specimens as follows:

1. $J_{Mb}$ can be determined as long as the B/b ratio is greater than 1.8 and there is sufficient remaining ligament.
2. For the materials investigated, the size limitation on the remaining ligament can be given as:

$$b > 30 \text{ to } 50 \left(\frac{J_{Mb}}{S_y}\right)$$

3. Deviations of $J_{Mb}$ from consistent values of $J_{Mb}$ for small remaining ligament are due to the fact that maximum load is no longer controlled by the onset of crack extension.
4. The size restriction on thickness automatically imposed by 1. and 2. above appears to be sufficient, i.e.

$$B > 30 \text{ to } 50 \left(1.8 \frac{J_{Mb}}{S_y}\right)$$

For the two materials investigated, the values of $J_{Mb}$ determined using the single specimen formula up to maximum load was found to be:

4340 ($S_y$ = 113 ksi); $\quad J_{Mb} = 960 \pm 3\% \ \frac{\text{in-lb}}{\text{in}^2}$

4340 ($S_y$ = 174 ksi); $\quad J_{Mb} = 474 \pm 5\% \ \frac{\text{in-lb}}{\text{in}^2}$

# REFERENCES


1. J. R. Rice and G. F. Rosengren, "Plane Strain Deformation Near a Crack Tip in a Power Law Hardening Material," J. Mech. Phys. Solids, Vol. 16, 1968, pp. 1-12.

2. J. R. Rice, "Mathematical Analysis in the Mechanics of Fracture," in Fracture, H. Liebowitz, Ed., Vol. 2, Academic Press, New York, 1968, pp. 191-311.

3. D. C. Drucker and J. R. Rice, "Plastic Deformation in Brittle and Ductile Fracture," Engr. Frac. Mech., Vol. 1, 1970, pp. 577-602.

4. J. R. Rice, "A Path Independent Integral and the Approximate Analysis of Strain Concentration by Notches and Cracks," J. Appl. Mech., Vol. 35, 1968, pp. 379-380.

5. J. A. Begley and J. D. Landes, "The J-integral as a Failure Criterion," in Fracture Toughness, ASTM STP 514, American Society for Testing and Materials, 1972, pp. 1-20.

6. "Standard Method of Test for Plane Strain Fracture Toughness of Metallic Materials," ASTM E399-73, Annual Book of ASTM Standards, 1973.

7. P. C. Paris, discussion to Ref. 5.

8. J. D. Landes and J. A. Begley, "The Effect of Specimen Geometry on $J_{Ic}$," in Fracture Toughness, ASTM STP 514, American Society for Testing and Materials, 1972, pp. 24-39.

9. R. H. Sailors, "Relationship between Tensile Properties and Microscropically Ductile Plane Strain Frasture Toughness," TAM Report No. 367, Univ. of Illinois, Urbana, Ill., 1973.

10. J. R. Rice, P. C. Paris, and J. G. Merkle, "Some Further Results of J-integral Analysis and Estimates," presented at the 1972 National Symposium on Fracture Mechanics, ASTM Headquarters, Philadelphia, Penn., 1972.

11. W. K. Wilson, "Stress Intensity Factors for Deep Cracks in Bending and Compact Tension Specimen," Engr. Fract. Mech., Vol. 2, 1970, pp. 167-171.

12. A. P. Green and B. B. Hundy, "Initial Plastic Yielding in Notched Bend Tests," J. Mech. Phys. Solids, Vol. 4, 1956, pp. 128-144.

TABLE 1

COMPOSITION OF MATERIAL USED IN INVESTIGATION

| | C | Mn | P | S | Si | Ni | Cr | Mo |
|---|---|---|---|---|---|---|---|---|
| From Vendor | .39 | .74 | .005 | .015 | .23 | 1.80 | .83 | .27 |
| Test Sample | .38 | .68 | ND | ND | ND | 1.71 | .79 | .26 |

ND - not determined

TABLE 2

MECHANICAL PROPERTIES

The mechanical properties were determined from a series of 0.25" diameter round tensile specimens with longitudinal axis along the rolling direction of the plate. A gage length of 1.0" was used.

| Heat Treatment | $S_y$ ksi | Ultimate Strength, ksi | %RA ($\epsilon_f$) | n |
|---|---|---|---|---|
| Austenitized at 1550° F for approx. 1 hr. Oil quenched Tempered at 1250° F for 18¼ hrs. Air cooled | 113 (116)[1] | 127 | 62 (0.97) | 0.11 |
| Austenitized at 1550° F for approx. 1 hr. Oil quenched Tempered at 980° F for 1½ hrs. Air cooled | 174[2] | 189 | 51.6 (0.71) | 0.054 |

1. lower yield point (upper yield point)
2. 0.2% offset

TABLE 3

J-INTEGRAL DATA FOR THICK BEND SPECIMENS
TEMPERED AT 1250° F. ($S_y$ = 113)
W = 1.0 in.

| Specimen No. | Thickness, B in. | Remaining Ligament, b in. | B/b | Maximum Load, $P_{max}$ kips | Displacement due to the crack at $P_{max}$, $\delta_{c\,max}$ in. | $J_{Mb}$* in-lb/in$^2$ |
|---|---|---|---|---|---|---|
| A1 | 0.25 | 0.135 | 1.85 | 0.208 | 0.063 | 625 |
| A2 | 0.25 | 0.452 | .583 | 1.88 | 0.049 | 1347 |
| A5 | 0.50 | 0.219 | 2.28 | 1.03 | 0.05475 | 827 |
| A6 | 0.50 | 0.187 | 2.67 | 0.79 | 0.0570 | 773 |
| A7 | 0.50 | 0.330 | 1.52 | 2.22 | 0.0498 | 1061 |
| A8 | 0.50 | 0.444 | 1.13 | 3.81 | 0.034 | 871 |
| A10 | 0.75 | 0.213 | 3.52 | 1.48 | 0.0620 | 951 |
| A11 | 0.75 | 0.298 | 2.52 | 2.79 | 0.0527 | 938 |
| A12 | 0.75 | 0.454 | 1.65 | 6.86 | 0.0317 | 949 |
| A16 | 1.0 | 0.282 | 3.35 | 3.54 | 0.047 | 962 |
| A17 | 1.0 | 0.393 | 2.54 | 6.30 | 0.038 | 970 |
| A20 | 1.5 | 0.185 | 8.10 | 2.55 | 0.0620 | 923 |
| A21 | 1.5 | 0.432 | 3.47 | 11.76 | 0.0465 | 952 |
| A25 | 2.0 | 0.198 | 10.1 | 3.74 | 0.0595 | 907 |
| A26 | 2.0 | 0.378 | 5.29 | 12.47 | 0.0400 | 976 |

*determined using single specimen formula at $P_{max}$

TABLE 4

J-INTEGRAL DATA FOR THIN BEND SPECIMENS
TEMPERED AT 1250° F. ($S_y$ = 113)

| Specimen No. | Depth, W in. | Thickness, B in. | Remaining Ligament, b in. | B/b | Maximum* Load, $P_{max}$ kips | Displacement** due to the crack at $P_{max}$, $\delta_{c\,max}$ in. | $J_{Mb}$*** in-lb/in$^2$ |
|---|---|---|---|---|---|---|---|
| A 50 | 0.9998 | 0.1175 | 0.1643 | 0.71 | 124.5 | 0.1005 | 1136 |
| A 51 | 0.8263 | 0.1257 | 0.0536 | 2.34 | 15.9 | 0.1275 | 513 |
| A 52 | 0.8066 | 0.1257 | 0.0515 | 2.44 | 15.6 | 0.1095 | 452 |
| A 53 | 0.8340 | 0.1264 | 0.0815 | 1.55 | 38.6 | 0.1020 | 595 |
| A 54 | 0.8472 | 0.1866 | 0.0772 | 2.42 | 50.3 | 0.1065 | 648 |
| A 55 | 0.8450 | 0.1864 | 0.0793 | 2.35 | 51.3 | 0.0925 | 534 |
| A 56 | 0.8616 | 0.1867 | 0.0792 | 2.36 | 51.5 | 0.1130 | 686 |
| A 57 | 0.8444 | 0.1864 | 0.1150 | 1.62 | 103.0 | 0.1085 | 899 |
| A 58 | 0.8444 | 0.2502 | 0.1131 | 2.21 | 143.0 | 0.0875 | 754 |
| A 59 | 0.8438 | 0.2490 | 0.1145 | 2.18 | 145.0 | 0.0835 | 715 |

* compensated for tare load

** assume $\delta_{Tot} = \delta_c$

*** determined using single specimen formula at $P_{max}$

TABLE 5

J-INTEGRAL DATA FOR THICK BEND SPECIMENS
TEMPERED AT 980° F. ($S_y$ = 174)

SSF - Single Specimen Formula
GM - Graphical Method

| Specimen No. | Thickness, B in. | Remaining Ligament, b in. | B/b | Maximum Load, $P_{max}$ kips | Displacement due to the crack at $P_{max}$, $\delta_{c\,max}$ in. | $J_{Mb}$ in-lb/in$^2$ Max. Load SSF | GM | Audible Emission SSF | GM |
|---|---|---|---|---|---|---|---|---|---|
| B0 | 0.25 | 0.233 | 1.07 | 0.69 | .0310 | 446 | - | 300 | - |
| B1 | 0.25 | 0.348 | 0.718 | 1.39 | .0273 | 546 | - | 394 | - |
| B2 | 0.25 | 0.489 | 0.511 | 2.49 | .0238 | 592 | - | 342 | - |
| B5 | 0.50 | 0.217 | 2.30 | 1.29 | .03185 | 459 | 440 | 347 | 340 |
| B6 | 0.50 | 0.178 | 2.81 | 0.96 | .03555 | 466 | 491 | 284 | 324 |
| B7 | 0.50 | 0.314 | 1.59 | 2.37 | .03085 | 593 | 491 | 376 | 340 |
| B8 | 0.50 | 0.451 | 1.10 | 4.55 | .0250 | 592 | - | 364 | - |
| B10 | 0.75 | 0.202 | 3.71 | 1.70 | .0336 | 470 | - | 255 | - |
| B11 | 0.75 | 0.416 | 1.80 | 5.87 | .0222 | 497 | - | 287 | - |
| B15 | 1.0 | 0.196 | 5.10 | 2.25 | .0332 | 462 | - | 361 | - |
| B16 | 1.0 | 0.304 | 3.29 | 4.62 | .0263 | 479 | 482 | 379 | 395 |
| B17 | 1.0 | 0.422 | 2.37 | 7.87 | .0215 | 463 | 482 | 340 | 395 |
| B21 | 1.5 | 0.446 | 3.36 | 13.20 | .02095 | 486 | - | 347 | - |
| B25 | 2.0 | 0.222 | 9.0 | 5.07 | .0335 | 460 | 471 | 258 | 290 |
| B26 | 2.0 | 0.301 | 6.68 | 9.17 | .02725 | 475 | 468 | 304 | 308 |
| B27 | 2.0 | 0.381 | 5.23 | 13.57 | .0245 | 494 | 493 | - | - |

TABLE 6

J-INTEGRAL DATA FOR THIN BEND SPECIMENS
TEMPERED AT 980° F. ($S_y$ = 174)

| Specimen No. | Depth, W in. | Thickness, B in. | Remaining Ligament, b in. | B/b | Maximum* Load, $P_{max}$ lbs. | Displacement** due to the crack at $P_{max}$, $\delta_{c\ max}$ in. | $J_{Mb}$*** in-lb/in$^2$ |
|---|---|---|---|---|---|---|---|
| B 50 | 0.8594 | 0.1224 | 0.0548 | 2.23 | 23.1 | 0.0450 | 200 |
| B 51 | 0.8368 | 0.1246 | 0.0511 | 2.44 | 20.0 | 0.0460 | 193 |
| B 52 | 0.8360 | 0.1202 | 0.0530 | 2.26 | 20.3 | 0.0420 | 204 |
| B 53 | 0.8510 | 0.1917 | 0.0795 | 2.42 | 76.5 | 0.0465 | 309 |
| B 54 | 0.8633 | 0.1894 | 0.0802 | 2.36 | 72.0 | 0.0460 | 289 |
| B 55 | 0.8413 | 0.2503 | 0.1058 | 2.36 | 158.0 | 0.0435 | 326 |

* compensated for tare load

** assume $\delta_{Tot} = \delta_c$

*** determined using single specimen formula at $P_{max}$

TABLE 7

CRACK GROWTH DATA ($S_y = 113$)

| Specimen No. | Crack length, a in. | Displacement due to the crack $\delta_c$, in. | Crack Advancement $\Delta a$, in. | $\Delta a / a$ % |
|---|---|---|---|---|
| A101 | 0.7756 | .03125 | 0.00158 | 0.203 |
| | | .04350 | 0.00622 | 0.802 |
| | | .05625 | 0.0124 | 1.601 |
| A102 | 0.6902 | .02825 | 0.00177 | 0.256 |
| | | .03800 | 0.00646 | 0.933 |
| | | .0490 | 0.0146 | 2.121 |
| | | .0640 | 0.0284 | 4.120 |
| A103 | 0.4625 | .01125 | 0.00355 | 0.778 |
| | | .0310 | 0.0224 | 4.817 |
| | | .0460 | 0.0580 | 12.54 |
| | | .0611 | 0.104 | 22.45 |
| A104 | 0.3762 | .01550 | 0.00417 | 1.104 |
| | | .02525 | 0.0205 | 5.423 |
| | | .03975 | 0.0635 | 16.844 |
| | | .0560 | 0.118 | 31.363 |

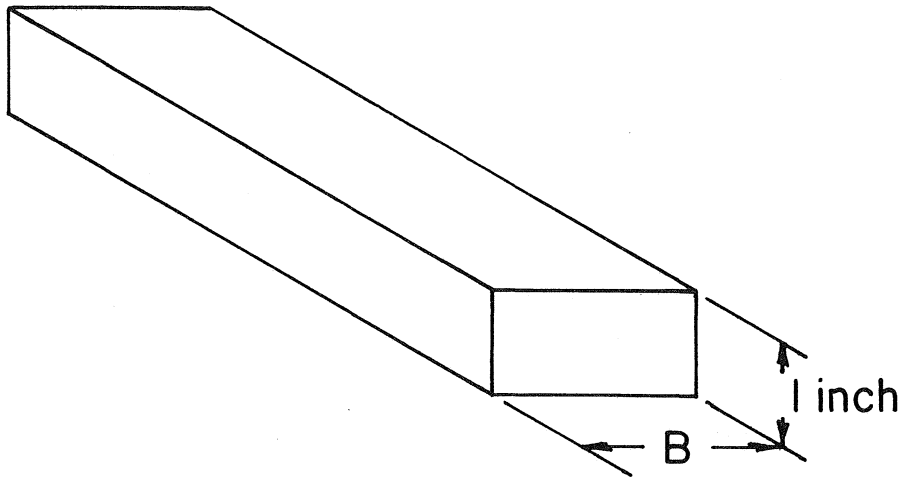


a) Thick Bend Bars

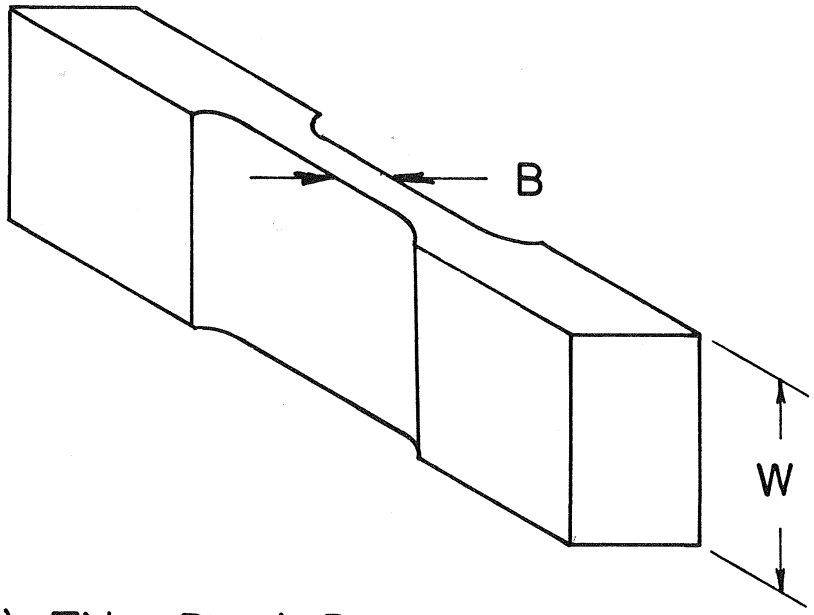


b) Thin Bend Bars

Fig. 1 Test Bend Specimens

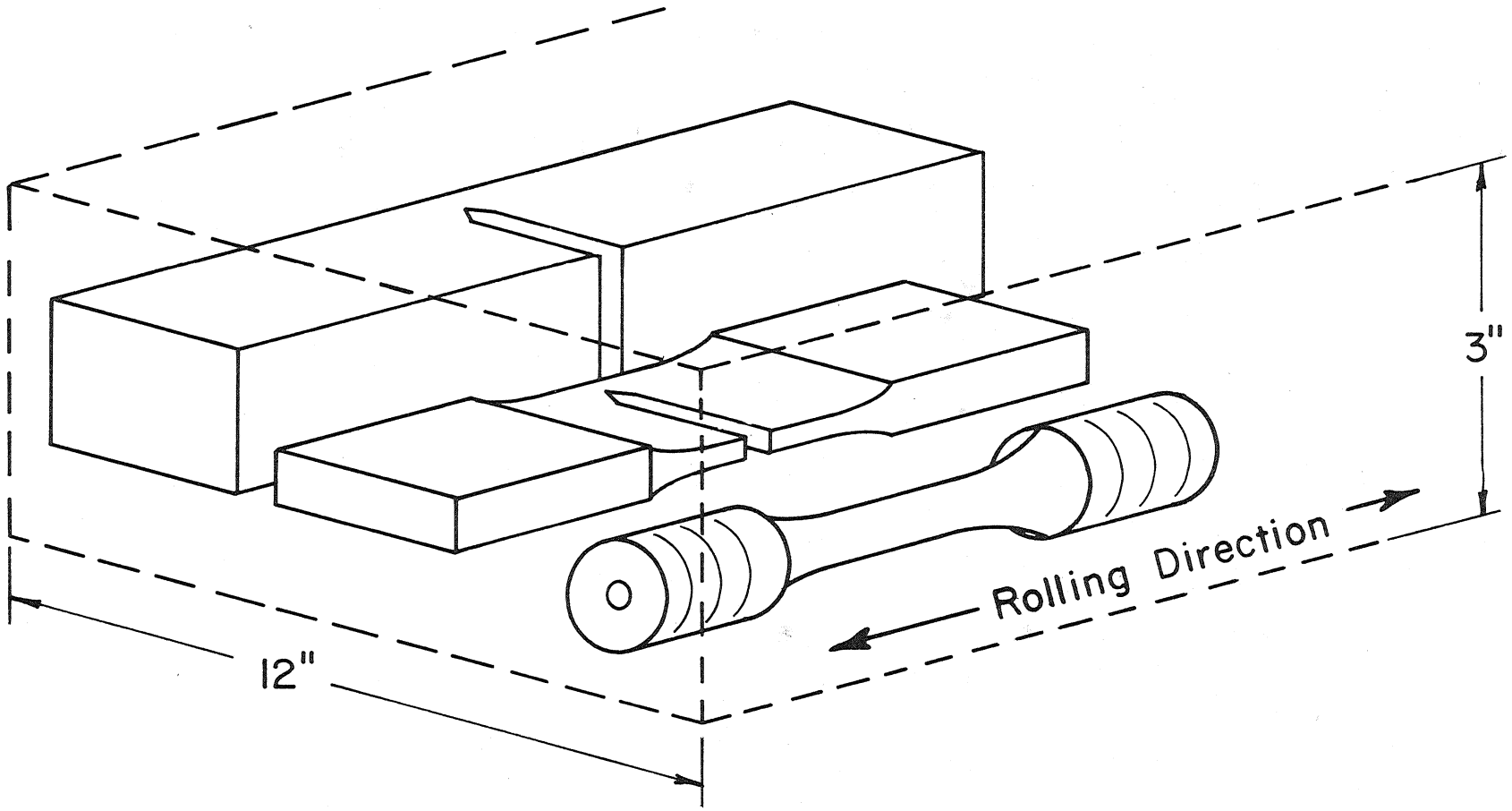


Fig. 2 Specimen Orientation

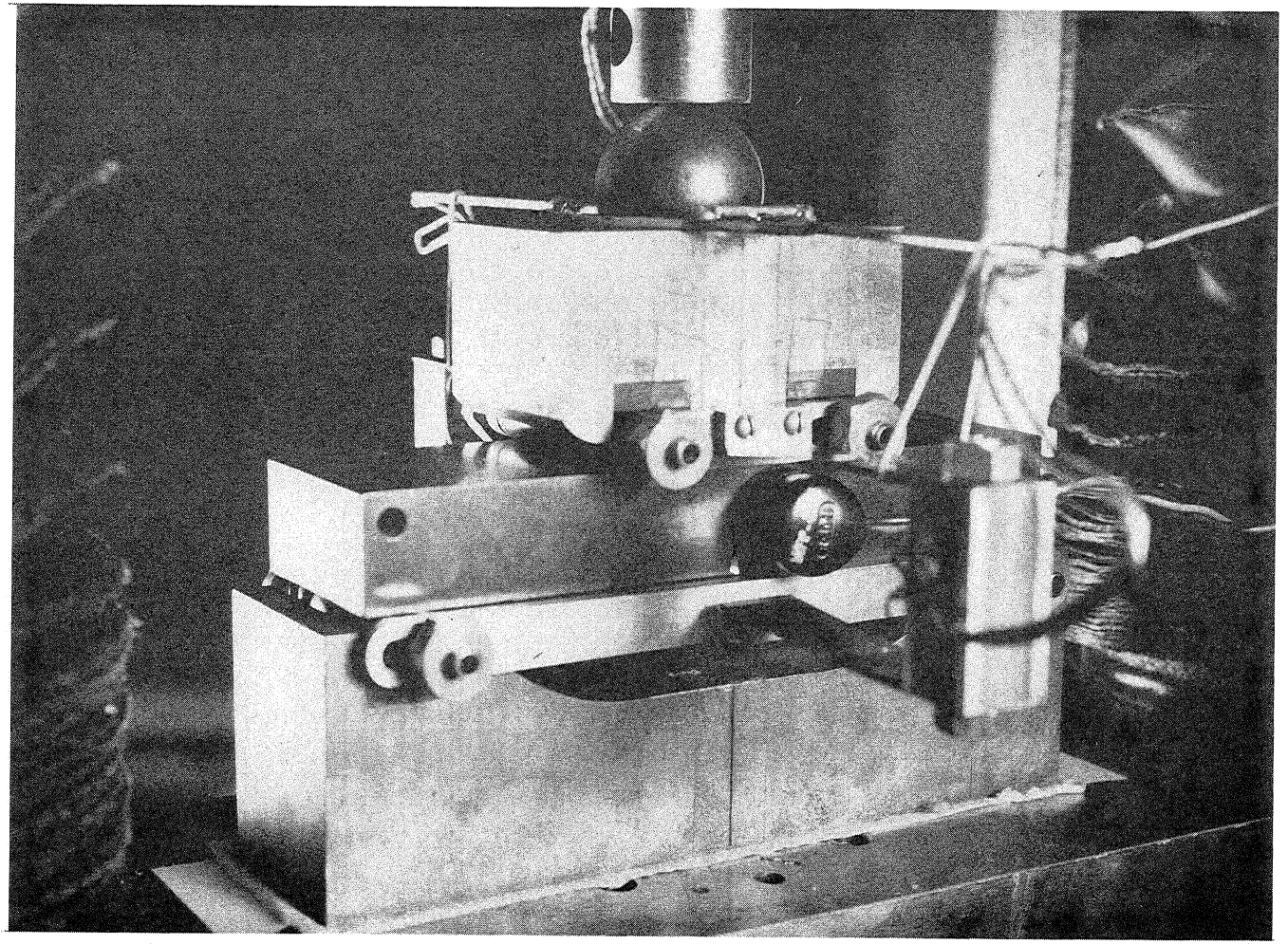

Fig. 3 Loading Apparatus

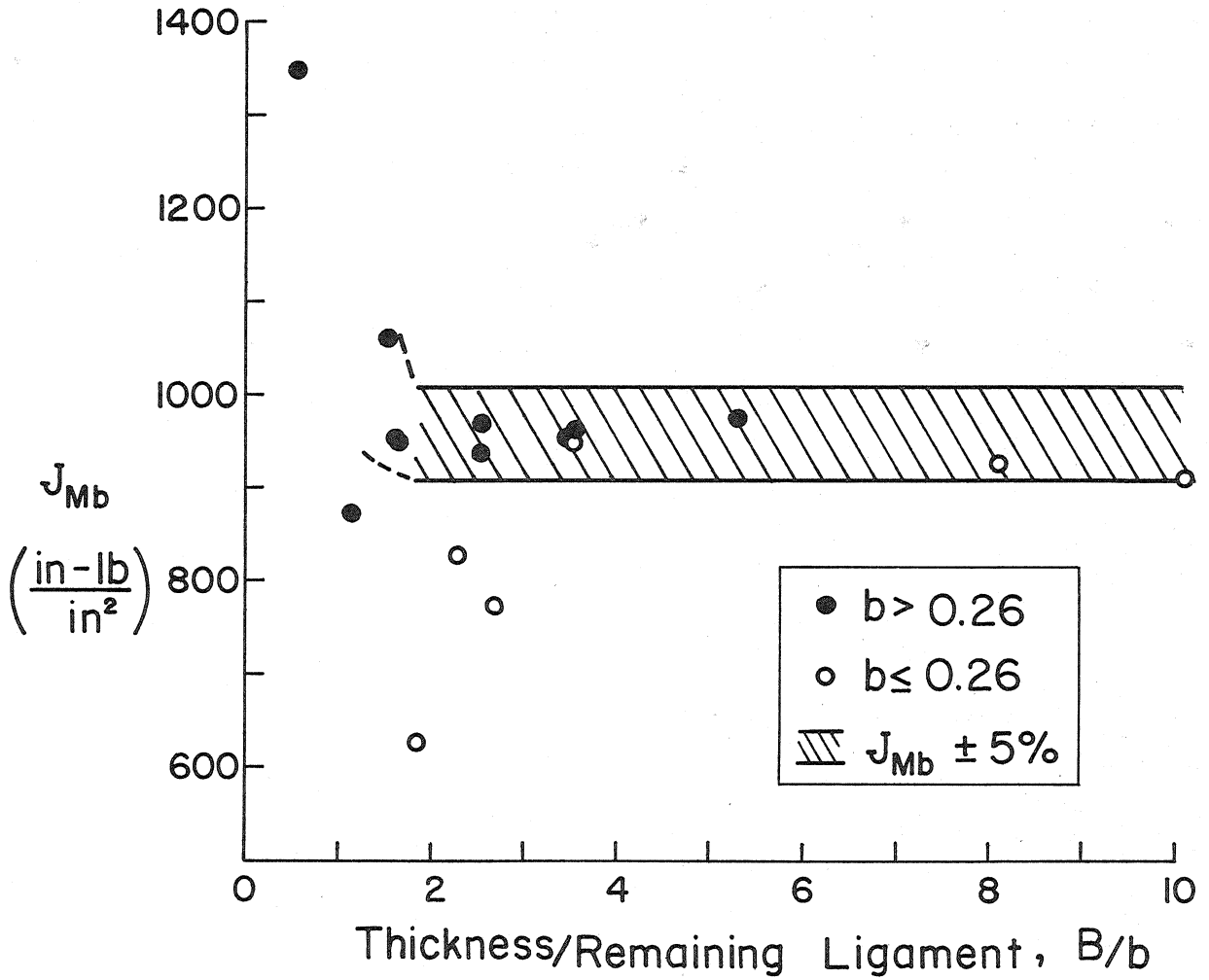


Fig. 4 Effect of B/b on $J_{Mb}$ for Thick Bend Specimens ($S_y$ = 113)

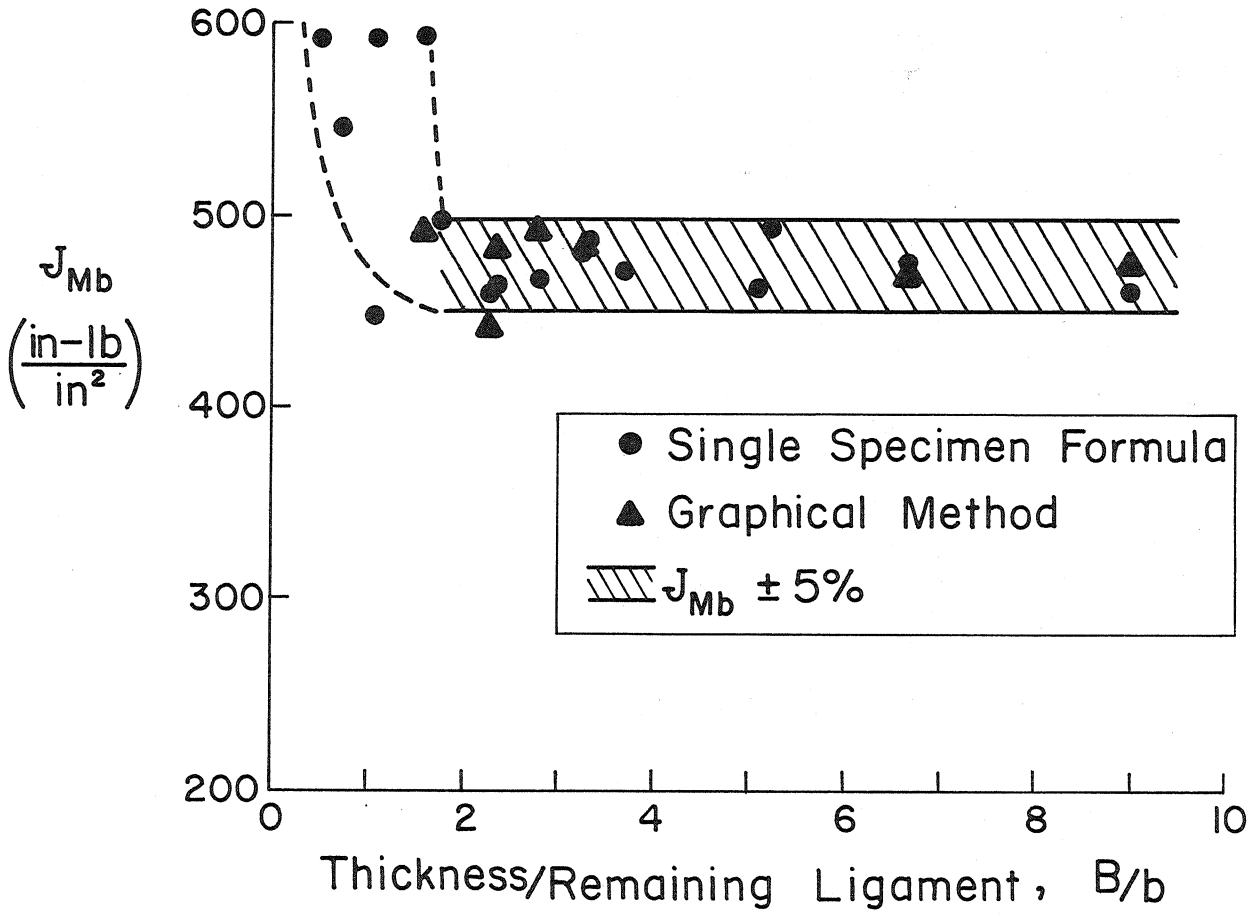


Fig. 5 Effect of B/b on $J_{Mb}$ for Thick Bend Specimens ($S_y$ = 174)

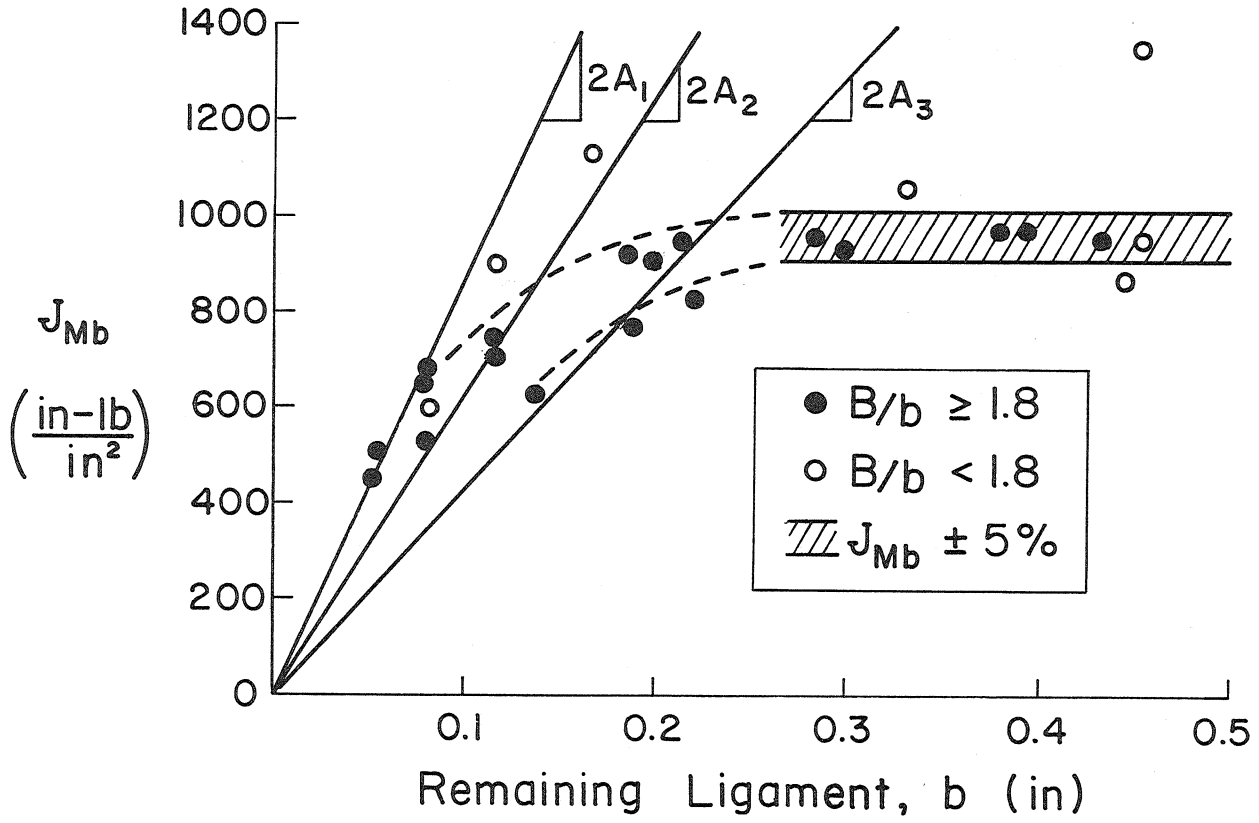


Fig. 6 Effect of Remaining Ligament on $J_{Mb}$ for Bend Specimens ($S_y$ = 113)

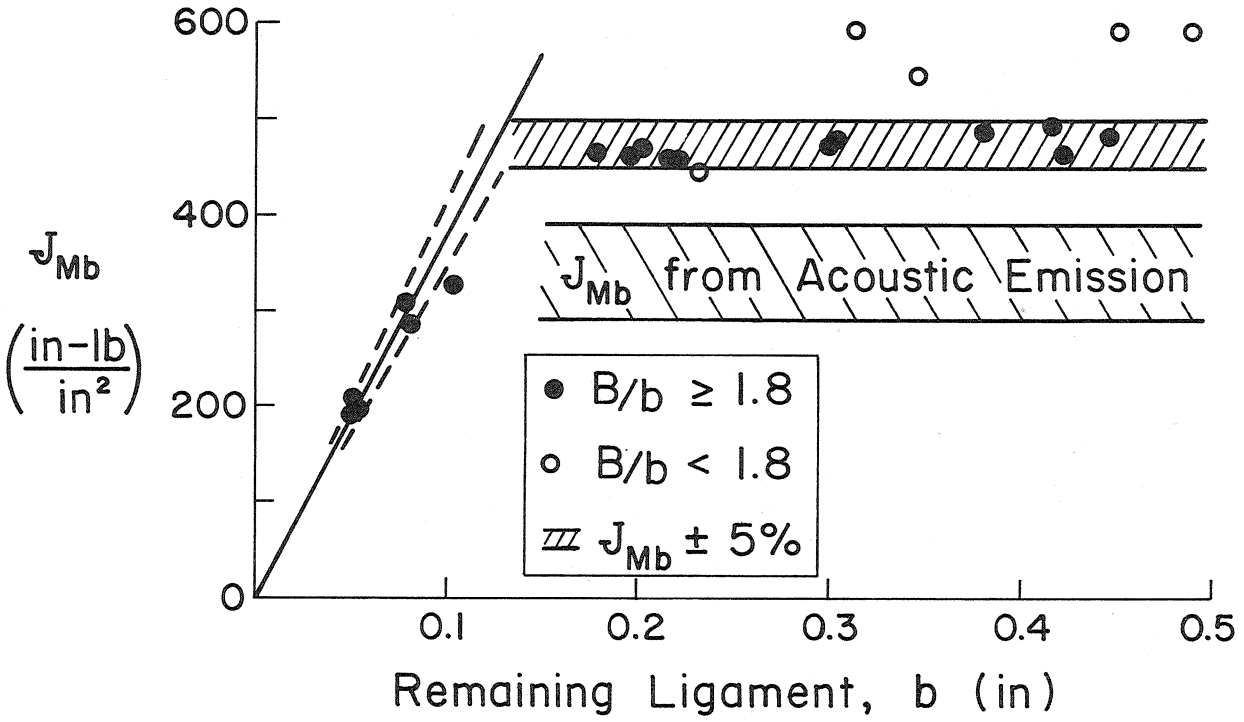


Fig. 7 Effect of Remaining Ligament on $J_{Mb}$ for Bend Specimens ($S_y = 174$)

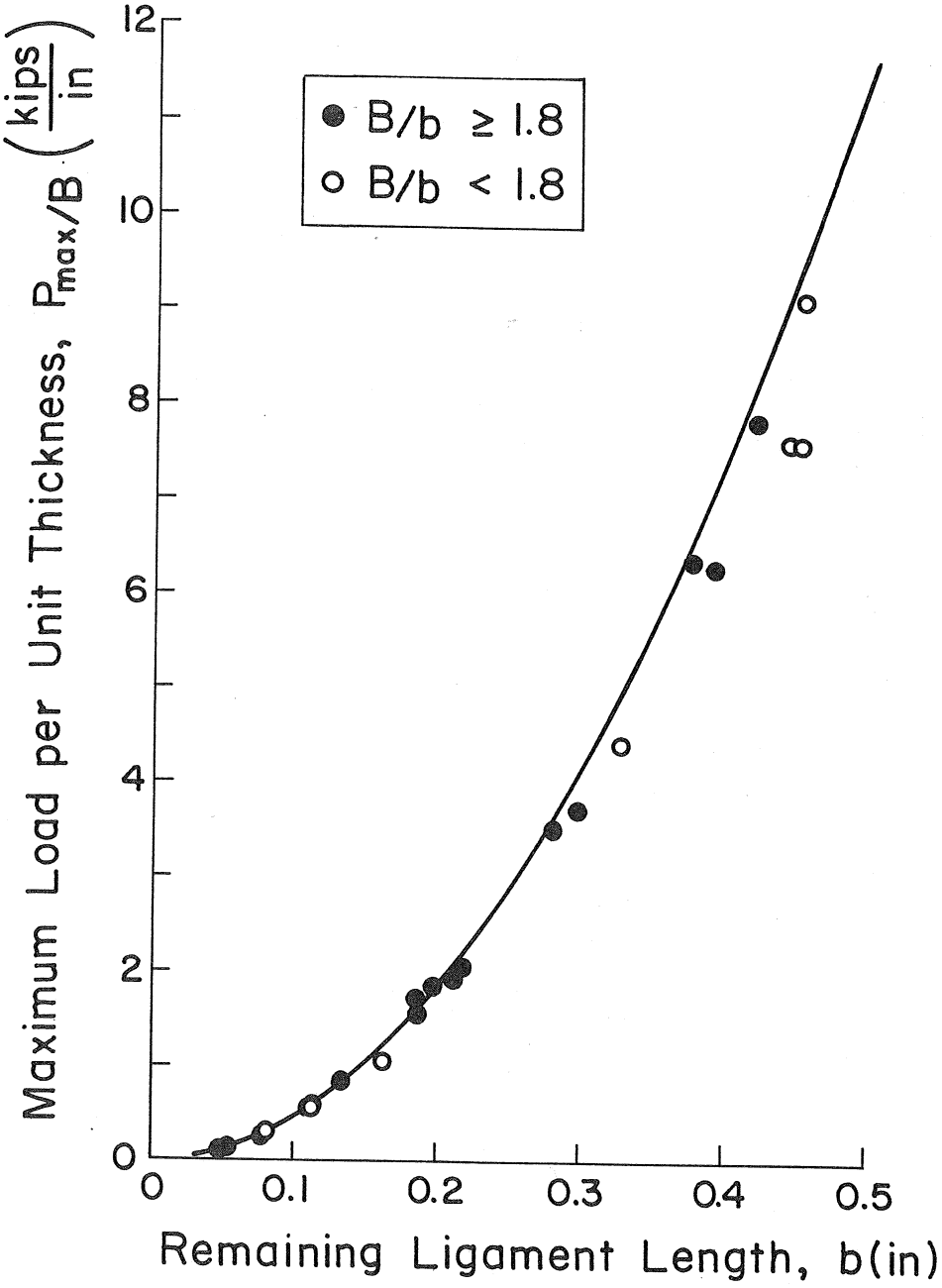


Fig. 8 Comparison between Maximum Load and Limit Load for Bend Specimens ($S_y$ = 113)

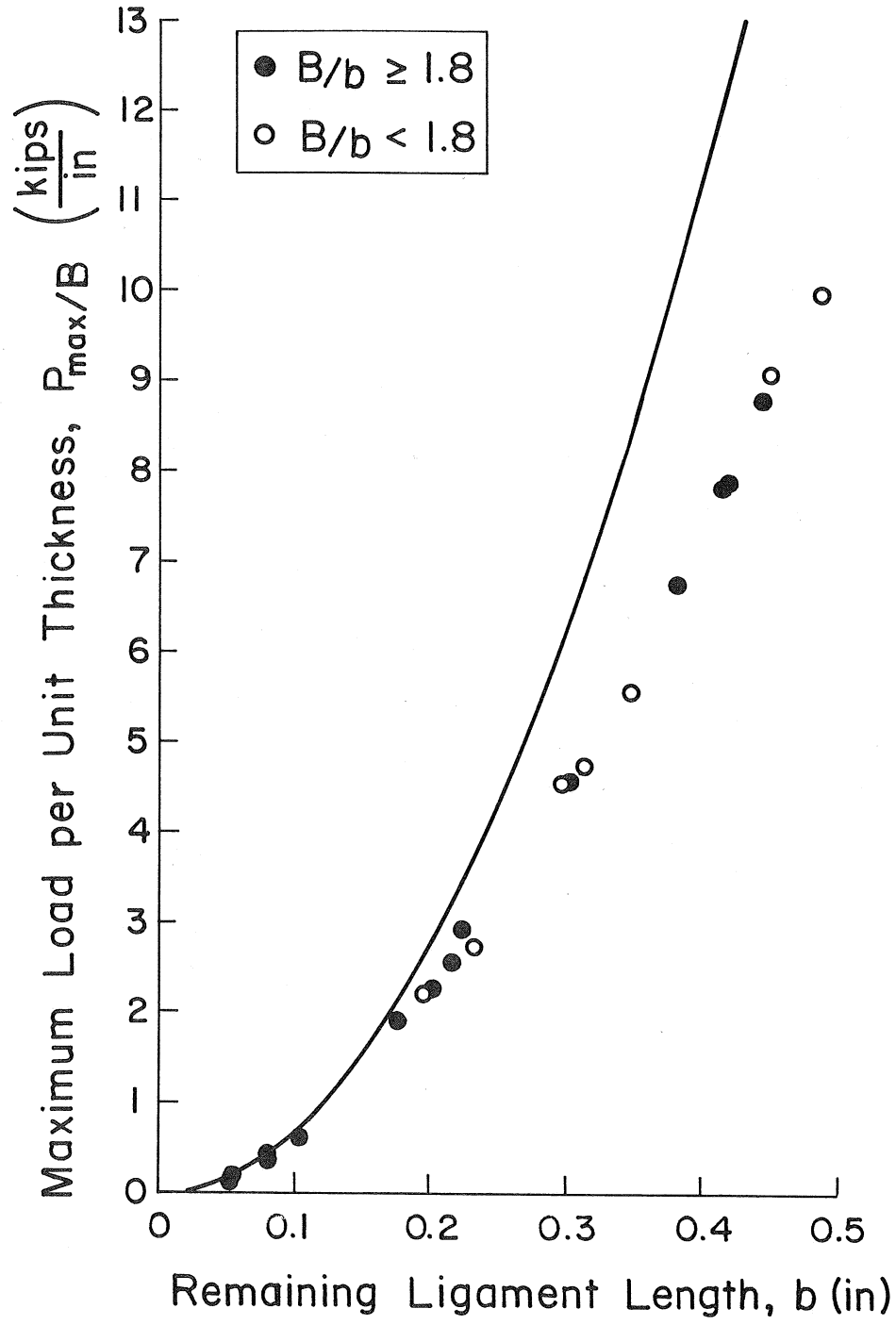


Fig. 9 Comparison between Maximum Load and Limit Load for Bend Specimens ($S_y$ = 174)

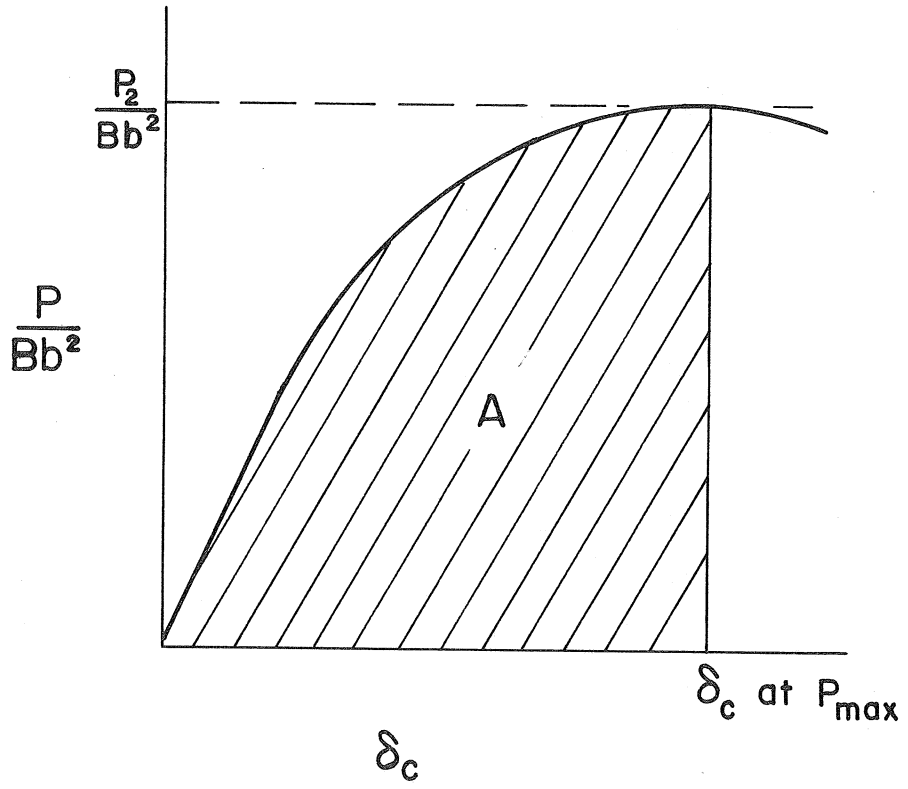


Fig. 10 Normalized Load-Displacement Diagram for Bend Specimens

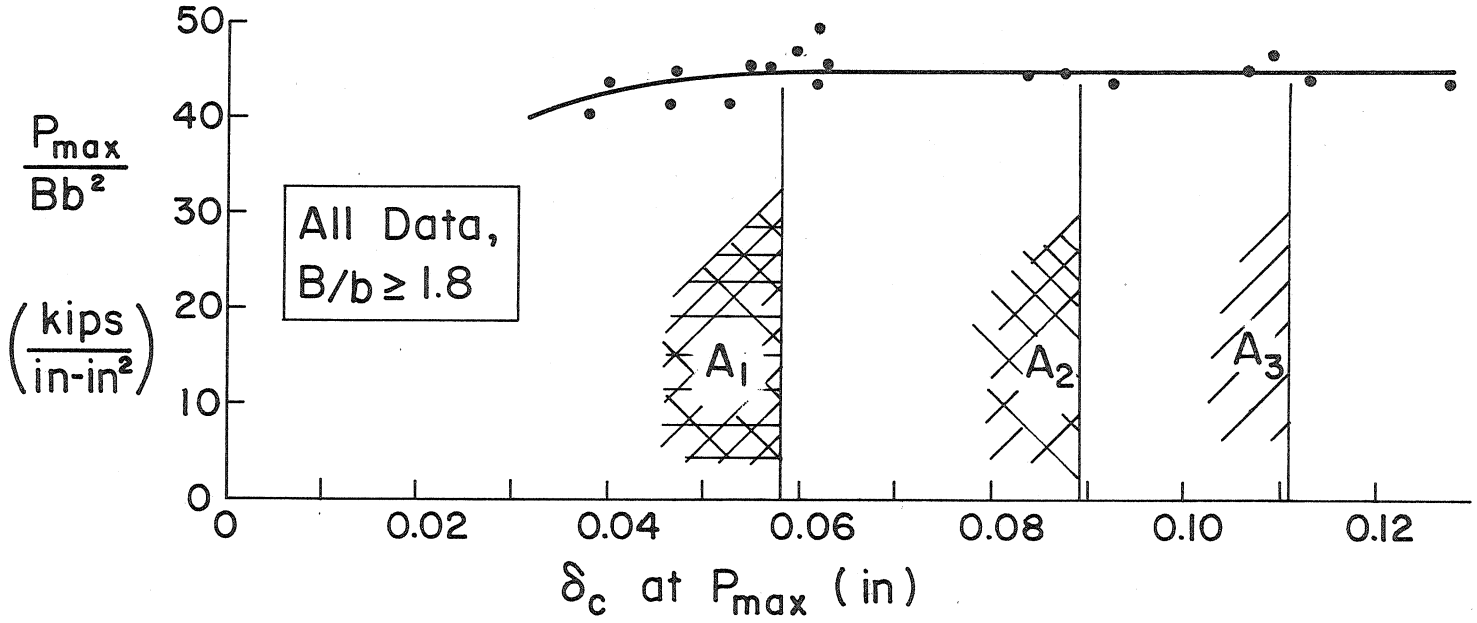


Fig. 11 Normalized Maximum Load Versus the Displacement Due to the Crack at Maximum Load ($S_y$ = 113)

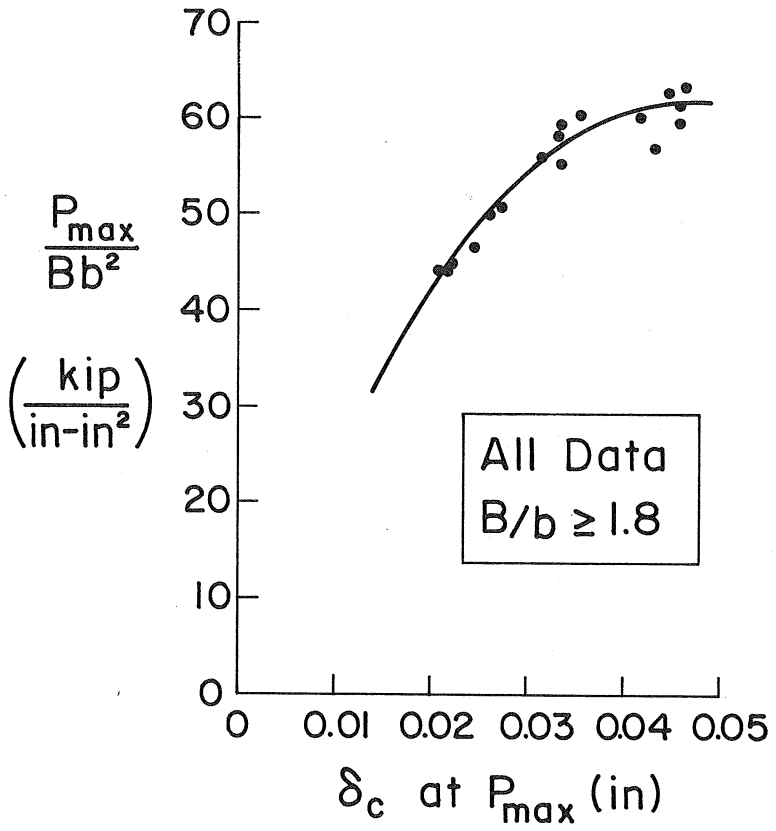


Fig. 12 Normalized Maximum Load Versus the Displacement Due to the Crack at Maximum Load ($S_y = 174$)

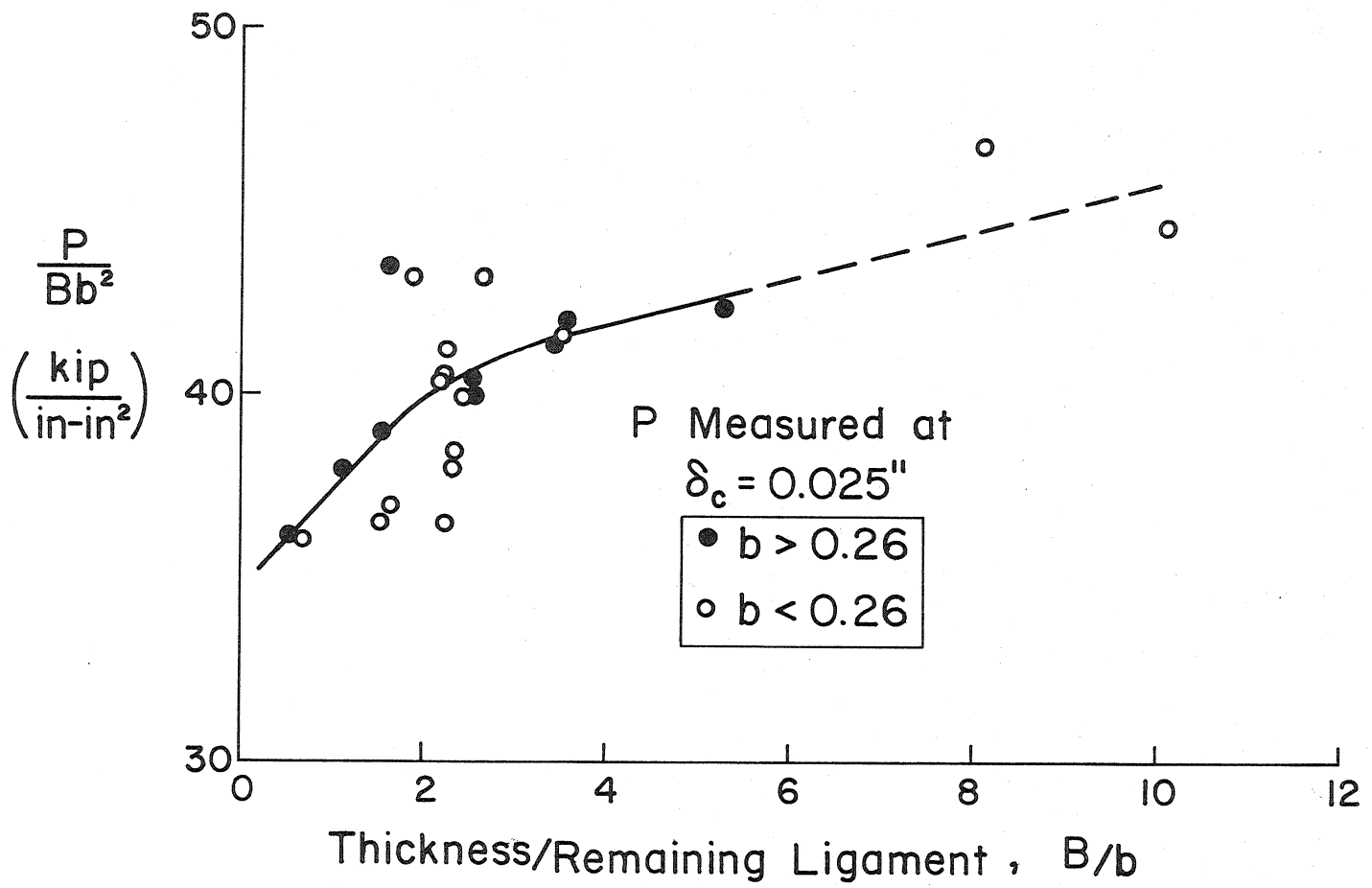


Fig. 13 Effect of Constraint on Load at a Given Displacement ($S_y$ = 113)

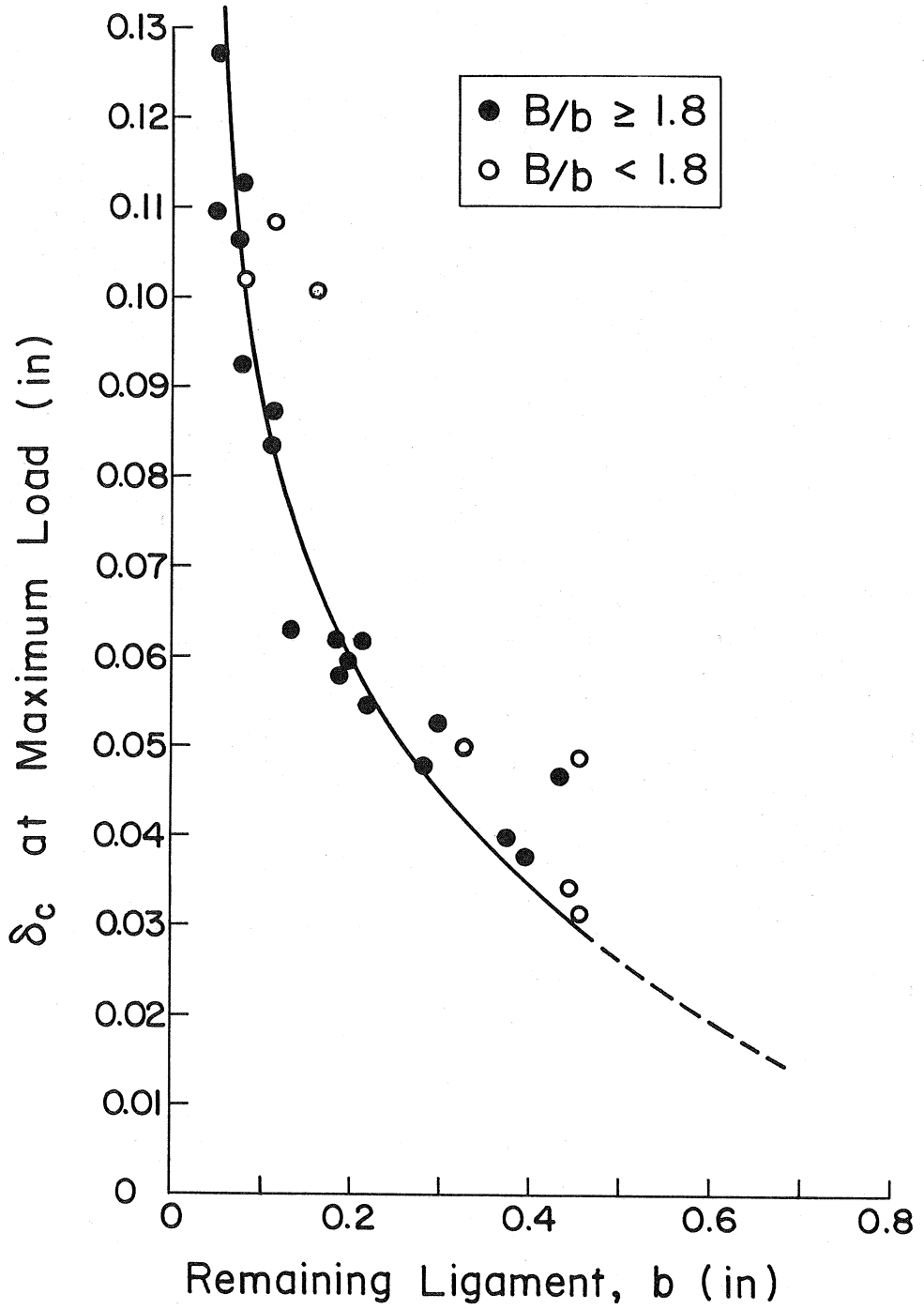


Fig. 14 Deflection Due to the Crack at $P_{max}$ for Bend Specimens ($S_y$ = 113)

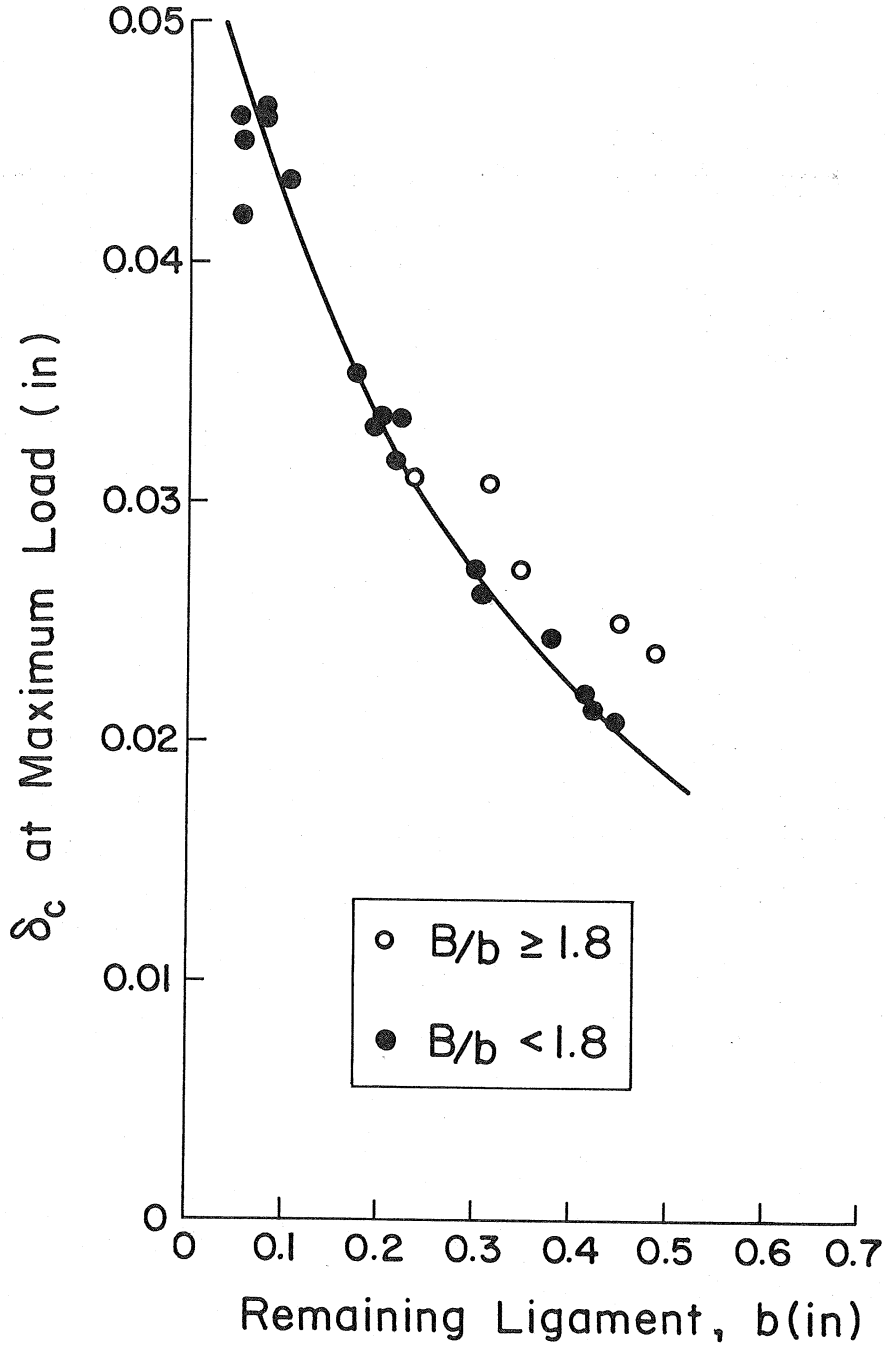


Fig. 15 Deflection Due to the Crack at $P_{max}$ for Bend Specimens ($S_y$ = 174)

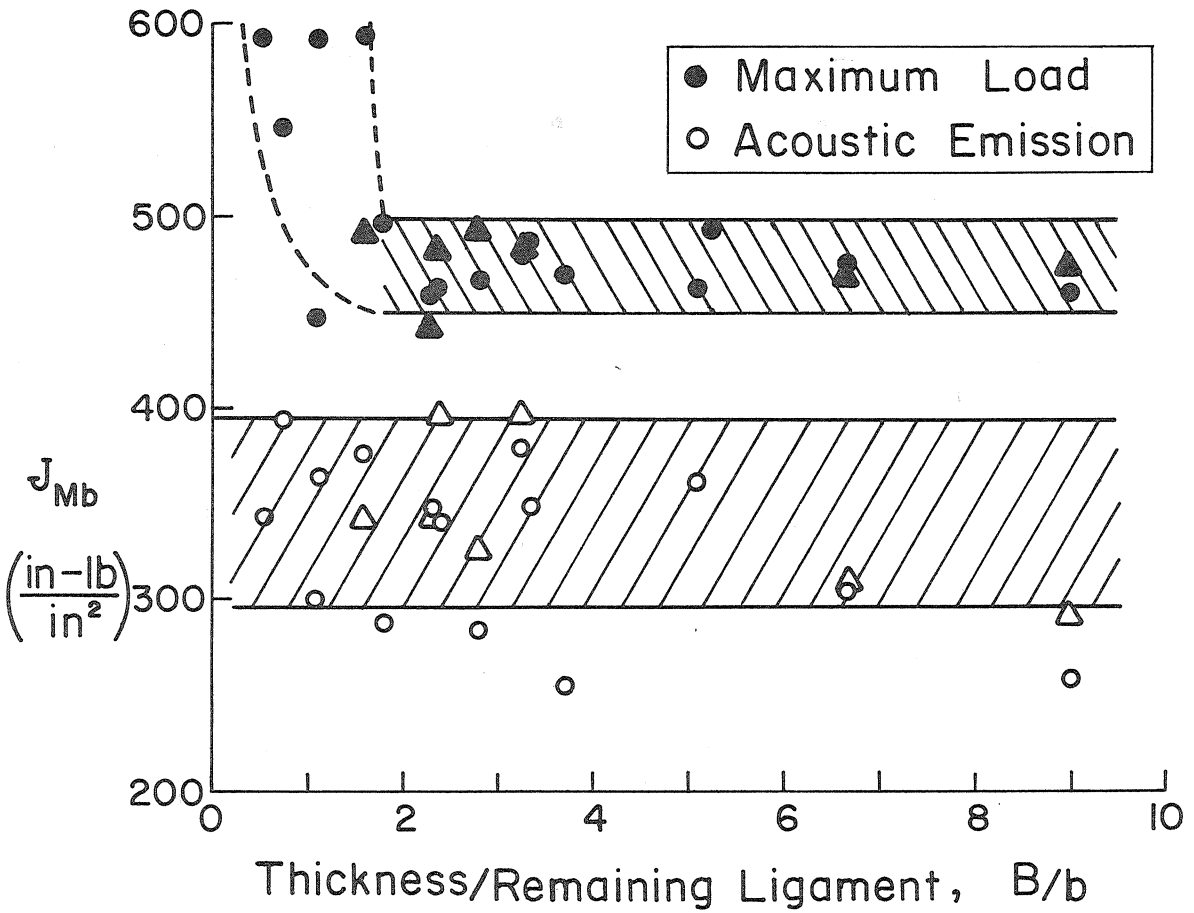


Fig. 16 Comparison Between $J_{Mb}$ Obtained at Maximum Load and Values at First Audible Acoustic Emission for Thick Bend Specimens ($S_y$=174)

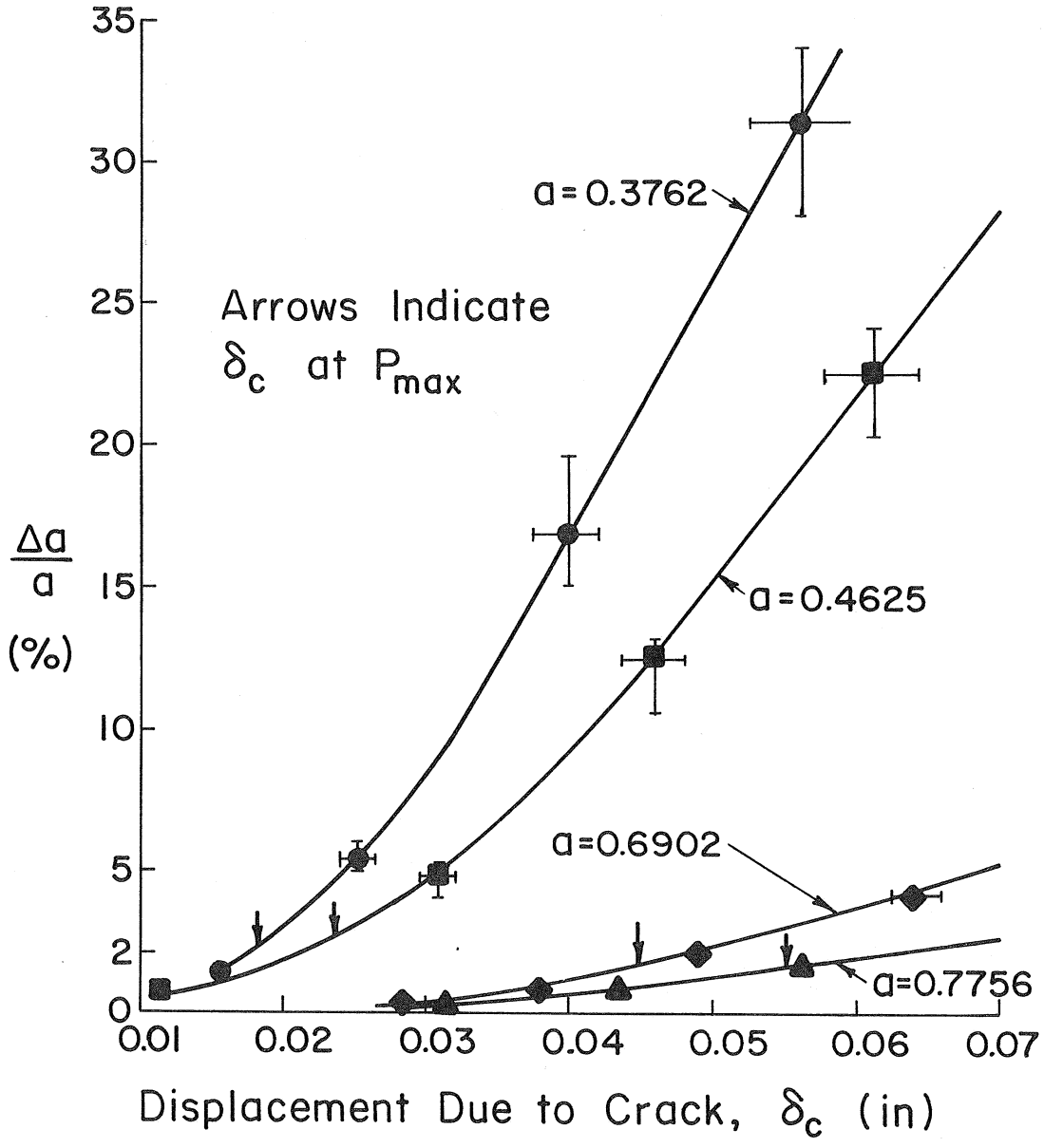


Fig. 17 Crack Growth as a Function of Displacement, $\delta_c$

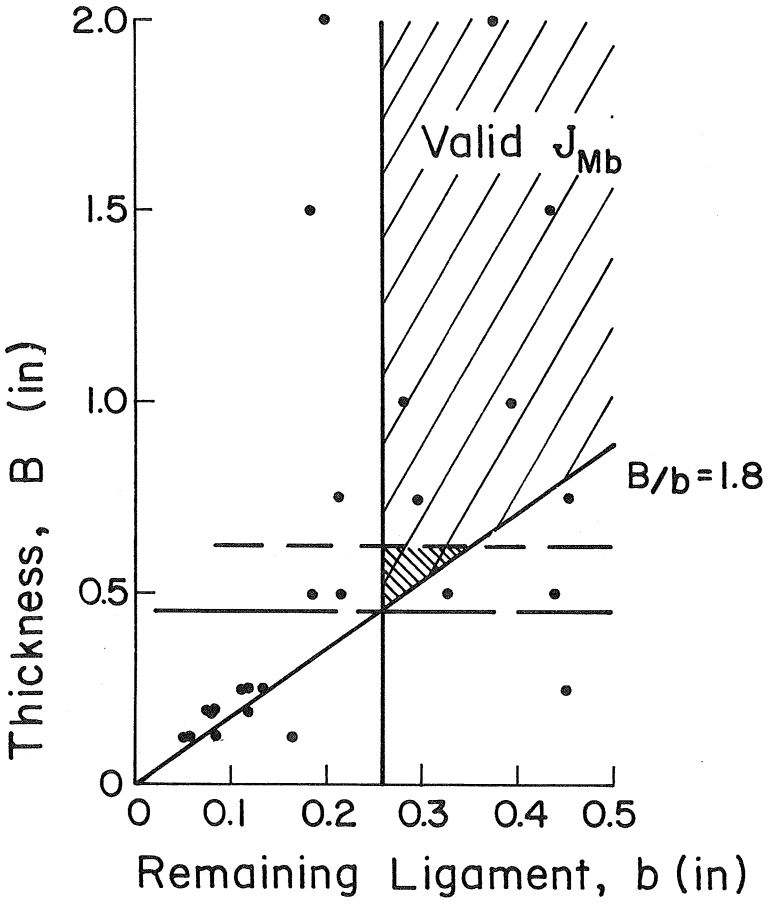


Fig. 18 Graphical Representation of the Specimen Size Restrictions for $J_{Mb}$ ($S_y$ = 113)

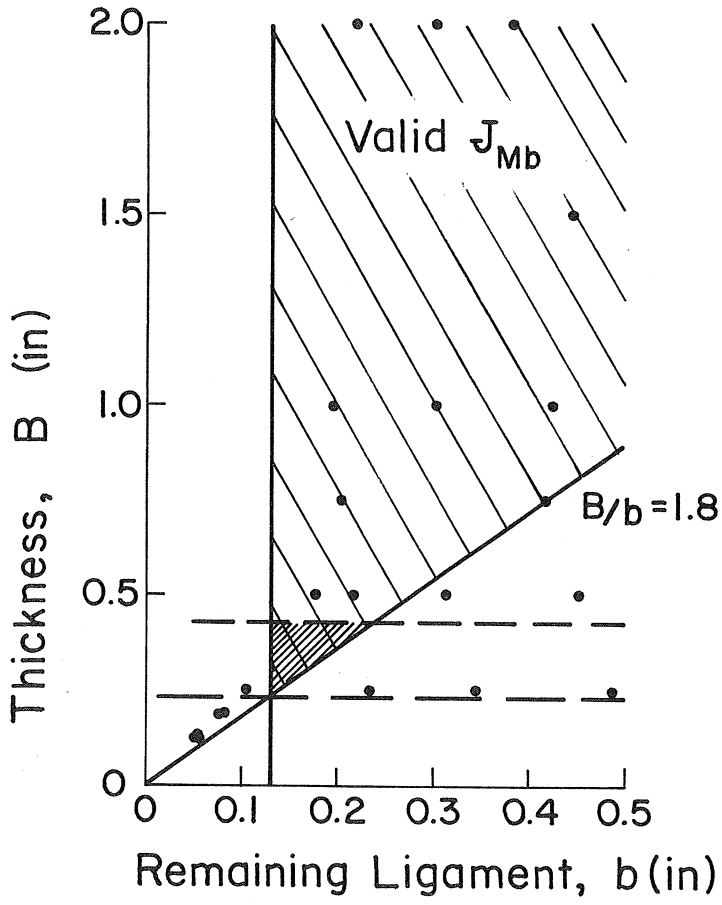


Fig. 19 Graphical Representation of the Specimen Size Restrictions for $J_{Mb}$ ($S_y$ = 174)

# APPENDIX A

## SINGLE SPECIMEN EVALUATION TECHNIQUE

The evaluation of the J-integral for several specimen geometries has produced a simple method of determining $J_c$ from a single specimen. The approach taken to determine $J_c$ in this manner is reviewed below.

For deep cracked bend specimens, the equation for the J-integral is:

$$J = \frac{2}{b} \int_0^{\theta} M d\theta_c \tag{1A}$$

where $M$ = Moment per unit thickness

$\theta_c$ = Angle of bend due to the crack

$b$ = Remaining ligament ahead of the crack

For a specimen subjected to four point loading, as illustrated below, this becomes

$$J = \frac{2}{b} \int \left(\frac{P}{2B} L\right) d\left(2 \frac{\delta_c}{L}\right) = \frac{2}{bB} \int P d\delta_c \tag{2A}$$

where $P$ = Load

$B$ = Thickness

$L$ = Span ($L' = L$)

$\delta_c$ = Vertical displacement of the load point due to the crack

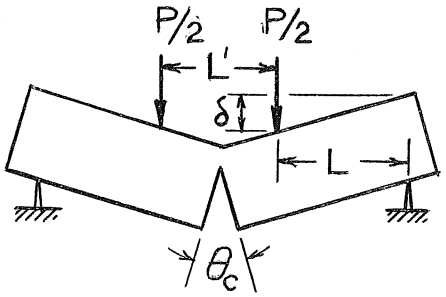

The integral in Eq. 2A can be interpreted as the area under the load-deflection curve less the elastic energy absorbed by the beam. Thus it can easily be seen that:

$$J = \frac{2}{bB} \left[\text{Area under the Load-}\delta_{Tot}\text{ curve} - \text{Area under the Load-}\delta_u\text{ curve}\right]$$

where $\delta_T$ = Total deflection

$\delta_u$ = Elastic deflection of the beam (this does not include the elastic deflection due to the crack)

For the test procedure used, the displacements measured also included the deflection of the contact rollers. Since this displacement is measured both times, it is automatically subtracted out. A pictoral description of the calculation is shown in Fig. 1A.

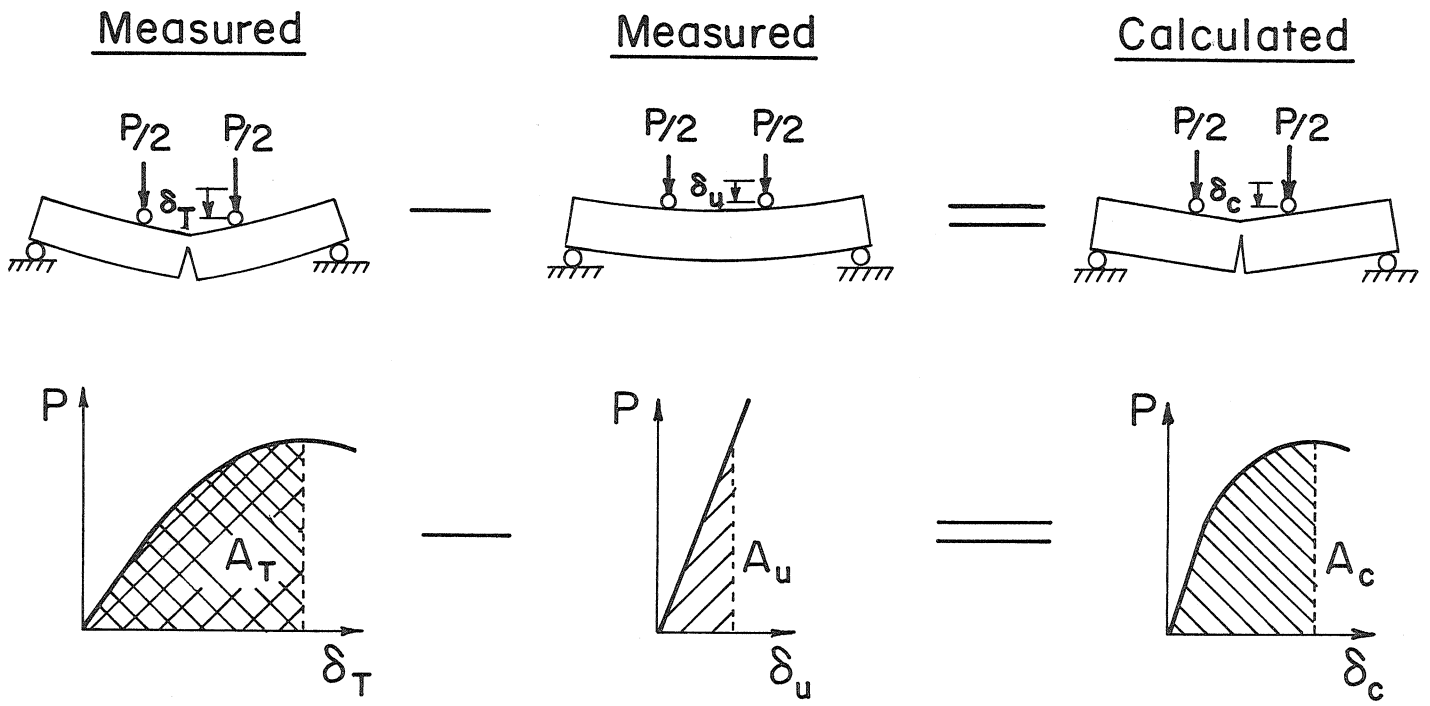


$$J = \frac{2}{bB}\int_0^{\delta_{c\,max}} P\, d\delta_c = \frac{2}{bB} A_c$$

$$J = \frac{2}{bB}\left[A_T - A_u\right]$$

Fig. I-A Pictoral Description of $J_{Mb}$ Evaluation Using Single Specimen Formula

## APPENDIX B

## GRAPHICAL EVALUATION TECHNIQUE

The procedure used to evaluate $J_{Mb}$ through the use of expression (2) is outlined below:

1. Load-displacement curves were obtained from several specimens with neighboring crack lengths and identical thicknesses, B.
2. The area under these curves (potential energy, U) was measured as a function of displacement for each specimen.
3. The potential energy was then plotted against crack length, a, for different values of displacement.
4. From the slopes of these plots, the change in the potential energy with respect to crack length was measured as a function of displacement, for a given crack length.
5. Thus the J-integral, $J = - 1/B \, \Delta U/\Delta \partial$ was easily determined as a function of displacement for each specimen.
6. With the critical value of displacement, from maximum load or acoustic emission, the critical value of the J-integral, was found.

$J_{Mb}$ for the higher strength material was determined in this manner using three groups of specimens, each group having identical thickness specimens. Tabulations of the potential energy versus crack length and J versus displacement for each group are given in the following tables. These relationships are graphically shown in Figs. 1-B through 3-B.

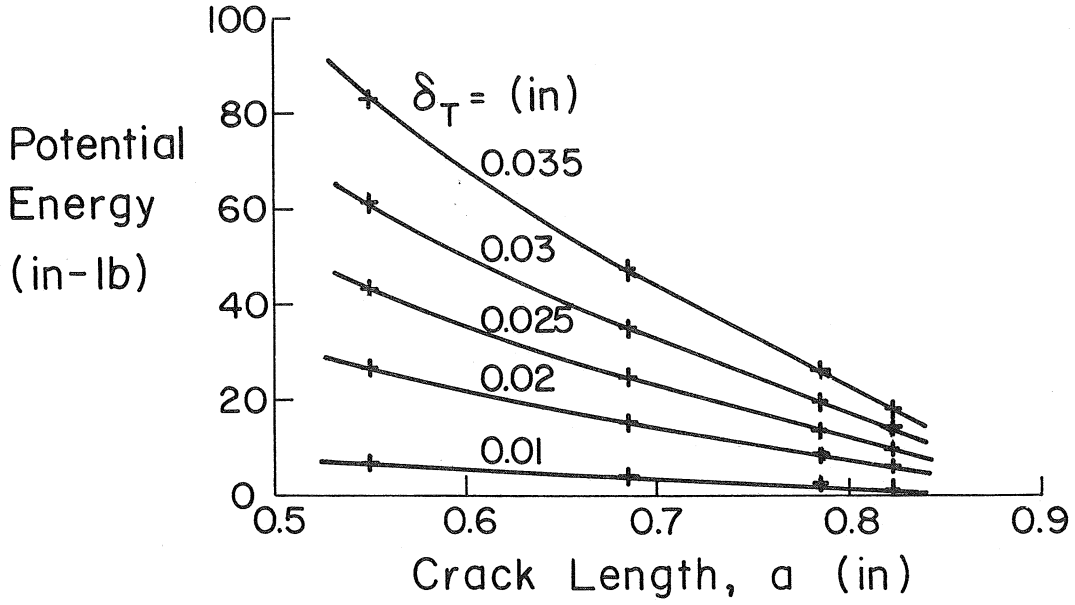


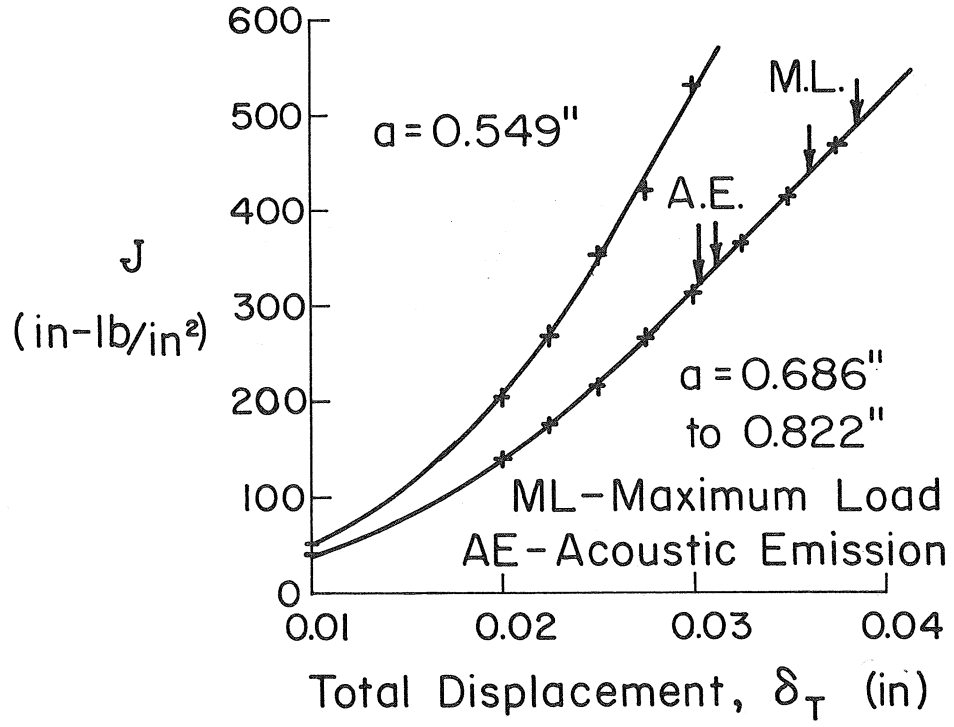


Fig. I-B Graphical Determination of J for Bend Specimens 0.5 in. Thick

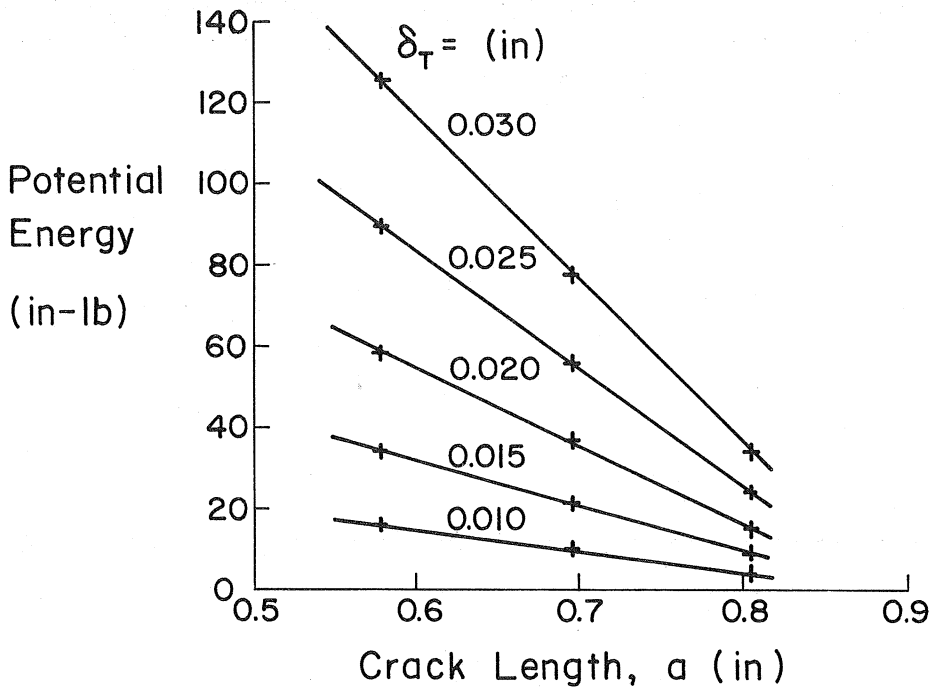


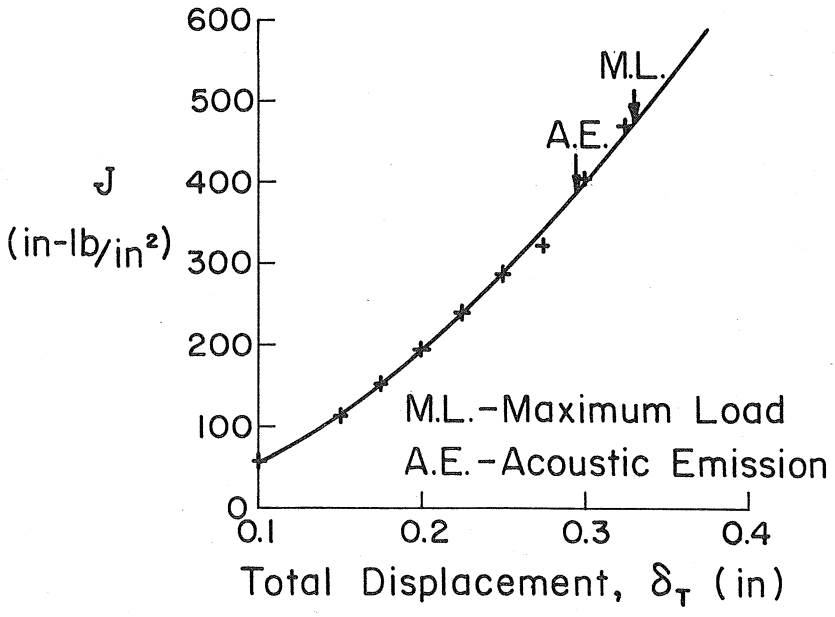


Fig. 2-B Graphical Determination of J for Bend Specimens 1.0 in. Thick

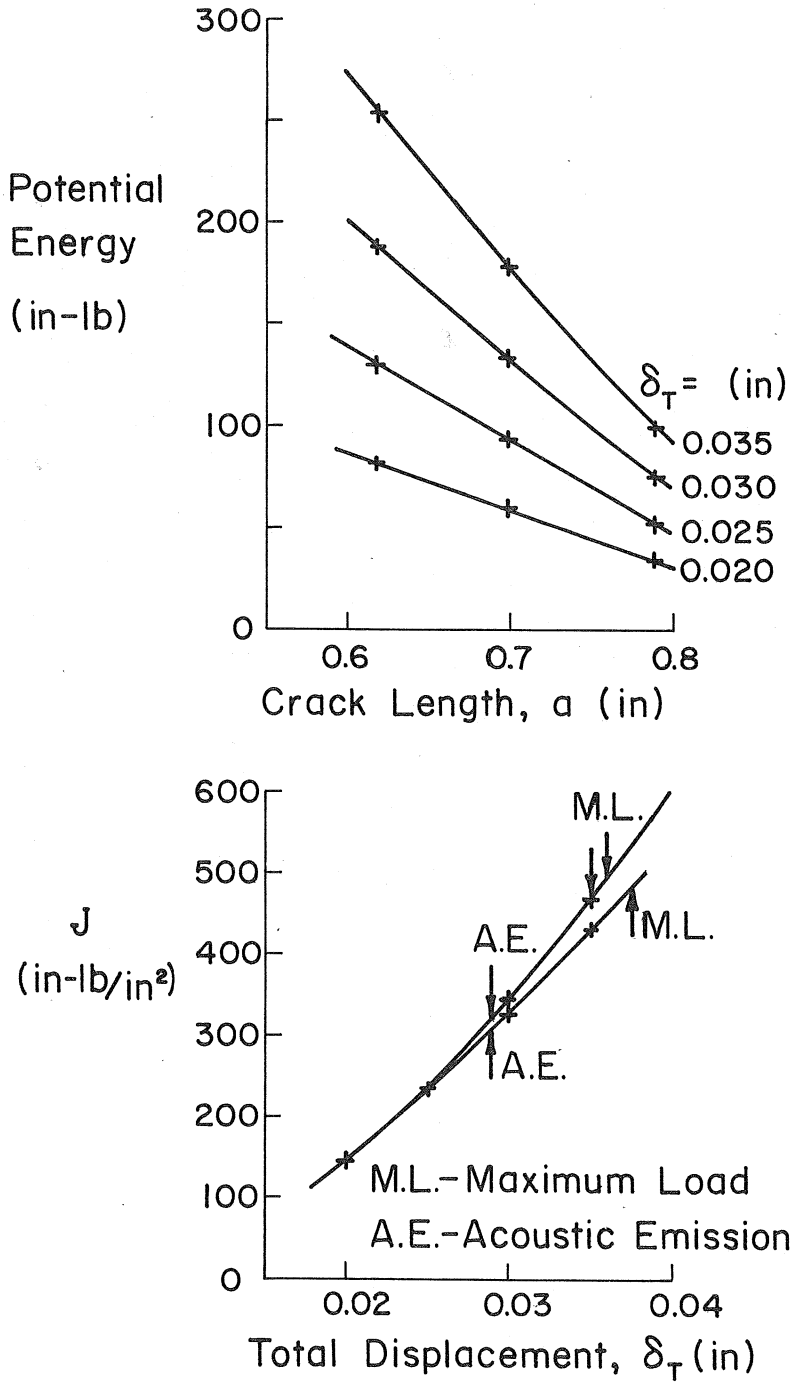


Fig. 3-B Graphical Determination of J for Bend Specimens 2.0 in. Thick

TABLE 1-B DATA FOR DETERMINING $J_{Mb}$ USING THE COMPLIANCE METHOD

Specimen Type: Bend Specimen
Thickness: 0.5 inch
$S_y$ = 174 ksi

| Specimen No. | Crack Length, a (in) | Potential Energy (in-lb) for Given Displacements, $\delta_T$ | | | | | | | | |
|---|---|---|---|---|---|---|---|---|---|---|
| | | 0.01 | 0.02 | 0.0225 | 0.025 | 0.0275 | 0.03 | 0.0325 | 0.035 | 0.0375 |
| B5 | .785 | 2.25 | 9.0 | 11.36 | 13.97 | 16.77 | 19.77 | 22.91 | 26.22 | -- |
| B6 | .822 | 1.56 | 6.28 | 7.94 | 9.78 | 11.81 | 14.01 | 16.31 | 18.66 | 21.07 |
| B7 | .686 | 4.13 | 15.74 | 20.03 | 24.76 | 29.94 | 35.46 | 41.20 | 47.03 | 52.92 |
| B8 | .549 | 6.75 | 27.0 | 34.88 | 43.03 | 51.97 | 61.68 | 72.05 | 82.97 | 94.20 |

| Specimen No. | $\delta_{c\ max}$ (in) | | J-integral for Given Displacements (in-lb/in$^2$) | | | | | | | | |
|---|---|---|---|---|---|---|---|---|---|---|---|
| | M. L. | A. E. | 0.01 | 0.02 | 0.0225 | 0.025 | 0.0275 | 0.03 | 0.0325 | 0.035 | 0.0375 |
| B5 | .03625 | .03125 | 39.4 | 139 | 177 | 218 | 266 | 314 | 364 | 416 | 470 |
| B6 | .03875 | .0305 | 39.4 | 139 | 177 | 218 | 266 | 314 | 364 | 416 | 470 |
| B7 | .03875 | .03125 | 39.4 | 139 | 177 | 218 | 266 | 314 | 364 | 416 | 470 |
| B8 | .0390 | -- | 48.8 | 303 | 269 | 353 | 421 | 531 | 631 | 754 | -- |

TABLE 2-B DATA FOR DETERMINING $J_{Mb}$ USING THE COMPLIANCE METHOD

Specimen Type: Bend Specimen
Thickness: 1.0 inch
$S_y$ = 174 ksi

| Specimen No. | Crack Length, a (in) | Potential Energy (in-lb) for Given Displacements, $\delta_T$ | | | | | | | | | |
|---|---|---|---|---|---|---|---|---|---|---|---|
| | | 0.010 | 0.015 | 0.0175 | 0.020 | 0.0225 | 0.025 | 0.0275 | 0.030 | 0.0325 | 0.035 |
| B15 | 0.804 | 3.92 | 8.75 | 11.9 | 15.5 | 19.5 | 24.06 | 28.93 | 34.1 | 39.52 | 45.08 |
| B16 | 0.696 | 10.5 | 21.67 | 28.8 | 36.83 | 45.83 | 55.75 | 62.25 | 77.48 | 88.97 | -- |
| B17 | 0.578 | 16.13 | 34.13 | 45.63 | 58.72 | 73.32 | 89.43 | 106.9 | 125.8 | 145.3 | -- |

| Specimen No. | $\delta_{c\ max}$ (in) | | J-integral for Given Displacements (in-lb/in$^2$) | | | | | | | | | |
|---|---|---|---|---|---|---|---|---|---|---|---|---|
| | M.L. | A.E. | 0.010 | 0.015 | 0.0175 | 0.020 | 0.0225 | 0.025 | 0.0275 | 0.030 | 0.0325 | 0.035 |
| B15 | .037 | .0325 | 57.4 | 112 | 151 | 189 | 240 | 290 | 345 | 405 | 471 | -- |
| B16 | .033 | .0295 | 57.4 | 112 | 151 | 189 | 240 | 290 | 345 | 405 | 471 | -- |
| B17 | .033 | .0295 | 57.4 | 112 | 151 | 189 | 240 | 290 | 345 | 405 | 471 | -- |

TABLE 3-B DATA FOR DETERMINING $J_{Mb}$ USING THE COMPLIANCE METHOD

Specimen Type: Bend Specimen
Thickness: 2.0 inch
$S_y$ = 174 ksi

| Specimen No. | Crack Length, a (in) | Potential Energy (in-lb) for Given Displacements 0.020 | 0.025 | 0.030 | 0.035 |
|---|---|---|---|---|---|
| B25 | 0.788 | 34.0 | 52.8 | 75.03 | 99.55 |
| B26 | 0.699 | 60.0 | 93.5 | 133.4 | 178.2 |
| B27 | 0.619 | 81.7 | 130.0 | 188.1 | 253.6 |

| Specimen No. | $\delta_T$ max M.L. | $\delta_T$ max A.E. | J-integral for Given Displacements (in-lb/in$^2$) 0.020 | 0.025 | 0.030 | 0.035 |
|---|---|---|---|---|---|---|
| B25 | .0375 | .0280 | 143 | 233 | 325 | 431 |
| B26 | .035 | .0285 | 143 | 233 | 344 | 468 |
| B27 | .036 | -- | 143 | 233 | 344 | 468 |

# APPENDIX C

## LOAD-DISPLACEMENT DATA

The following pages contain the load-displacement data obtained for all bend specimens. The solid curves indicate the load as a function of total displacement for the cracked specimen. The dashed line is the elastic response of the uncracked specimen. For the thin bars, the total displacement is considered as the displacement due to the crack. These smaller specimens failed at such small loads that the tare weight was considered as contributing to the response, which is indicated as the dotted portion of the curve. At the end of this data, photographs of the fracture surfaces are shown.

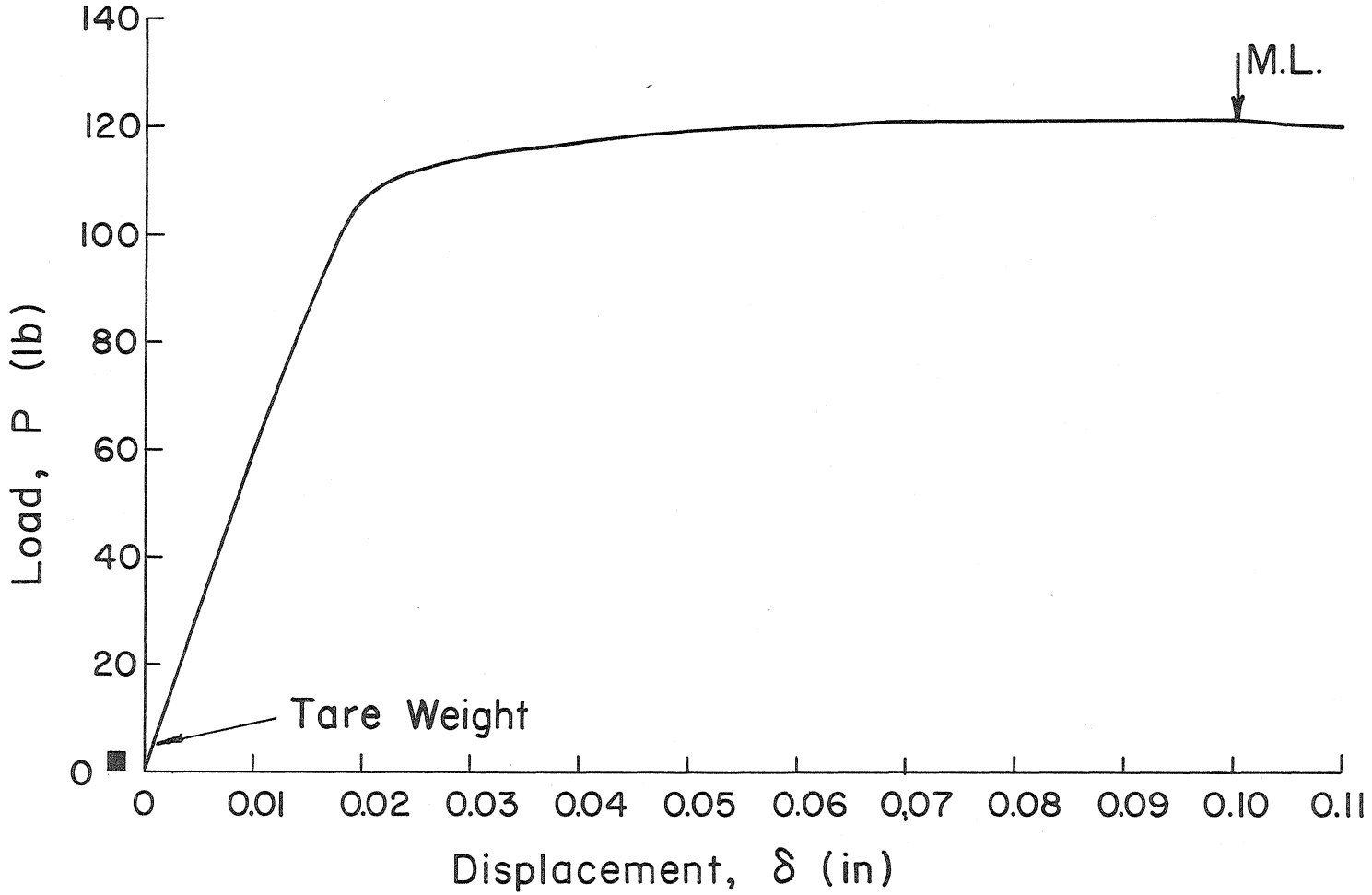


Fig. I-C P-δ Curve, A50 ($S_y$ = 113, B = 0.125, b = 0.1643)

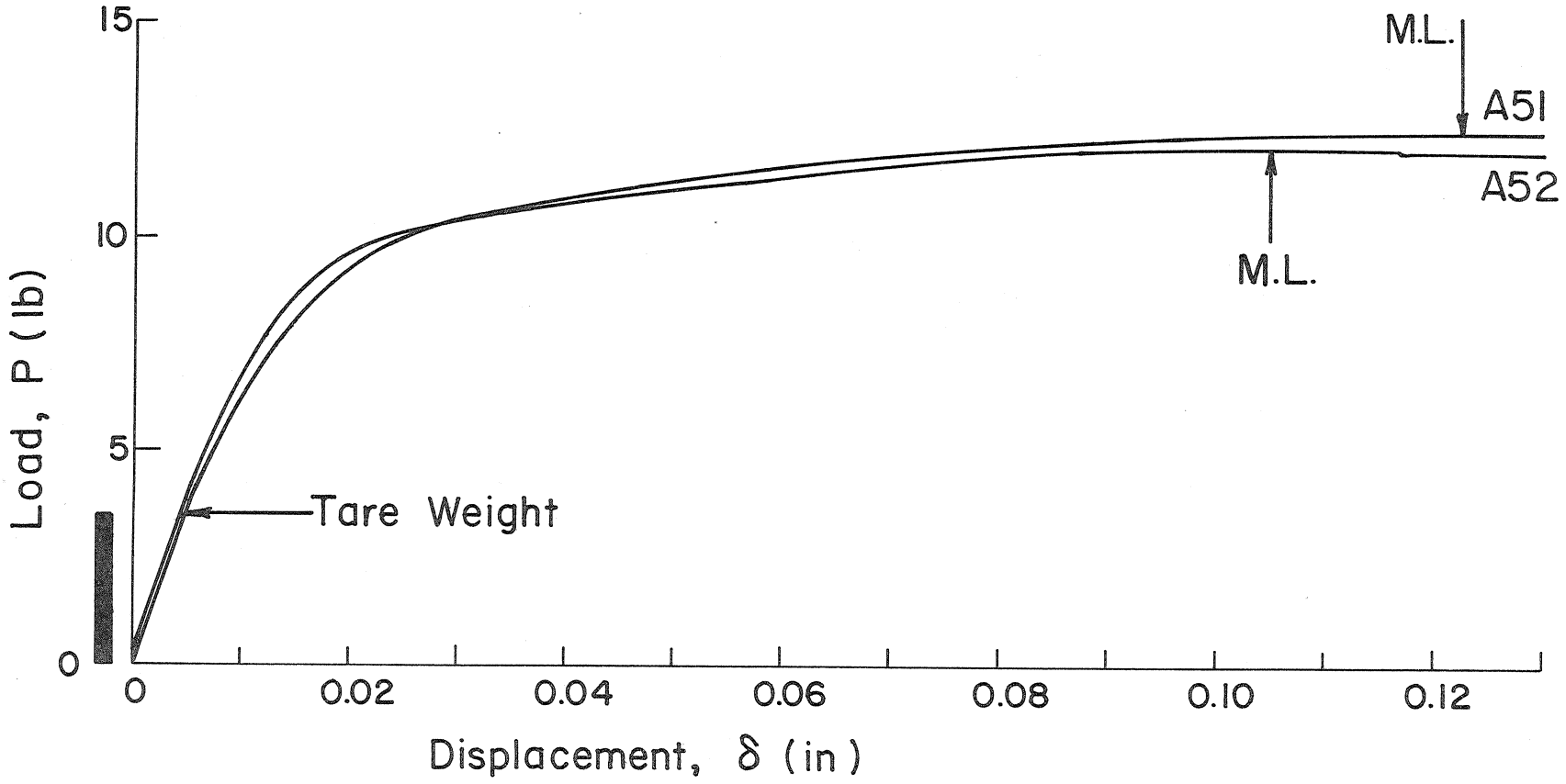


Fig. 2-C P-δ Curve, A51 ($S_y$=113, B=0.125, b=0.0536) and A52 ($S_y$=113, B=0.125, b=0.0515)

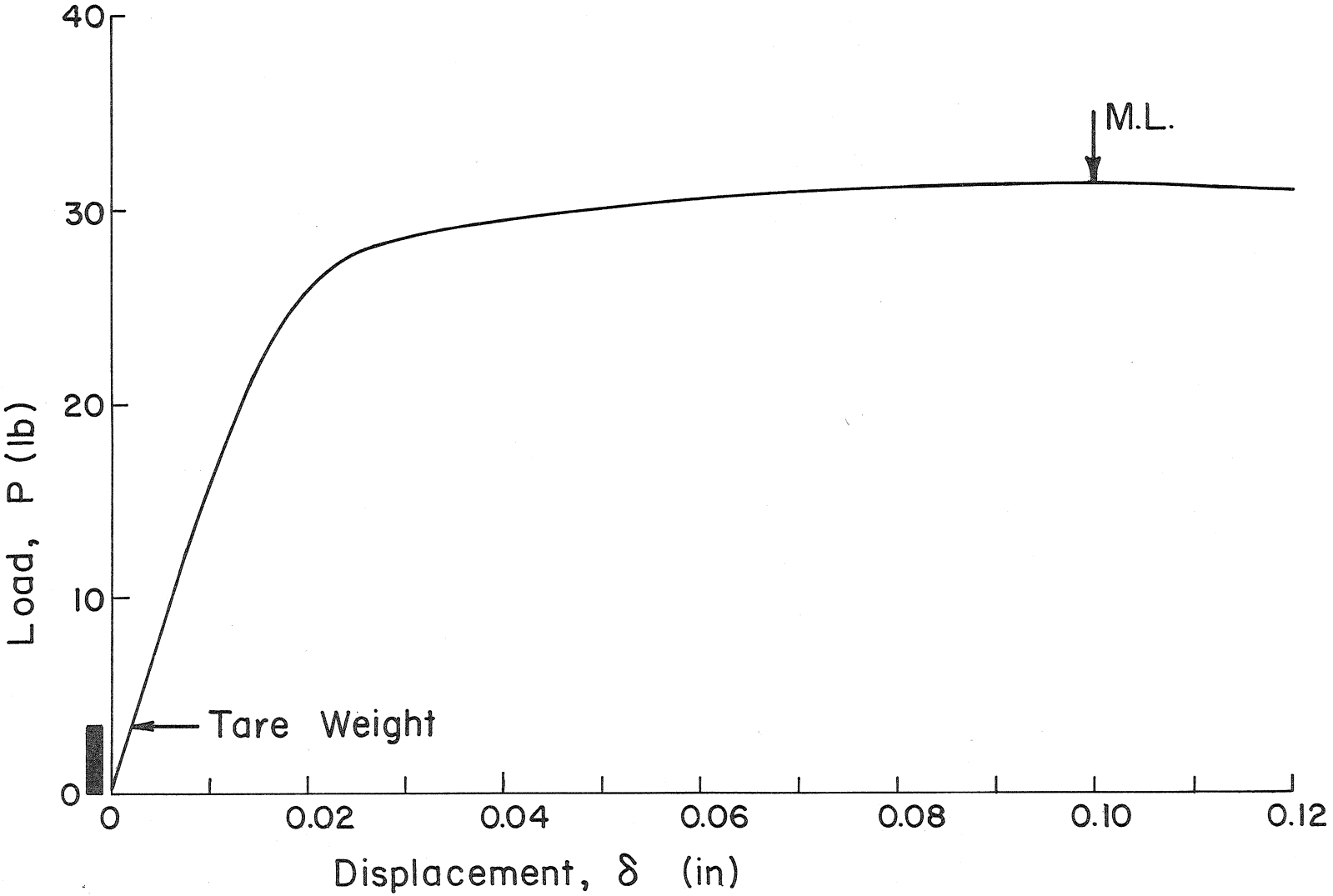


Fig. 3-C P-δ Curve, A53 ($S_y$ = 113, B=0.125, b=0.0815)

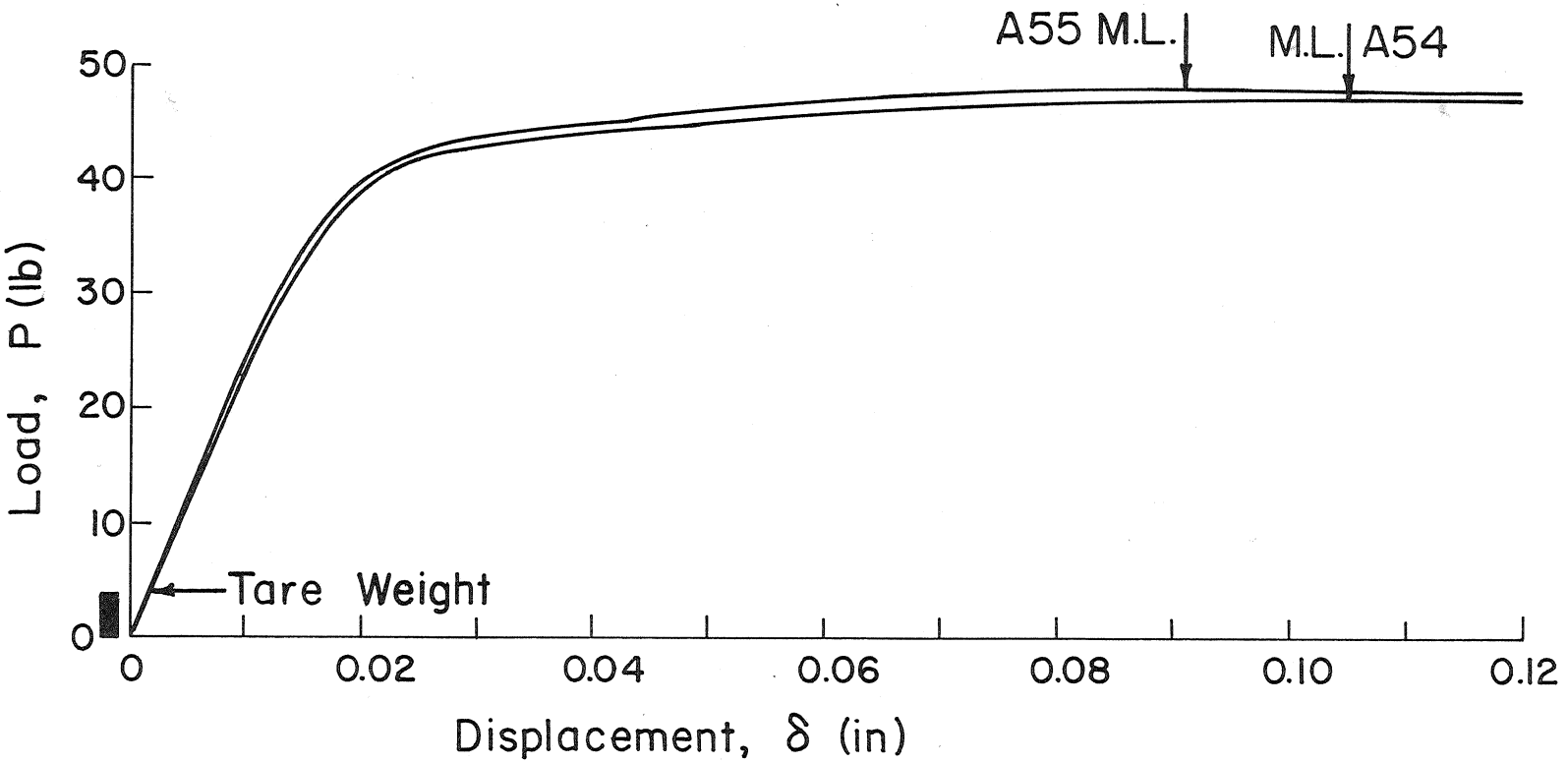


Fig. 4-C P-δ Curve, A54 ($S_y$ = 113, B = 0.1875, b = 0.0772) and A55 ($S_y$ = 113, B = 0.1875, b = 0.0793)

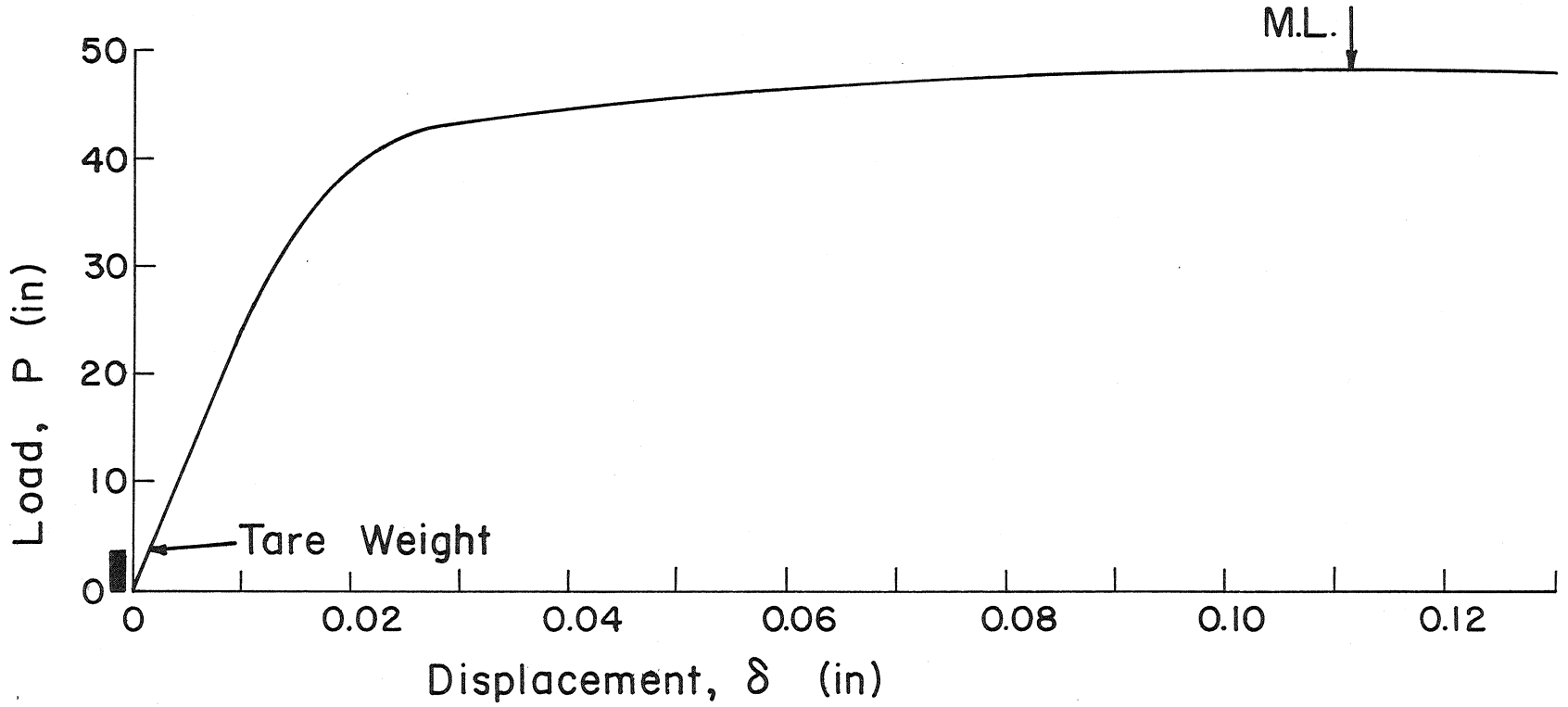


Fig. 5-C P-δ Curve, A56 ($S_y$ = 113, B= 0.1875, b= 0.0792)

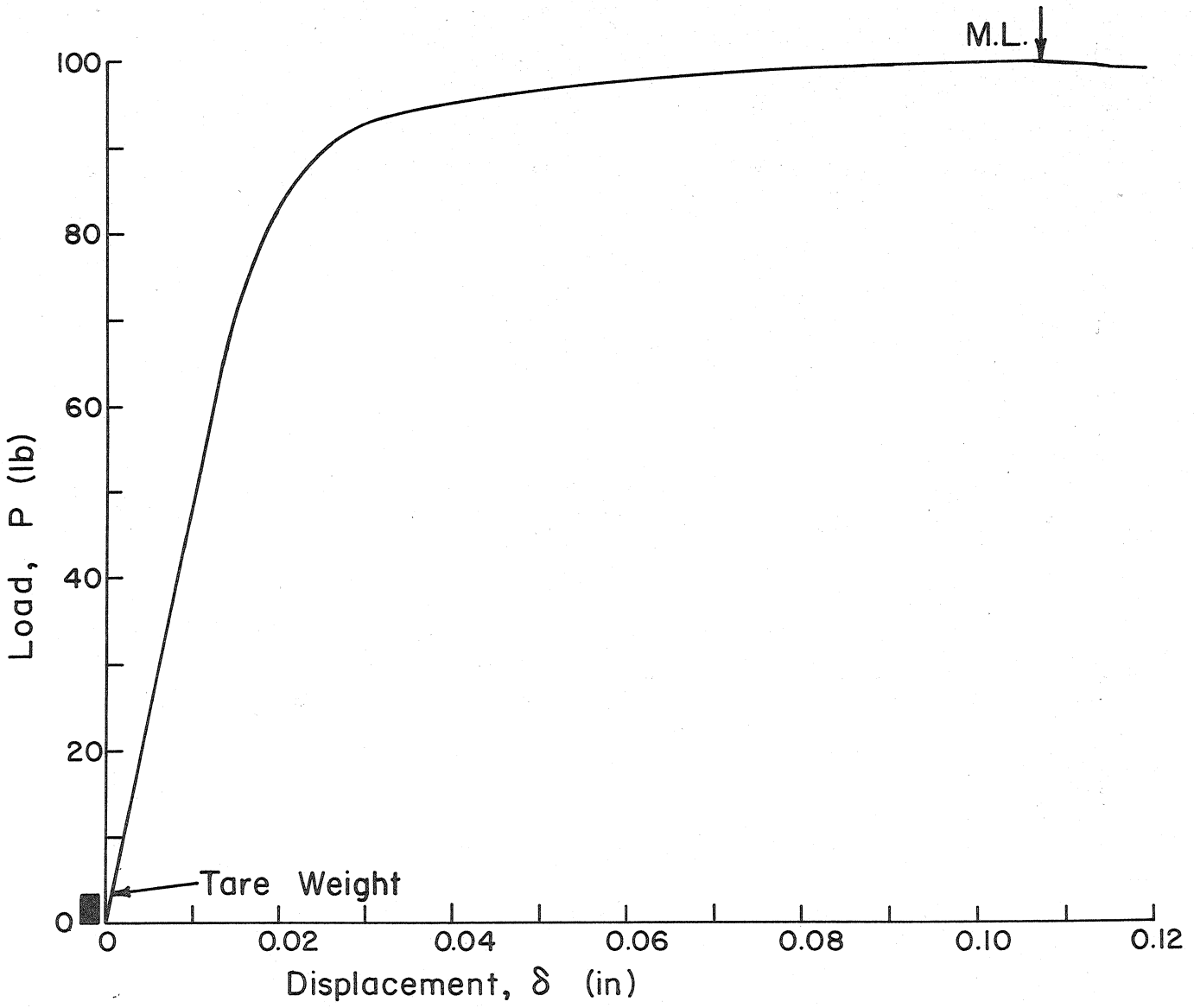


Fig. 6-C P-δ Curve, A57 ( $S_y$ = 113, B= 0.1875, b= 0.1150)

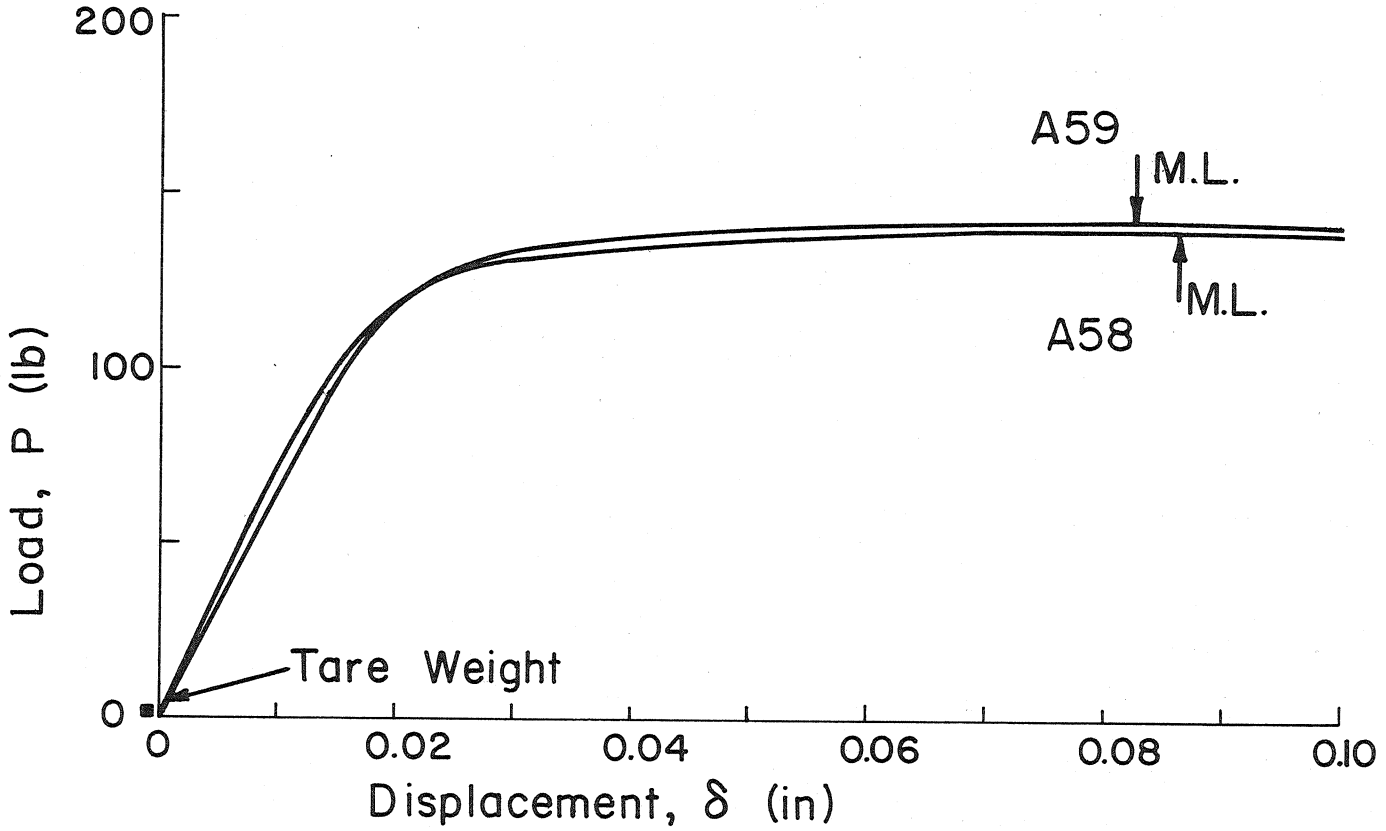


Fig. 7-C P-δ Curve, A58 ($S_y$ = 113, B= 0.250, b= 0.1131) and A59 ($S_y$ = 113, B= 0.250, b= 0.1145)

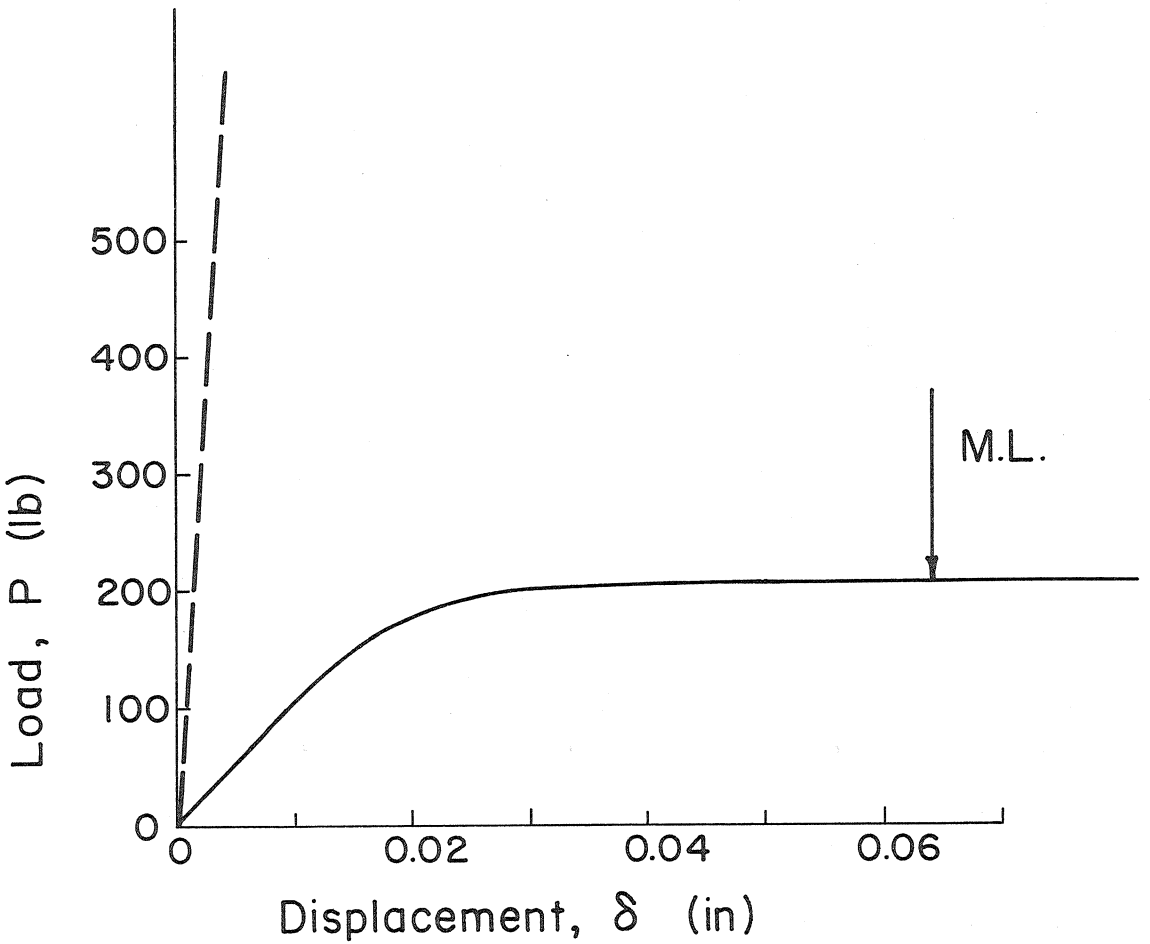


Fig. 8-C P-δ Curve, Al ($S_y$ = 113, B = 0.250, b = 0.135)

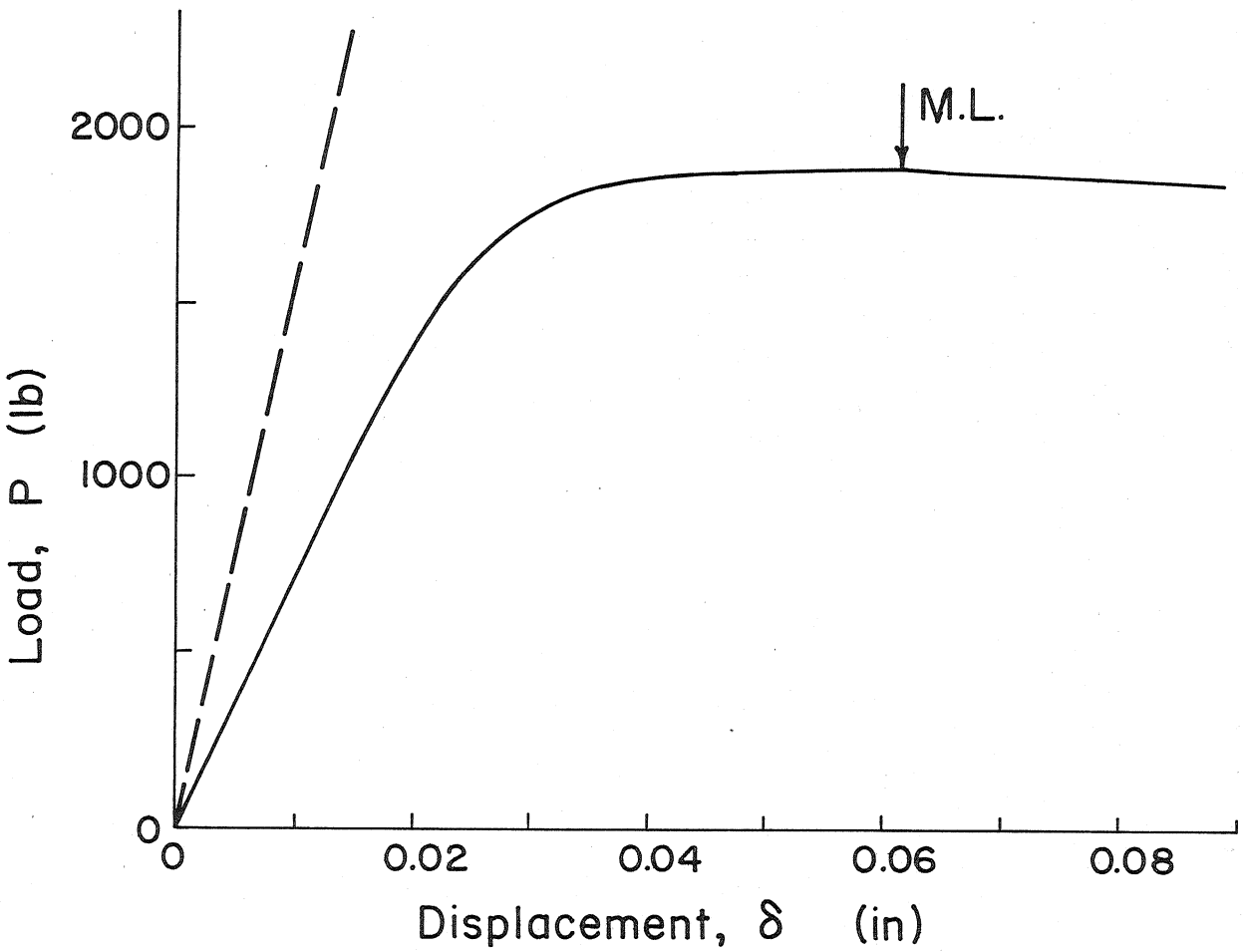


Fig. 9-C P-δ Curve, A2($S_y$ = 113, B= 0.250, b= 0.452)

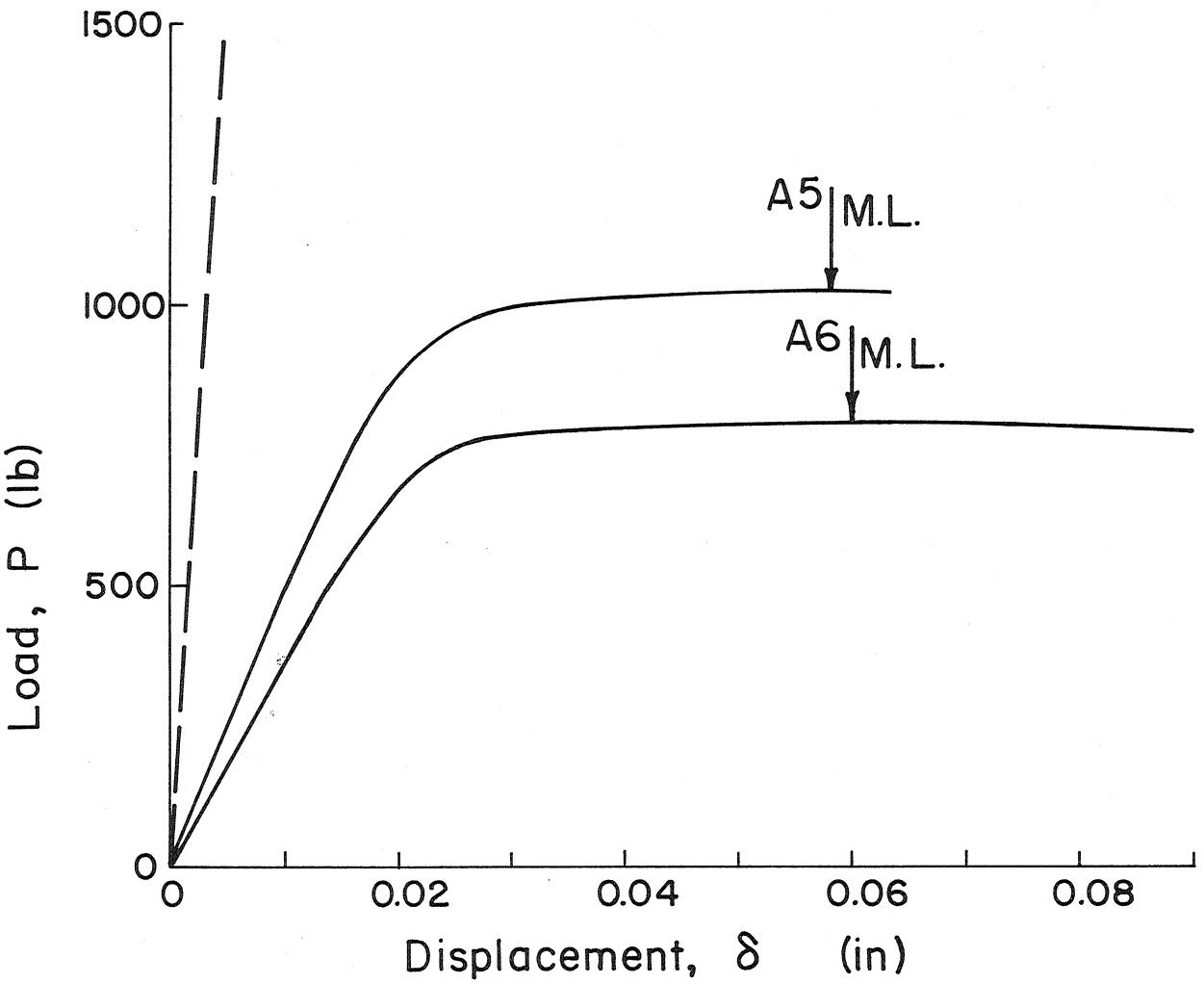


Fig. 10-C P-δ Curve, A5 ($S_y$= 113, B= 0.50, b= 0.219) and A6 ($S_y$= 113, B= 0.50, b= 0.187)

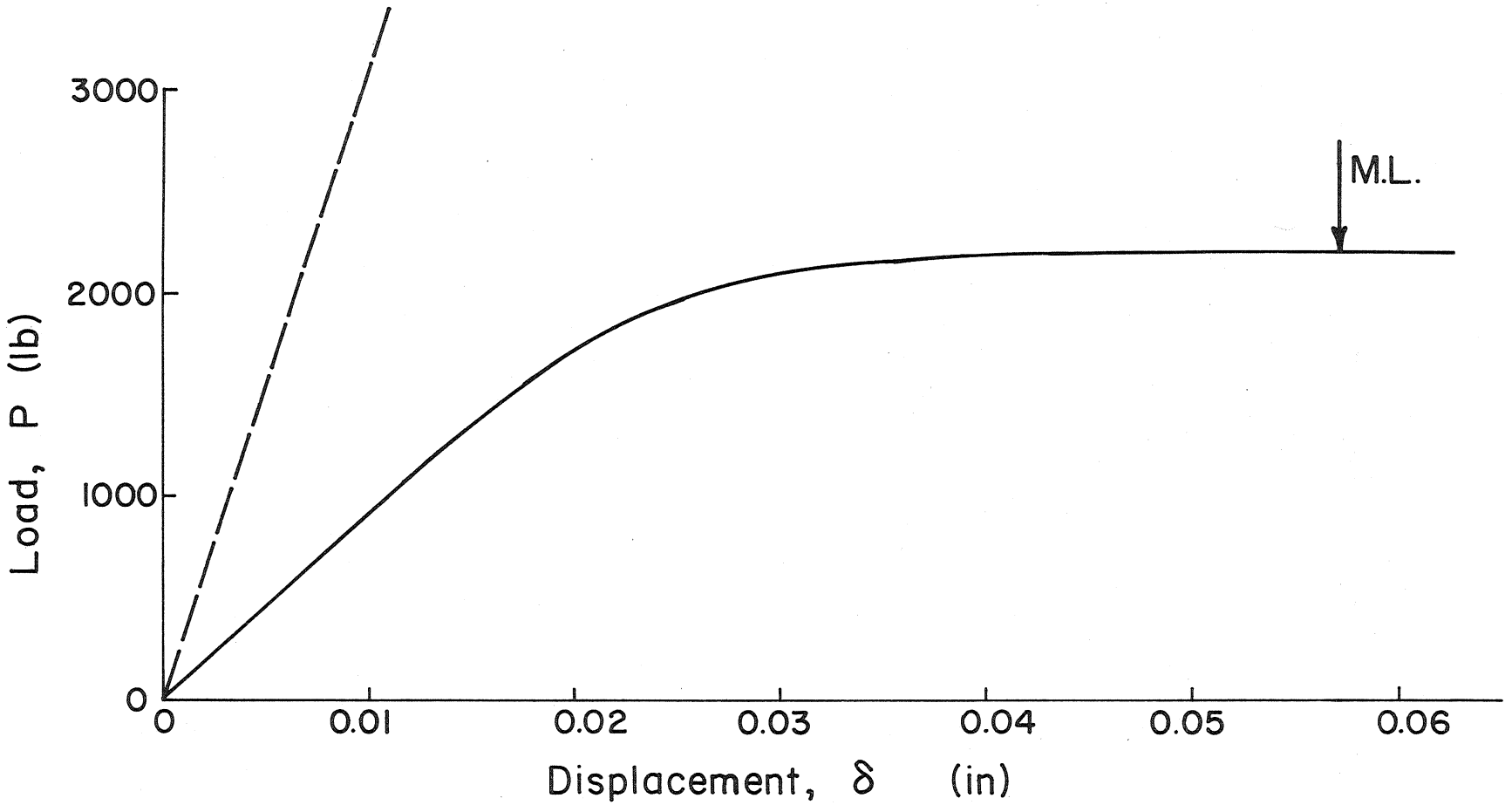


Fig. II-C P-δ Curve, A7 ($S_y$ = 113, B = 0.50, b = 0.330)

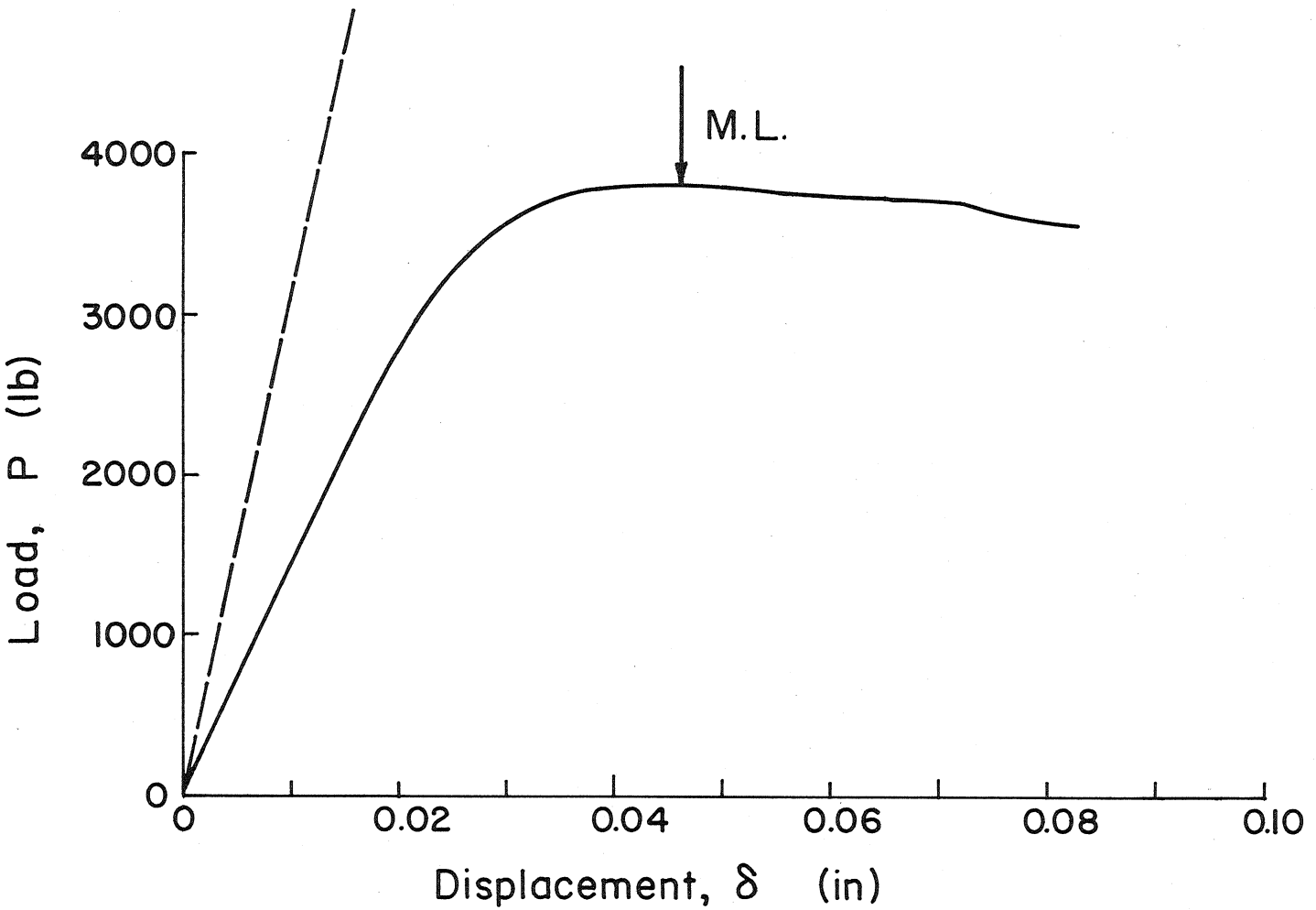


Fig. 12-C P-δ Curve, A8($S_y$= 113, B= 0.50, b= 0.444)

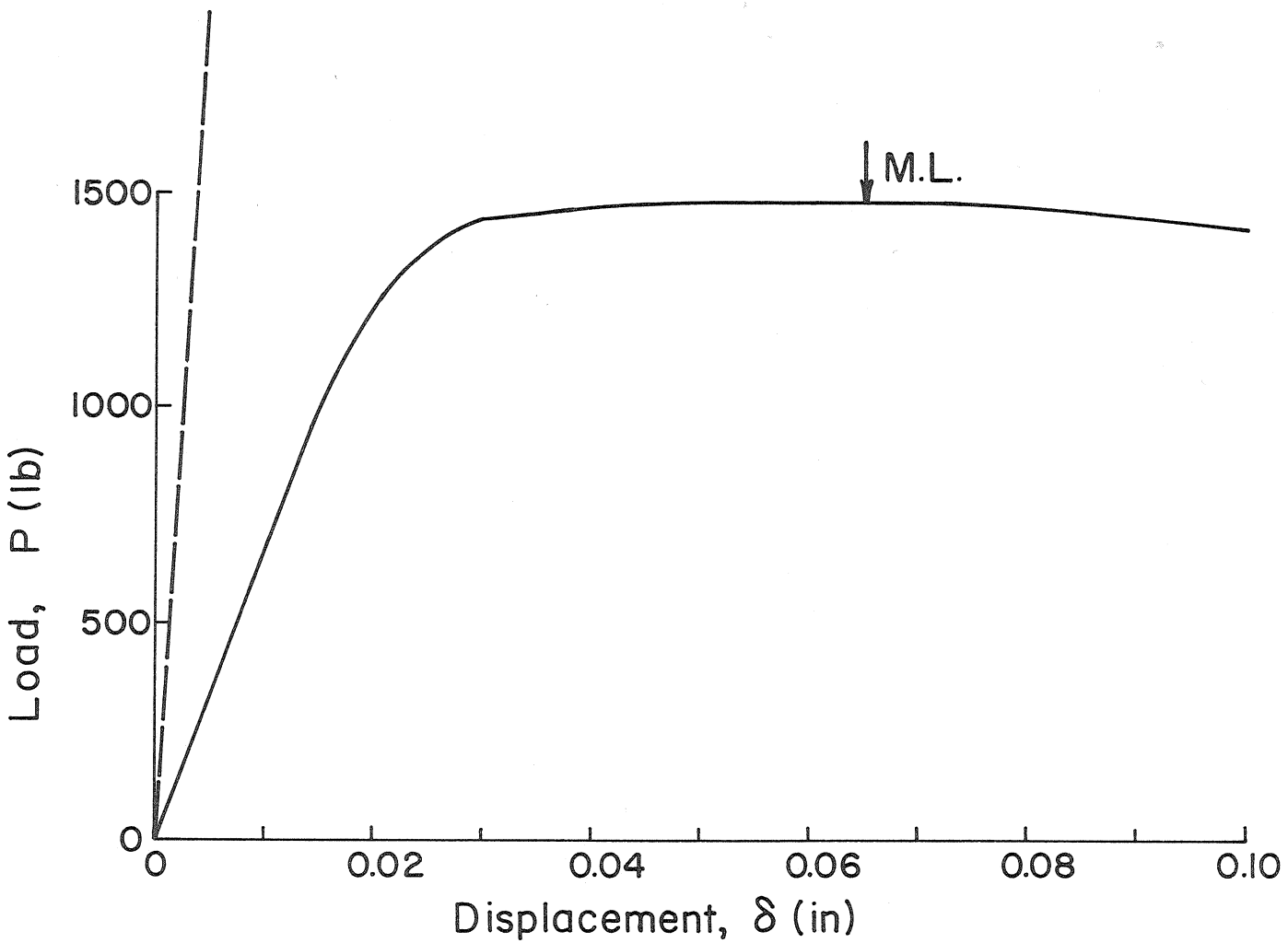


Fig. 13-C P-δ Curve, A10 ($S_y$ = 113, B= 0.75, b= 0.213)

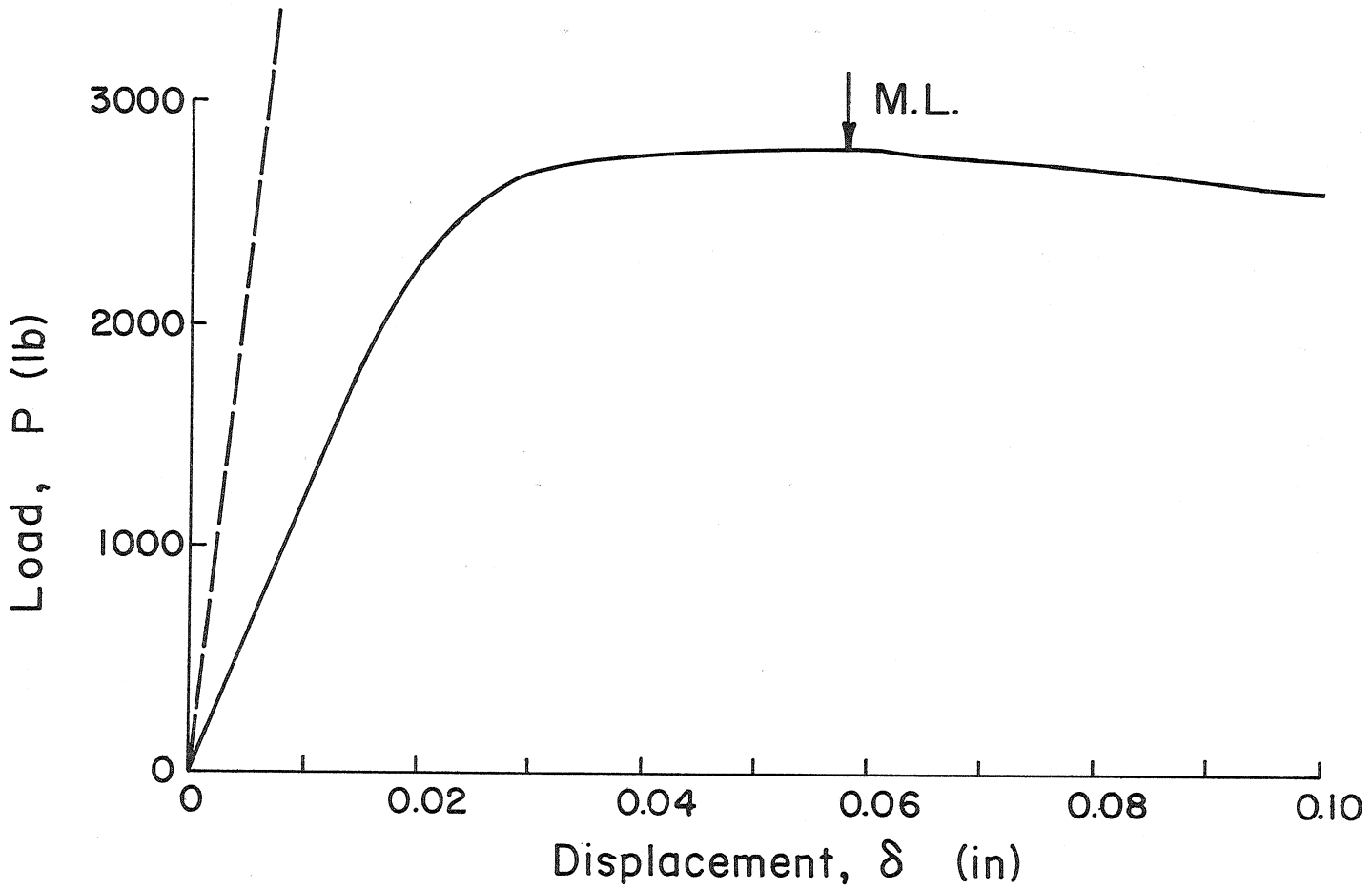


Fig. 14-C P-δ Curve, All ($S_y$ = 113, B = 0.75, b = 0.298)

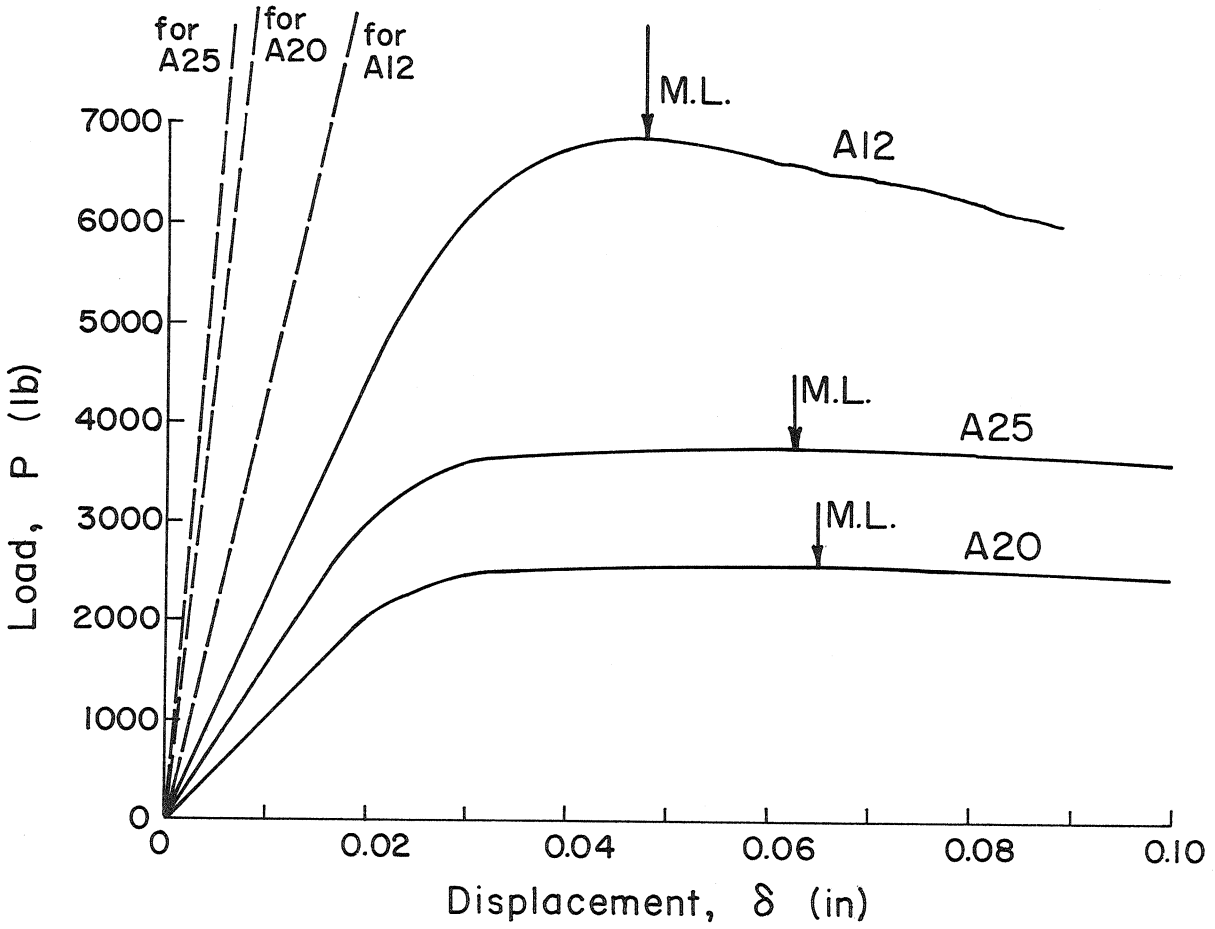


Fig. 15-C P-δ Curve, A12 ($S_y$=113, B=0.75, b=0.454), A20 ($S_y$=113, B=1.5, b=0.185), and A25 ($S_y$=113, B=2.0, b=0.198)

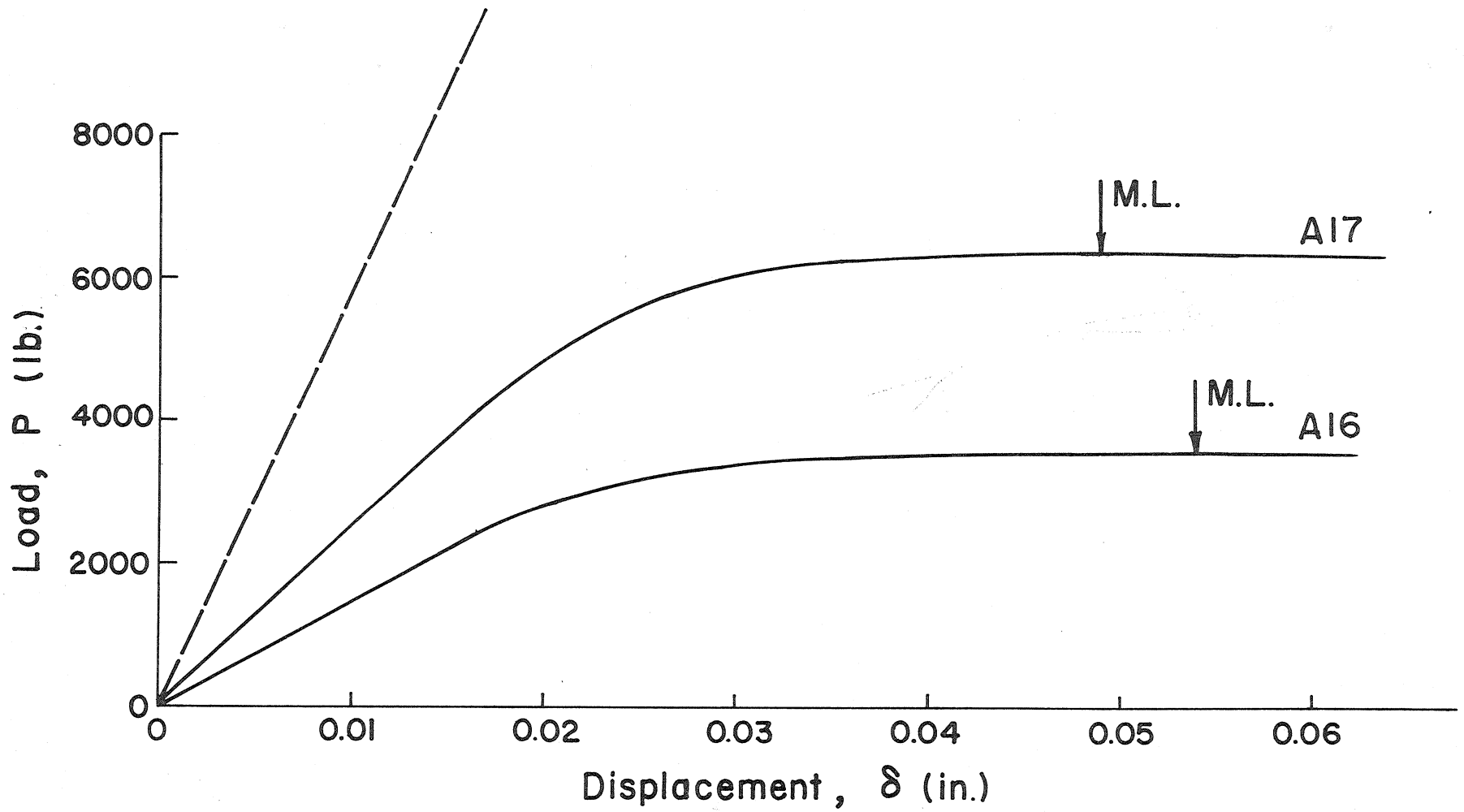


Fig. 16–C P–δ Curve, A16 ($S_y$ = 113, B = 1.0, b = 0.282), and A17 ($S_y$ = 113, B = 1.0, b = 0.393)

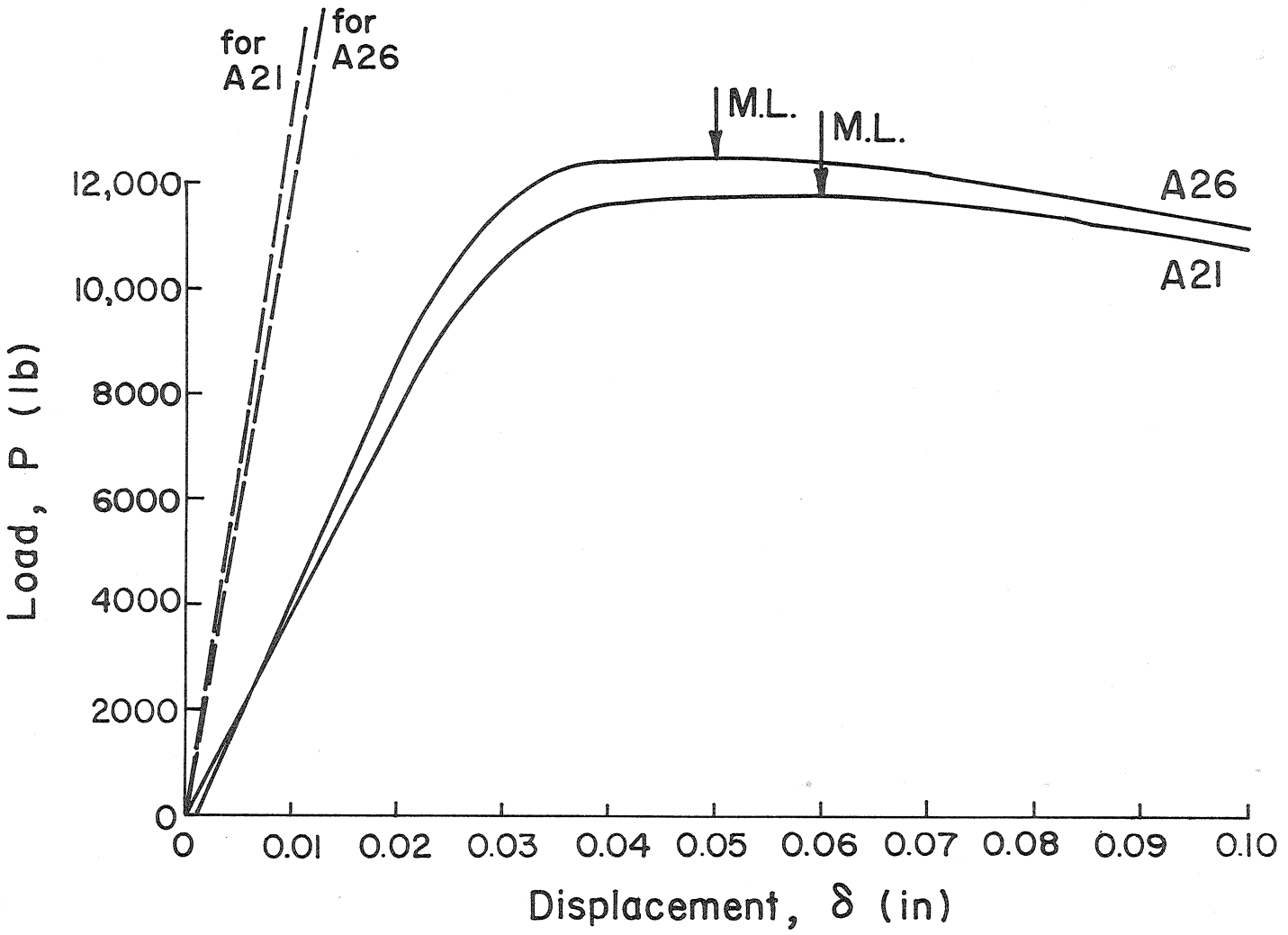


Fig. 17-C P-δ Curve, A21 ( $S_y$ = 113, B = 1.5, b = 0.432 ), and A26 ( $S_y$ = 113, B = 2.0, b = 0.378 )

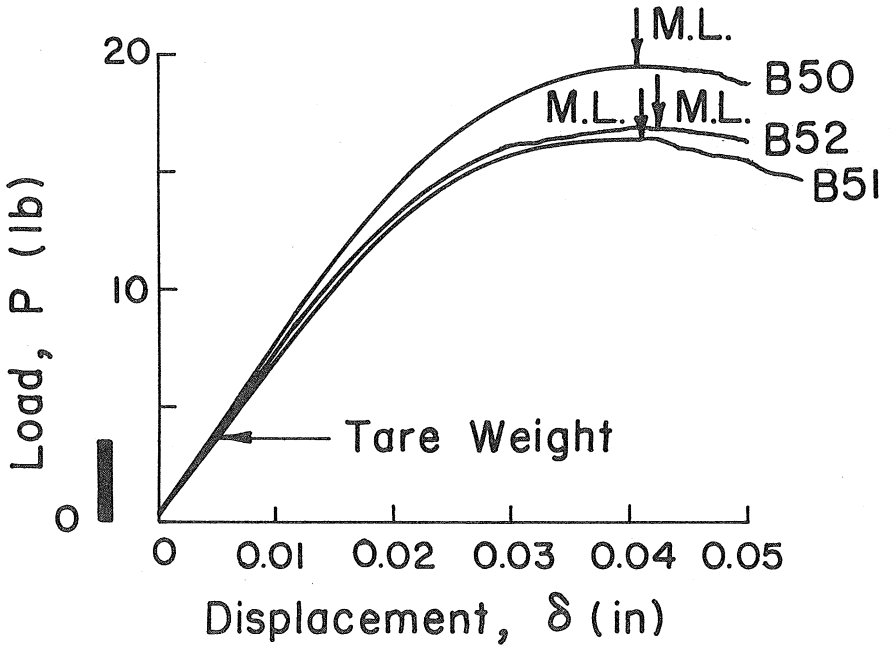


Fig. 18-C P-δ Curve, B50 ($S_y$ = 174 B = 0.125, b = 0.0548), B51 ($S_y$ = 174 B = 0.125, b = 0.0511), and B52 ($S_y$ = 174, B = 0.125, b = 0.053)

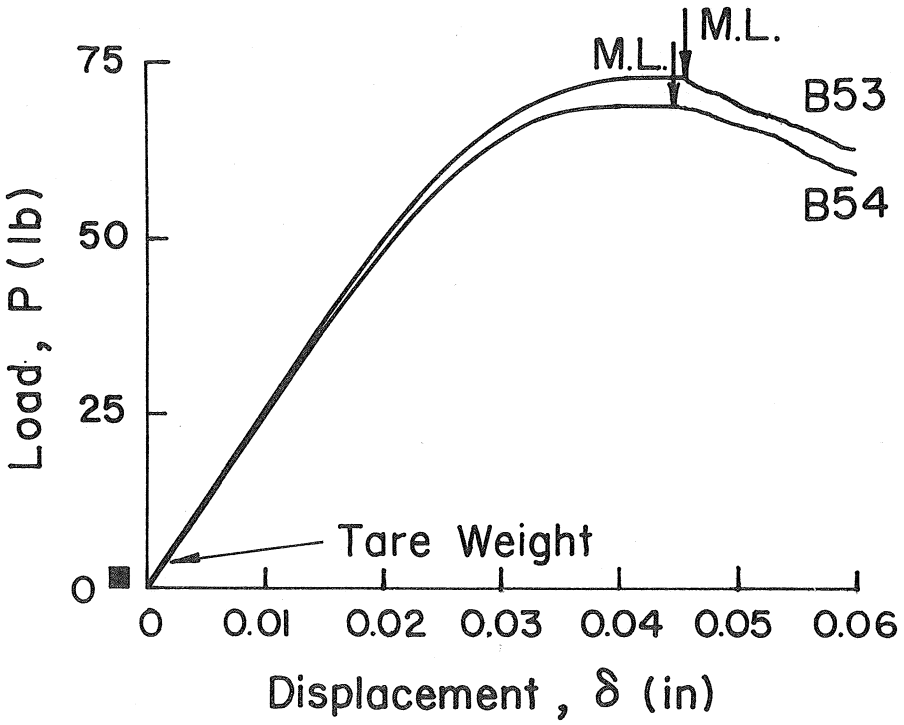


Fig. 19-C P-δ Curve, B53 ($S_y$ = 174, B = 0.1875, b = 0.0795 ), and B54 ($S_y$ = 174, B = 0.1875, b = 0.0802 )

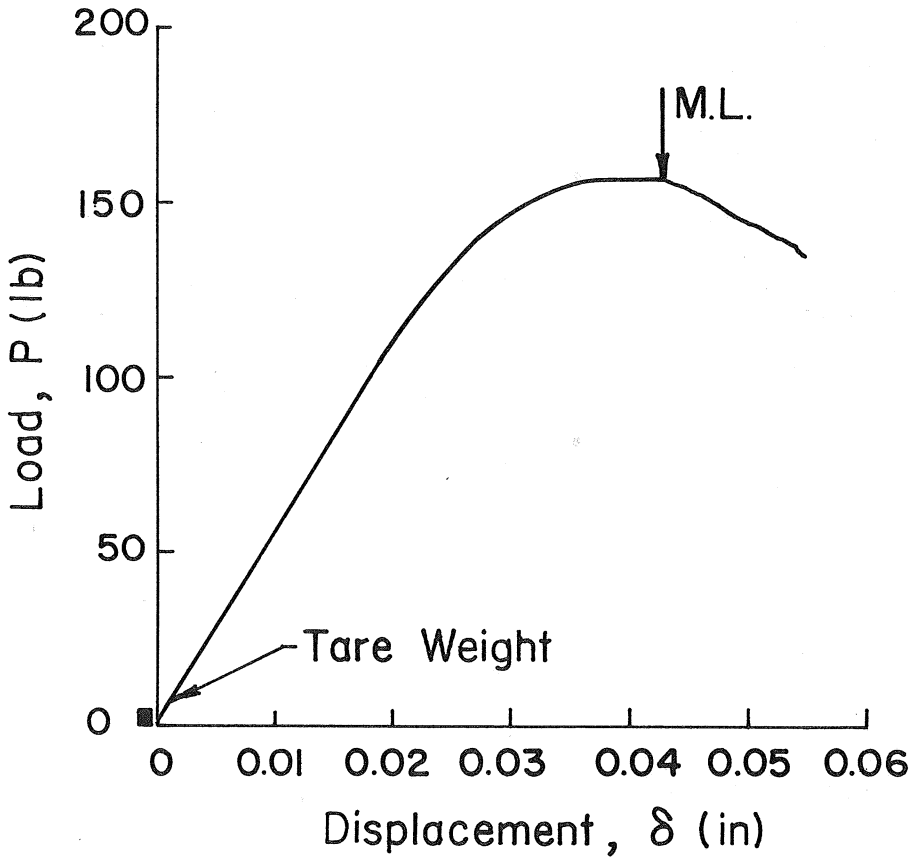


Fig. 20-C P-δ Curve, B55 ($S_y$ = 174, B = 0.25, b = 0.1058)

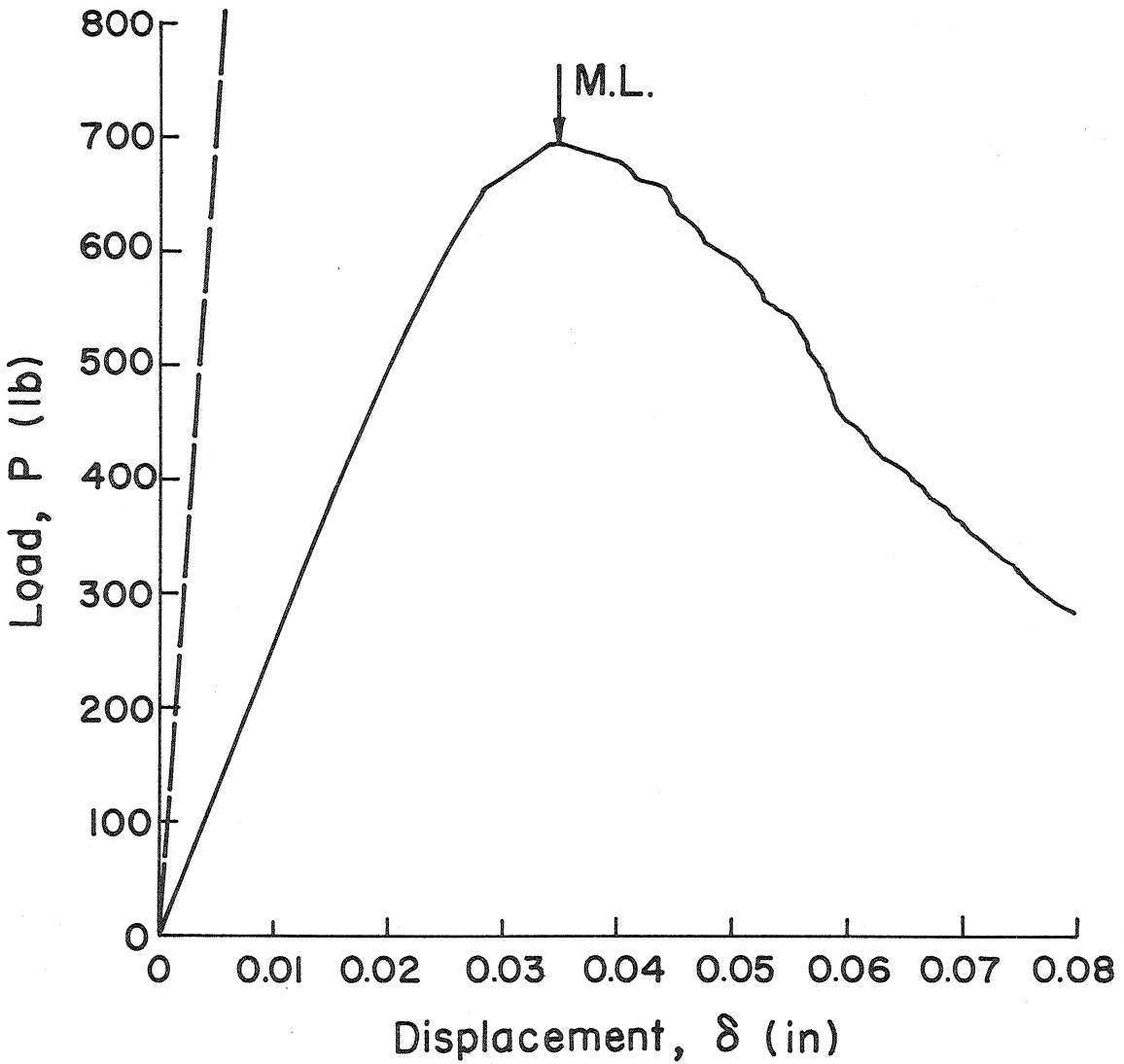


Fig. 21-C P-δ Curve, BO ($S_y$ = 174, B = 0.25, b = 0.233)

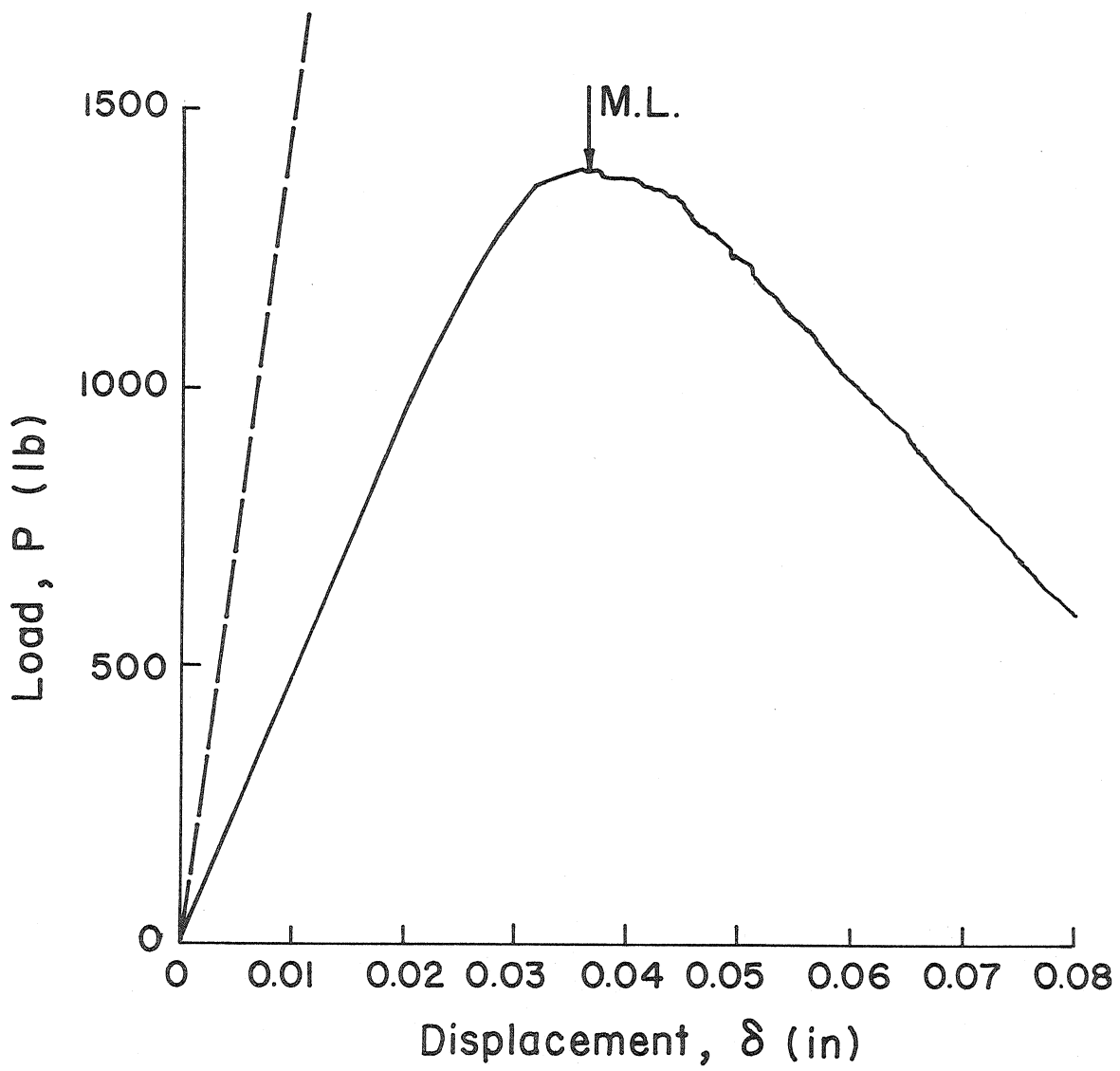


Fig. 22-C P-δ Curve, BI ($S_y$ = 174, B = 0.25, b = 0.348)

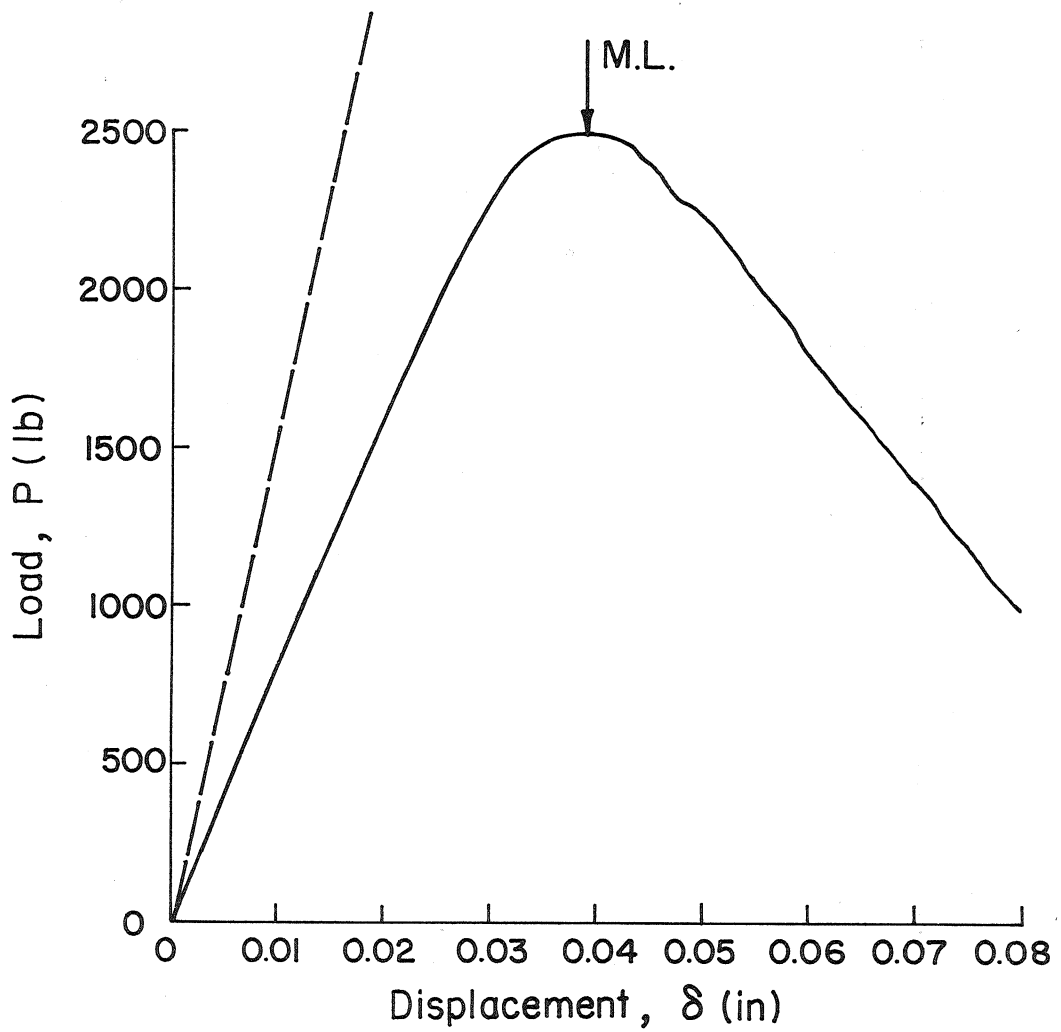


Fig. 23 P-δ Curve, B2 ($S_y$ = 174, B = 0.25, b = 0.489)

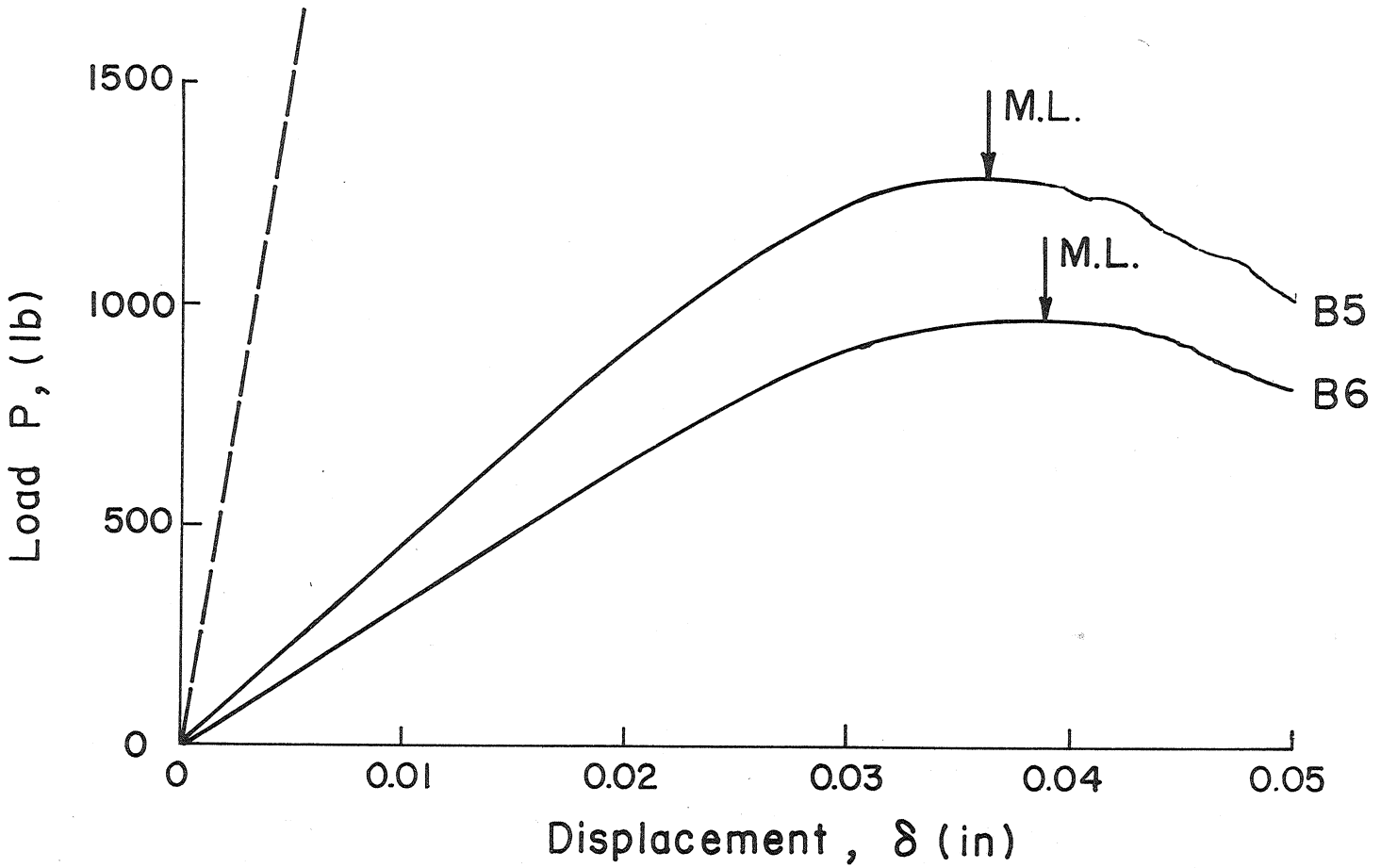


Fig. 24 P - δ Curve, B5 ($S_y$ = 174, B = 0.50, b = 0.217), and B6 ($S_y$ = 174, B = 0.50, b = 0.178)

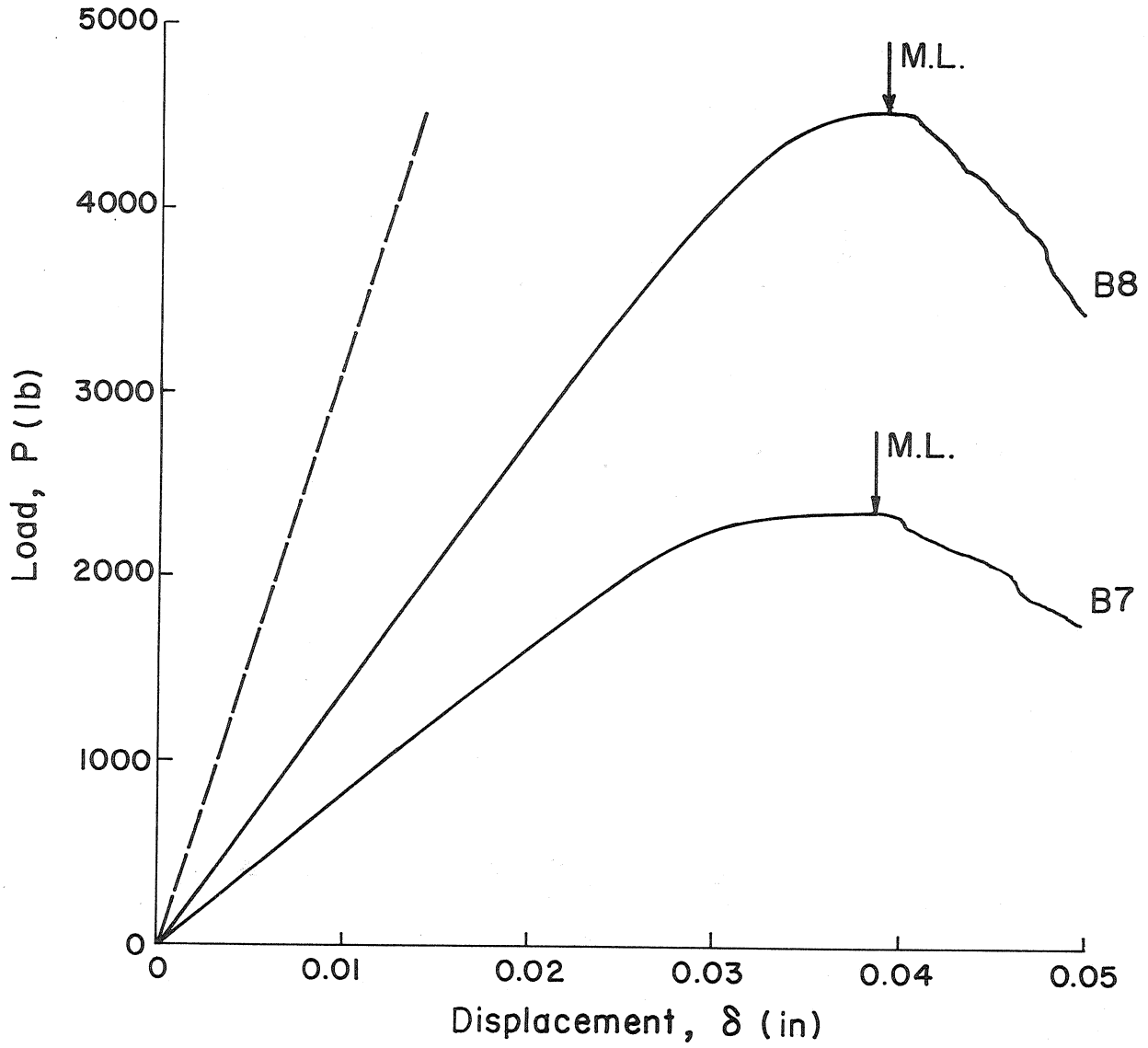


Fig. 25-C P-δ Curve, B7($S_y$=174, B=0.50, b=0.314), B8($S_y$=174, B=0.50, b=0.451)

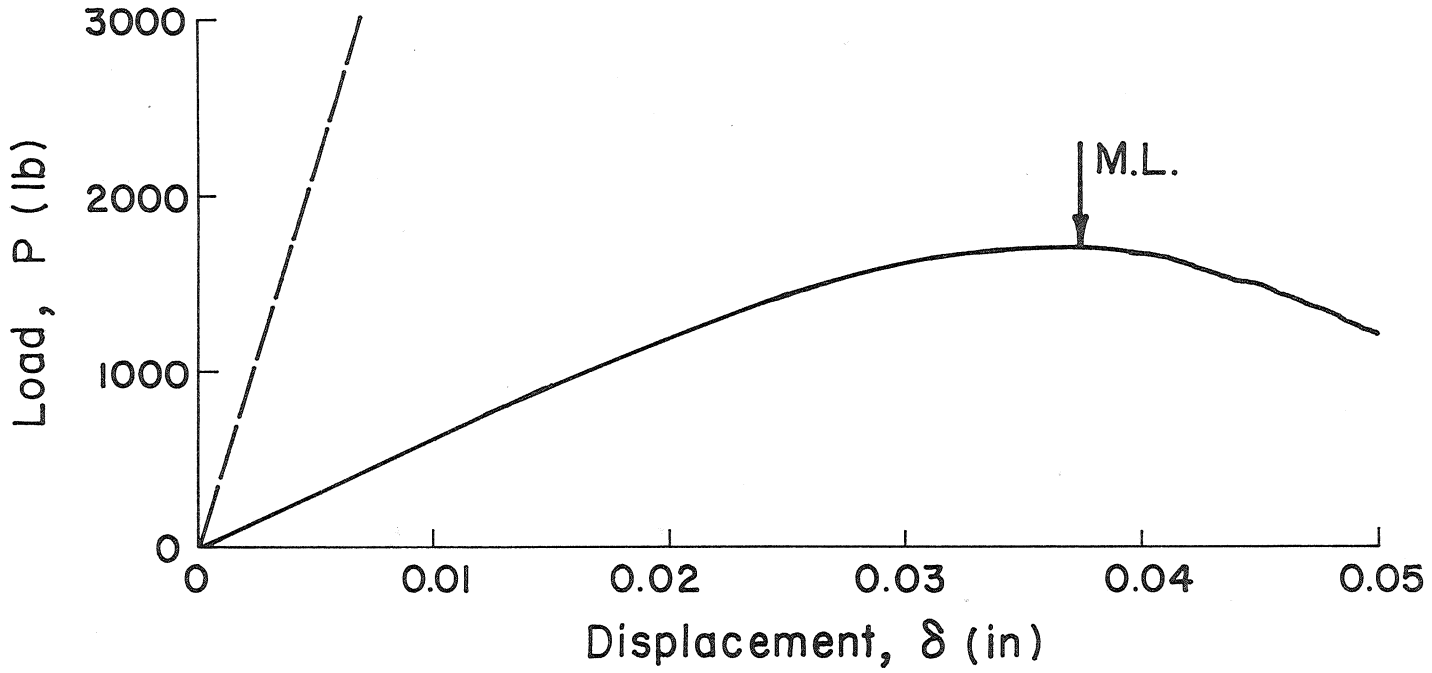


Fig. 26-C P-δ Curve, B10 ( $S_y$ = 174, B = 0.75, b = 0.202 )

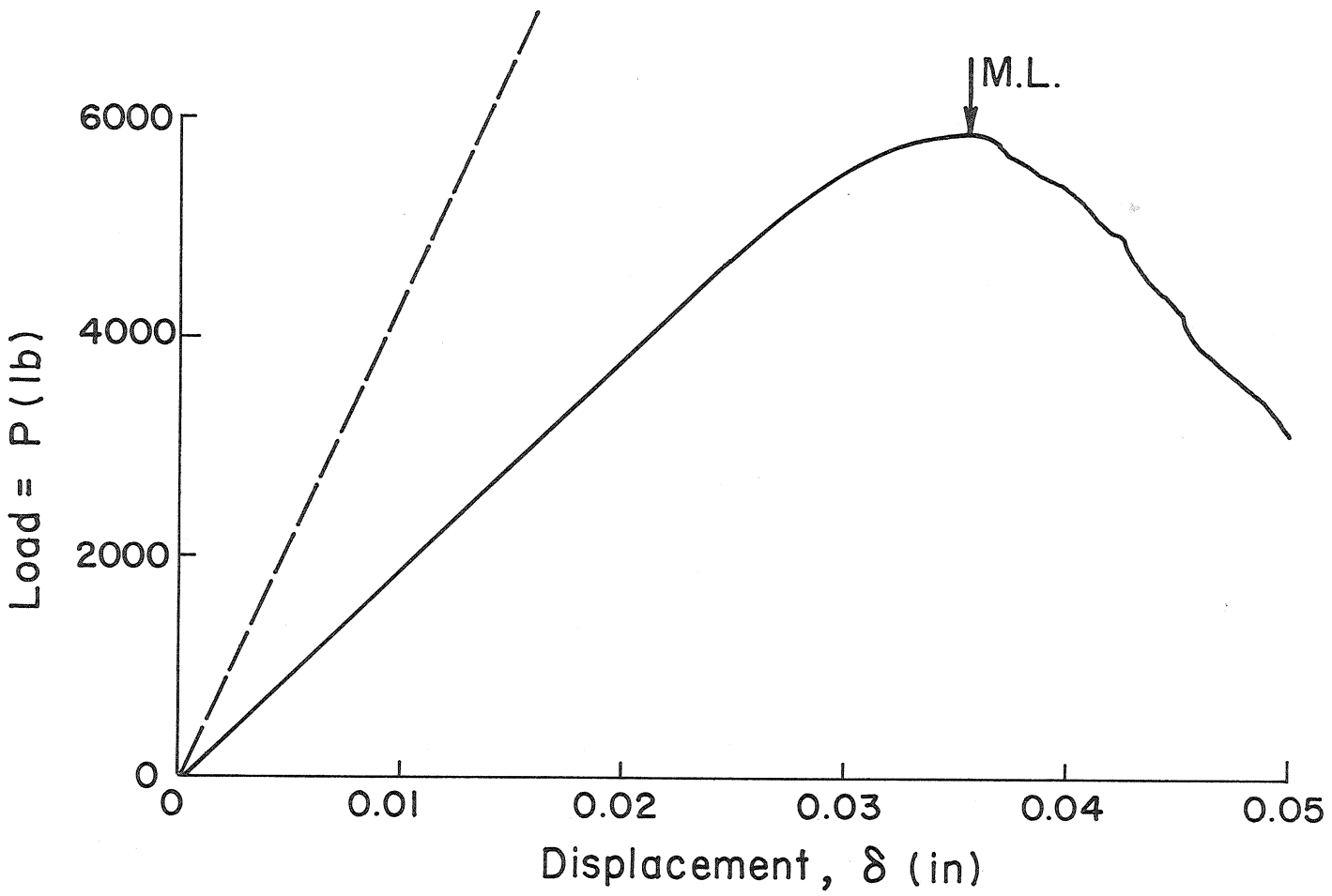


Fig. 27-C P-δ Curve, B11 ($S_y$ = 174, B = 0.75, b = 0.416)

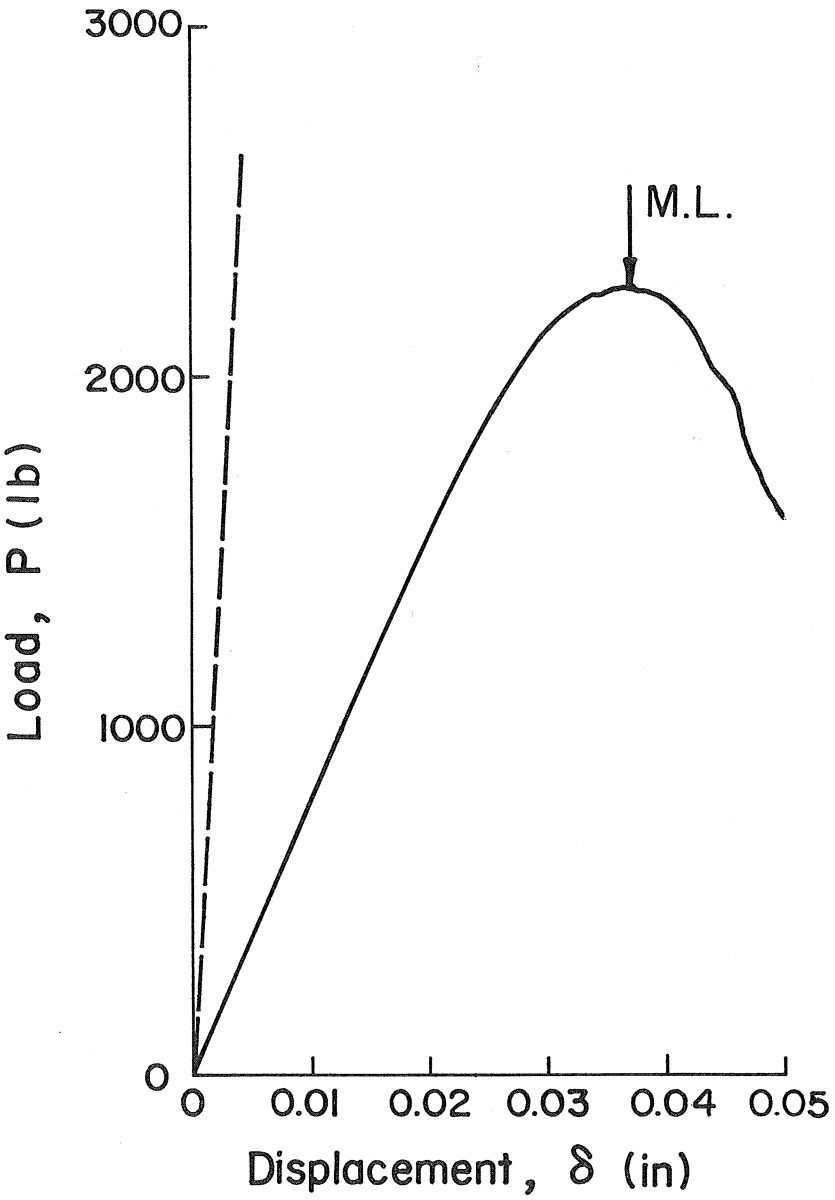


Fig. 28-C P-δ Curve, B15 ($S_y$ = 174, B = 1.0, b = 0.196 )

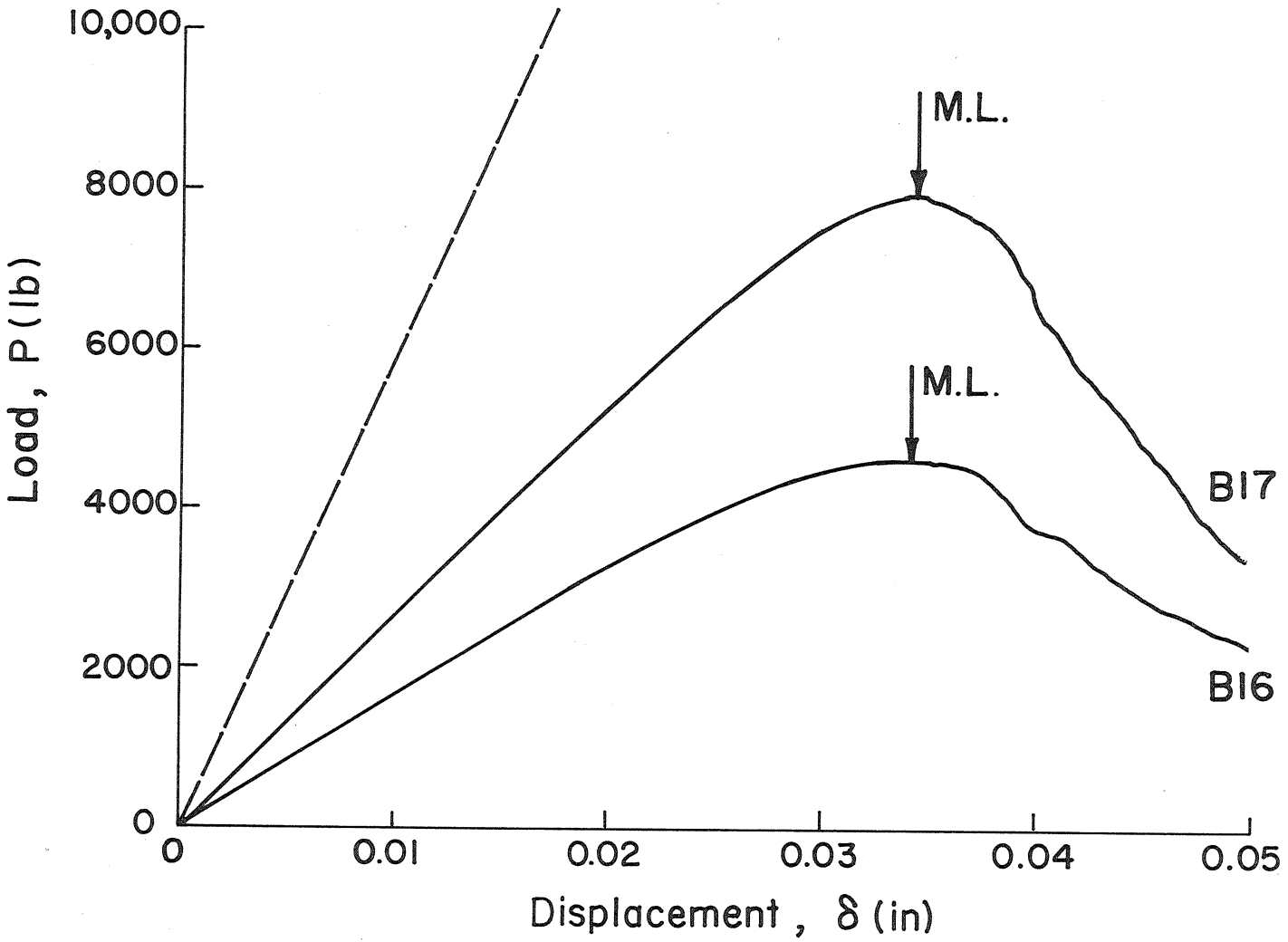


Fig. 29-C P-δ Curve, B16 ($S_y$ = 174, B = 1.0, b = 0.304 ), and B17 ($S_y$ = 174, B = 1.0, b = 0.422 )

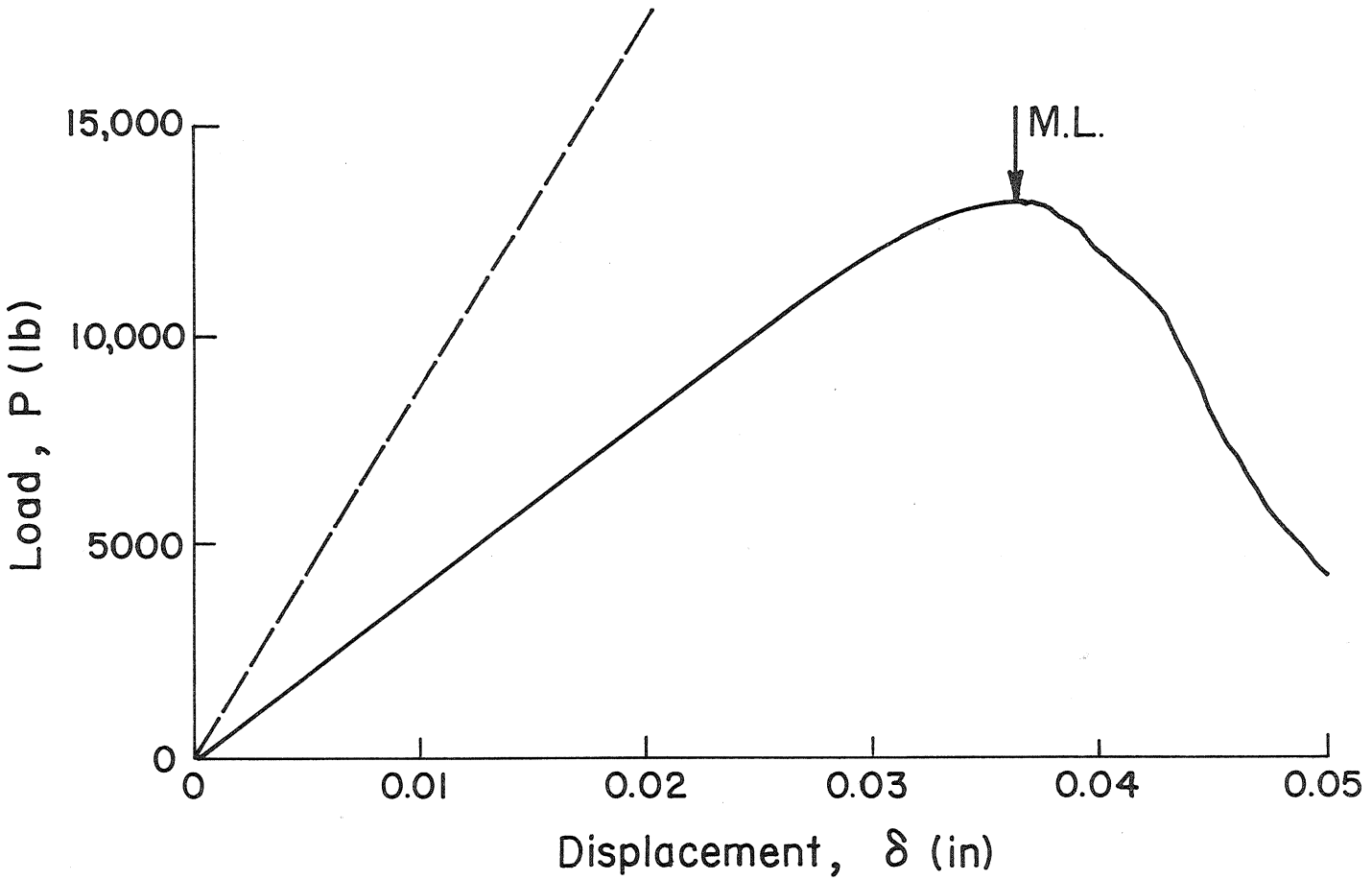


Fig. 30-C P-δ Curve, B21 ($S_y$ = 174, B = 1.5, b = 0.446 )

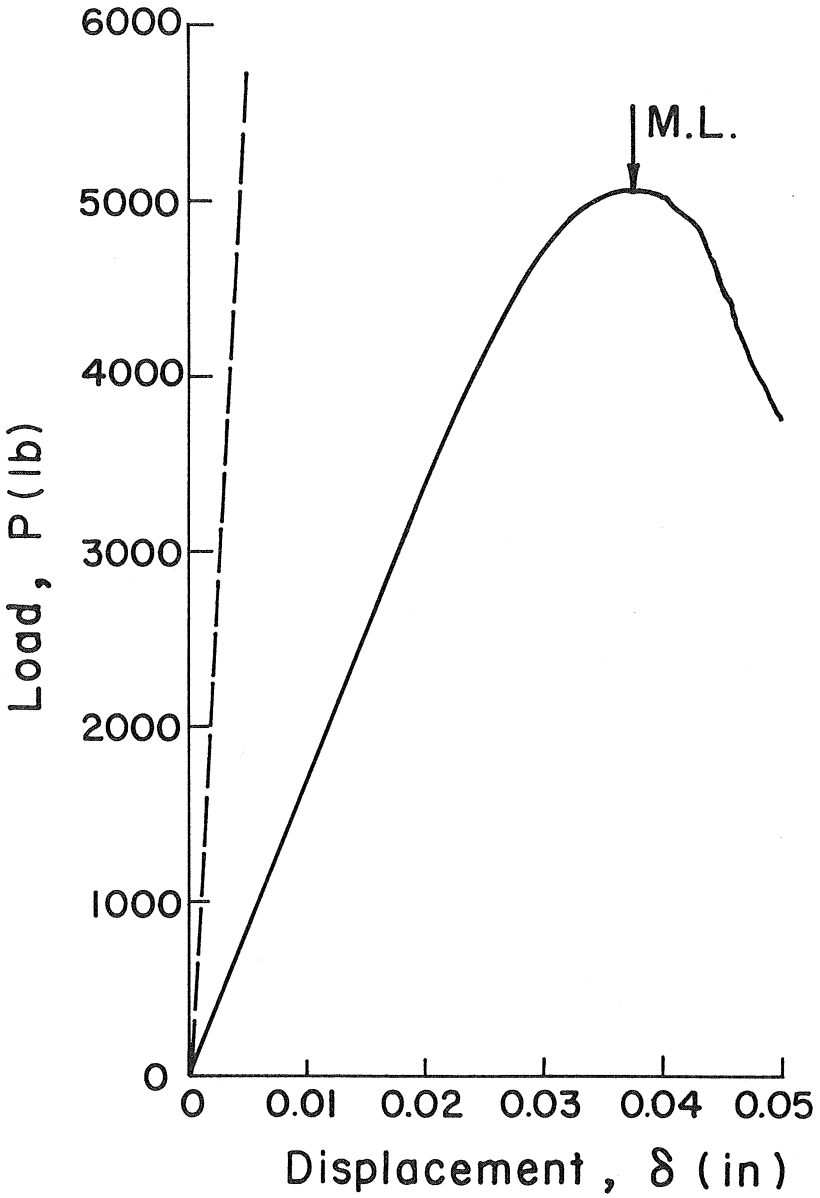


Fig. 31-C P-δ Curve, B25 ($S_y$ = 174, B = 2.0, b = 0.222)

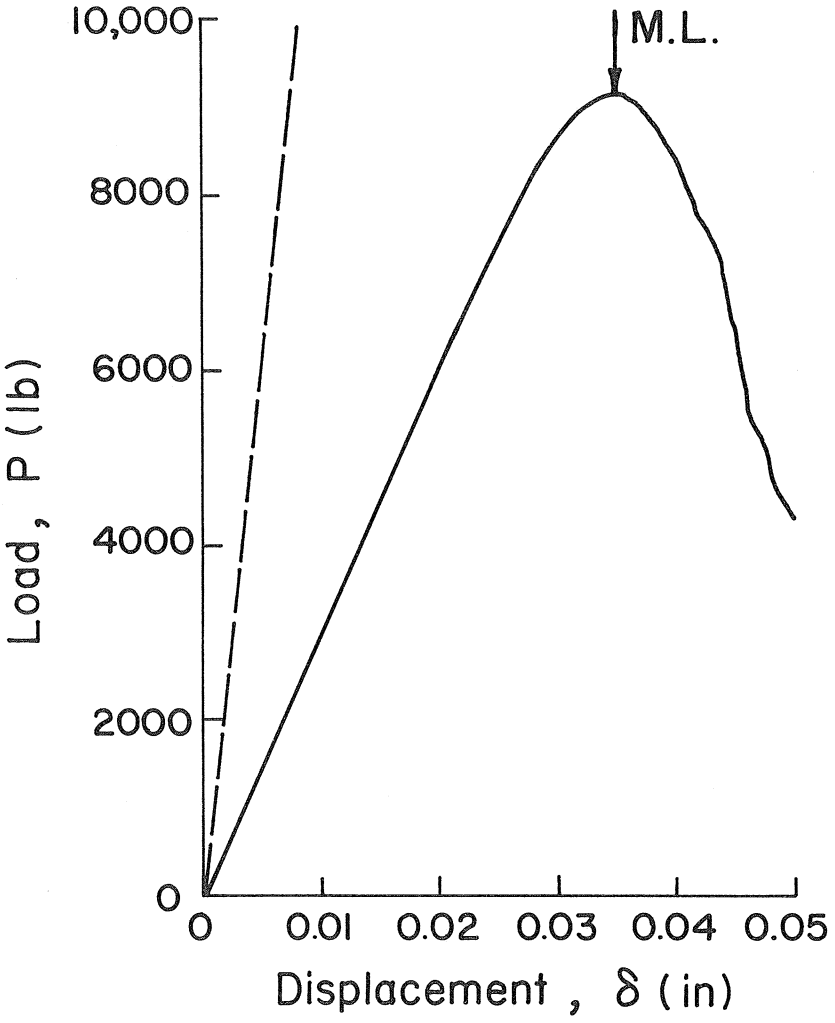


Fig. 32-C P-δ Curve, B26 ($S_y$ = 174, B = 2.0, b = 0.301)

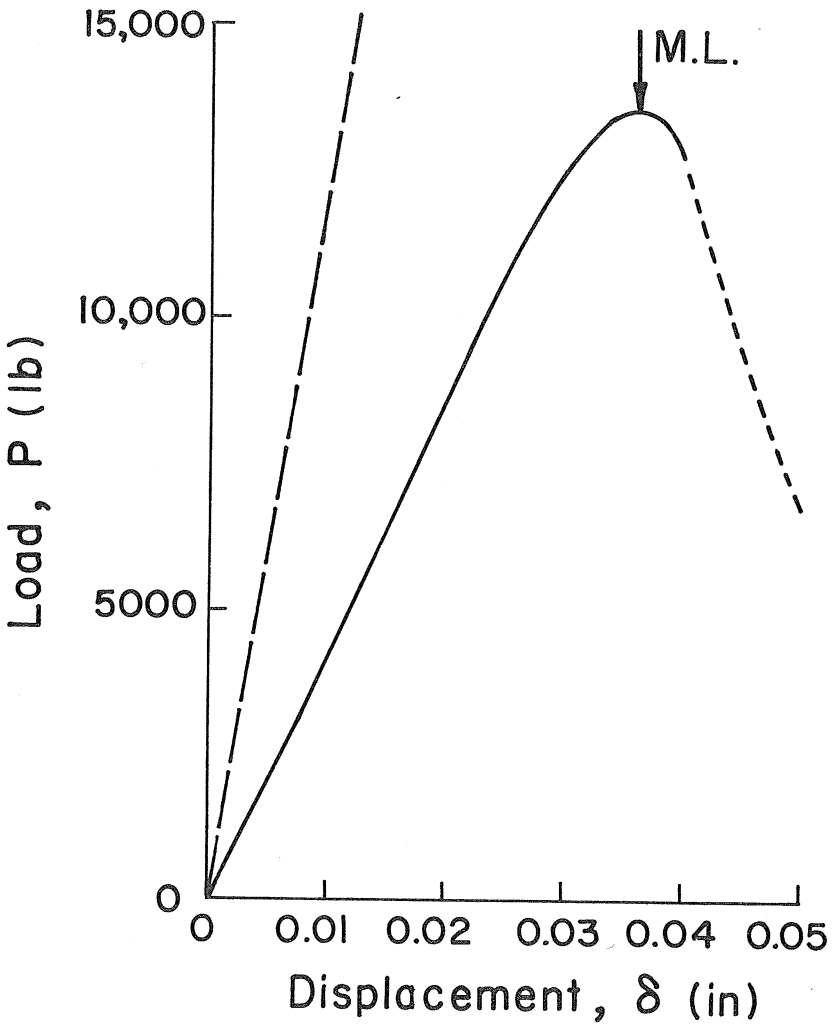


Fig. 33-C P-δ Curve, B27 ($S_y$ = 174, B = 2.0, b = 0.381 )

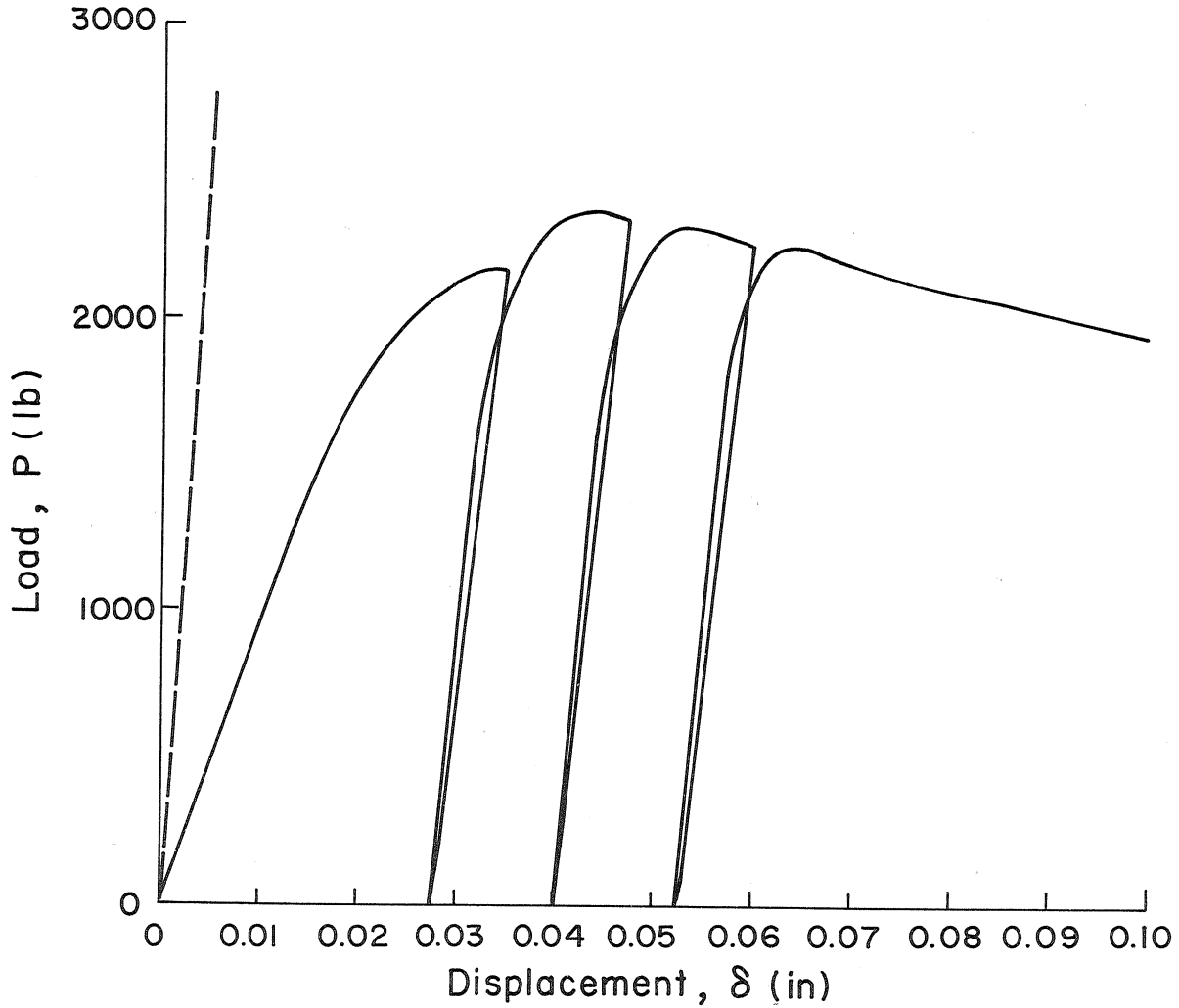


Fig. 34-C P-δ Curve, A101 ($S_y$ = 113, B = 0.75, b = 0.224)

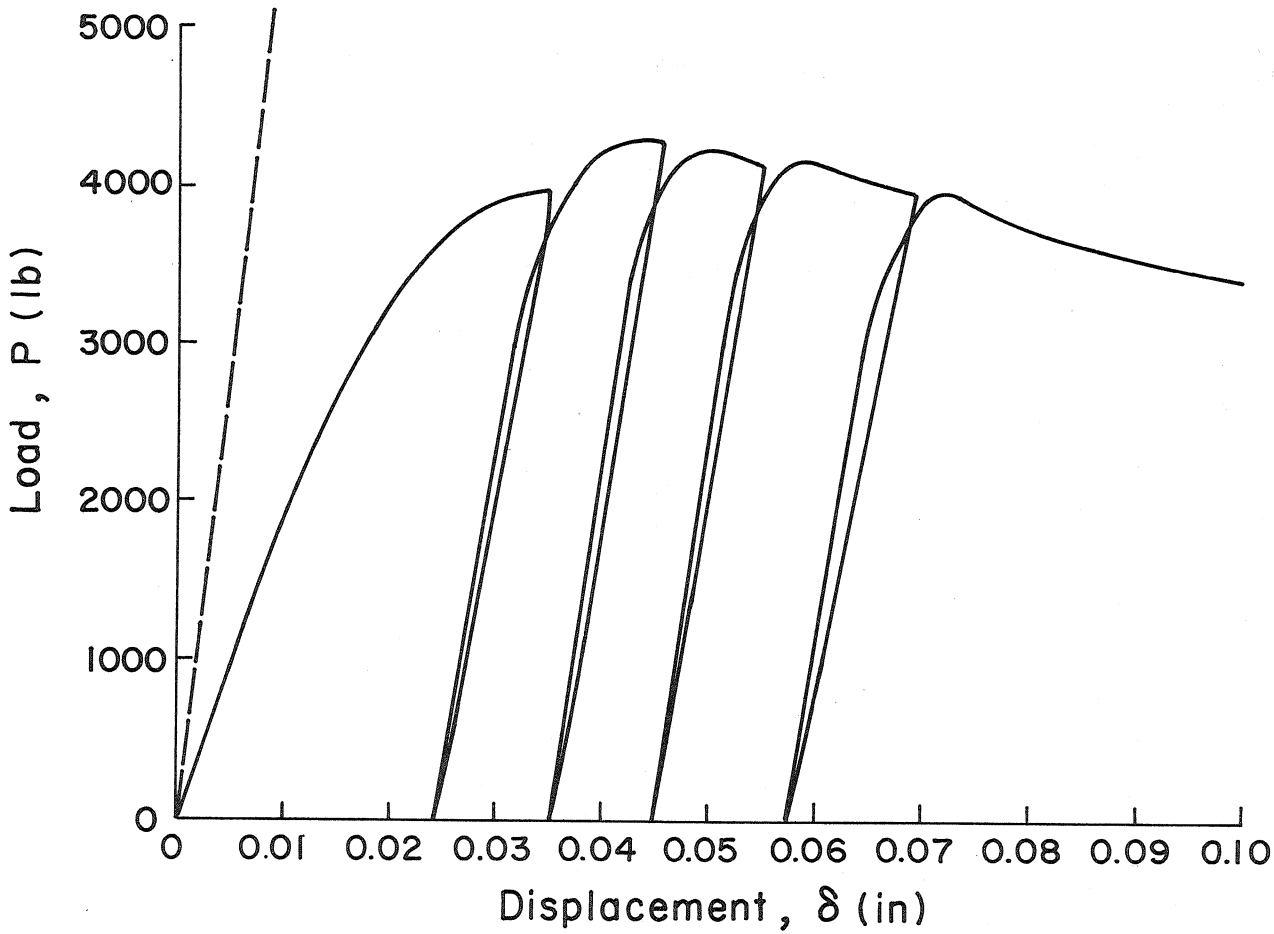


Fig. 35-C P-δ Curve, A102 ($S_y$ = 113, B = 0.75, b = 0.310)

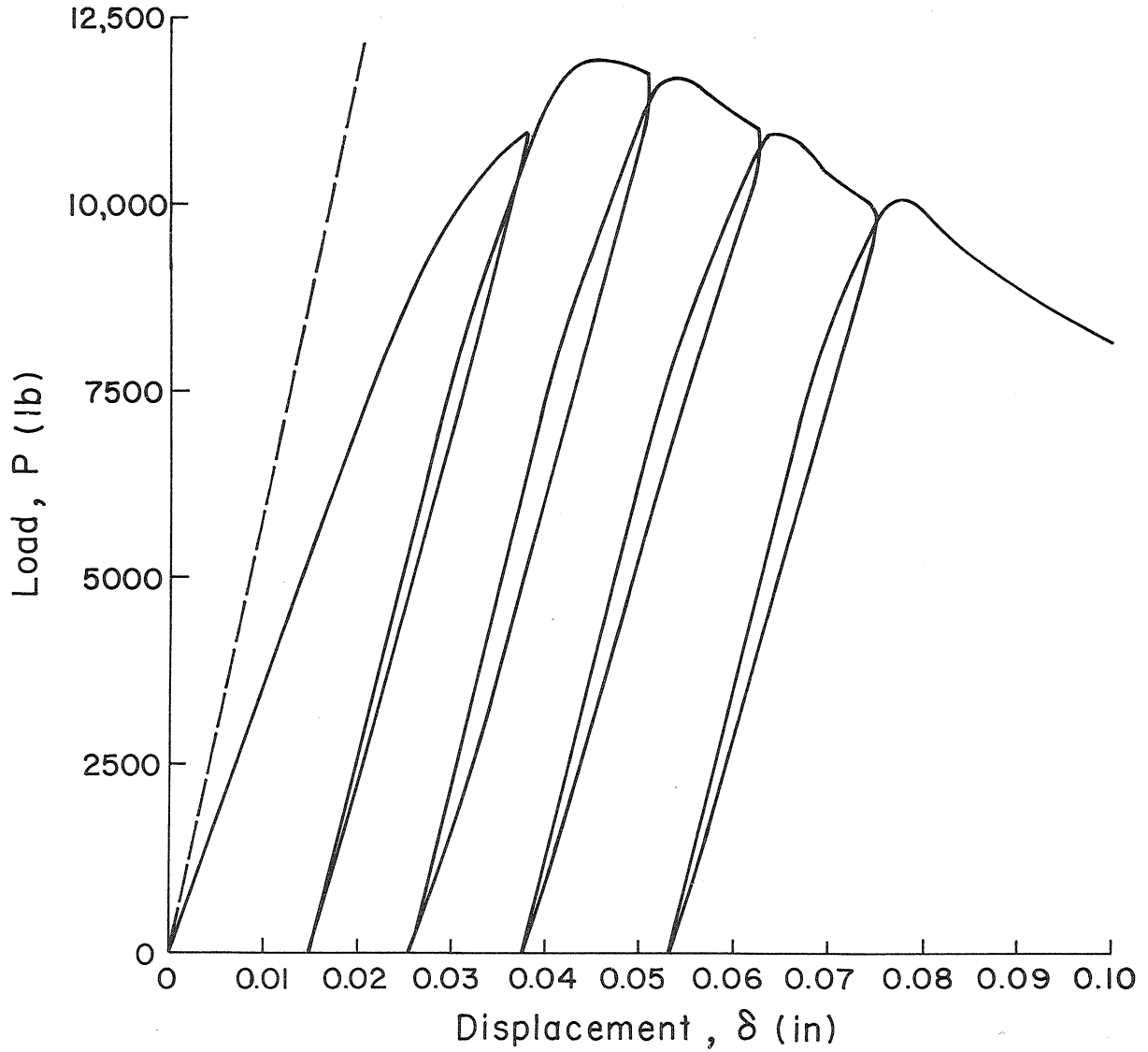


Fig. 36-C P-δ Curve , A103 ($S_y$ = 113, B = 0.75, b = 0.537 )

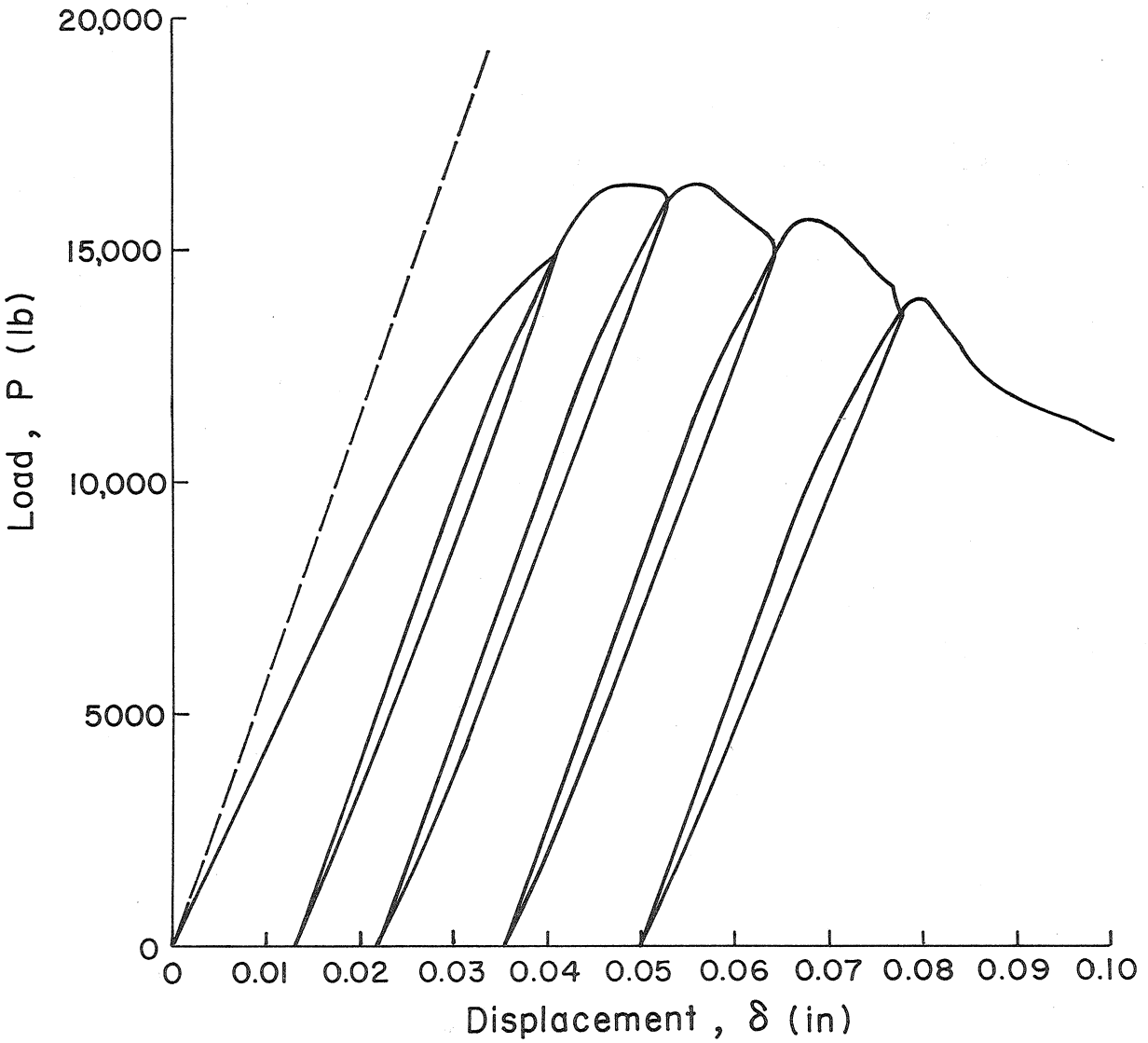


Fig. 37-C P-δ Curve, A104 ($S_y$ = 113, B = 0.75, b = 0.624)

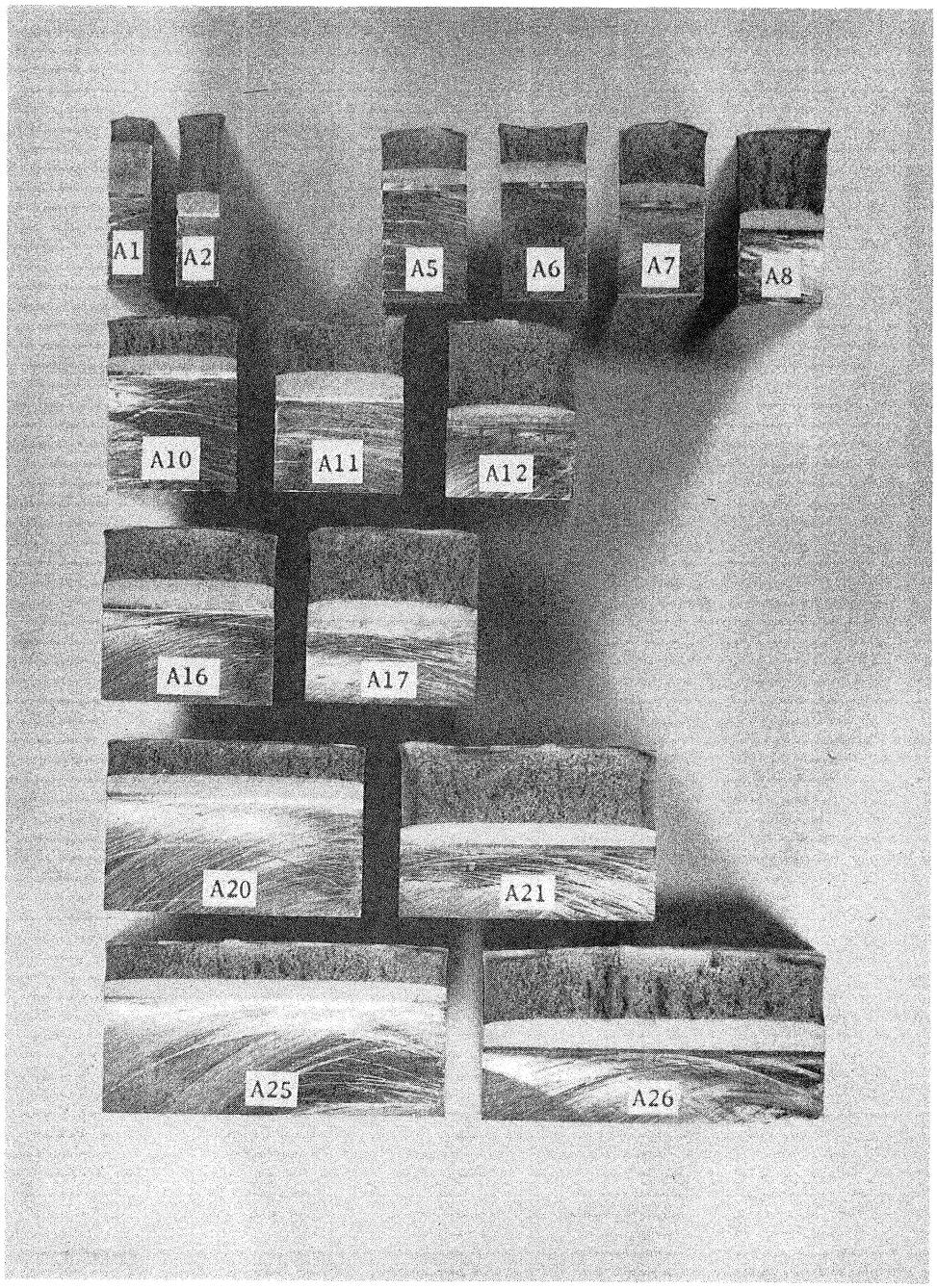


Fig. 38 – C Fracture Surfaces of Thick Bend Specimens ($S_y$ = 113)

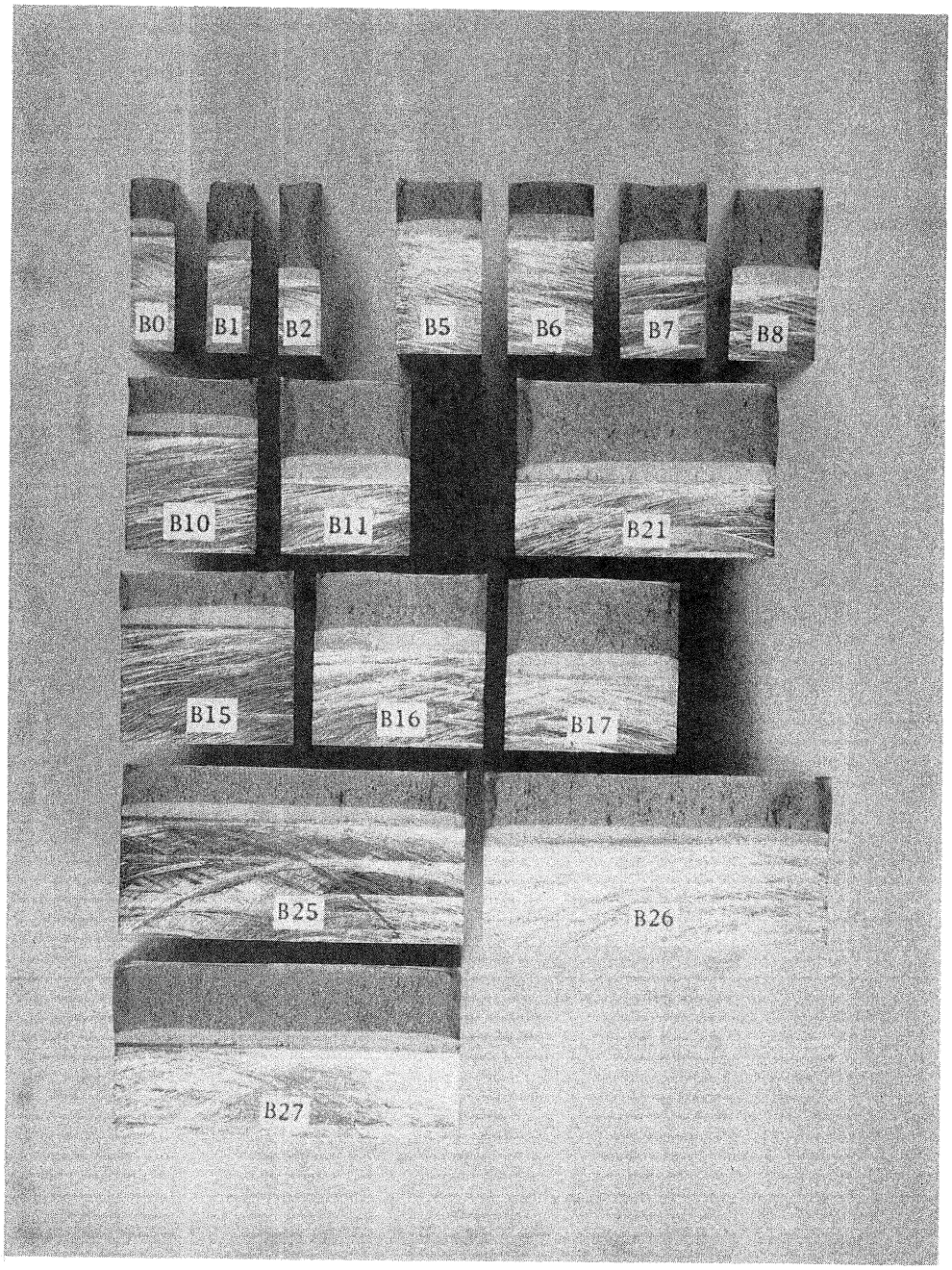


Fig. 39 - C Fracture Surfaces of Thick Bend Specimens ( $S_y = 174$ )

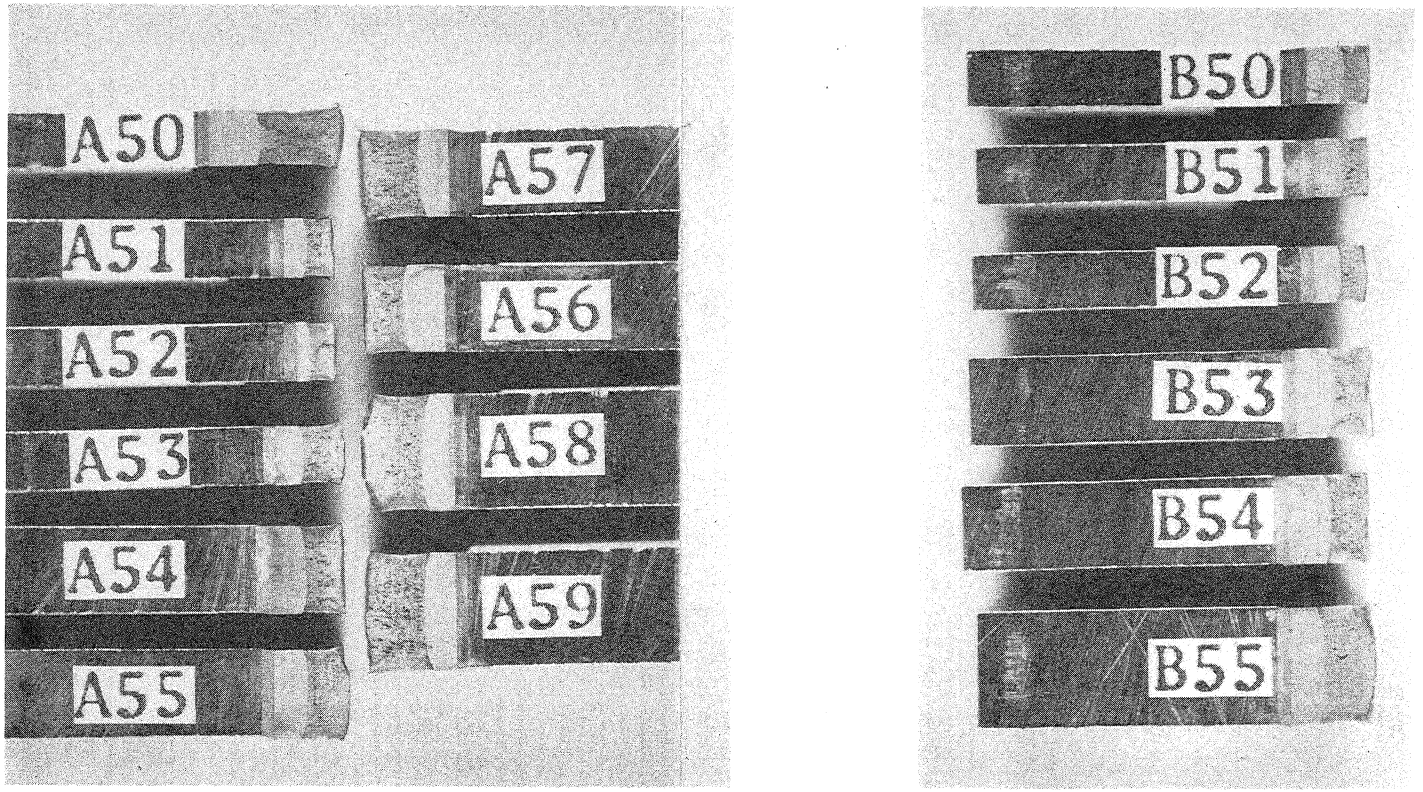


(a) $S_y$ = 113

(b) $S_y$ = 175

Fig. 40 – C Fracture Surfaces of Thin Bend Specimens

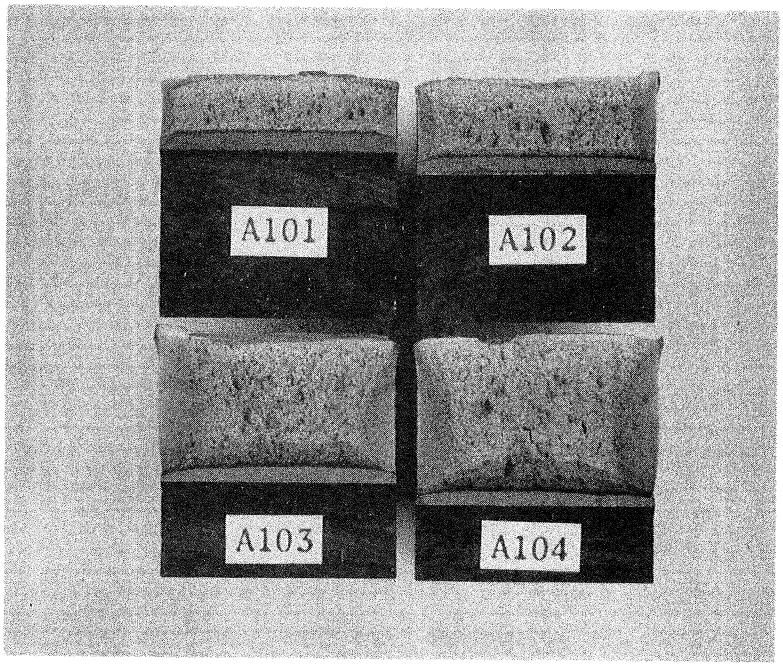


Fig.41 - C Fracture Surfaces of Heat Treated Specimens